

# Quantum Monte Carlo

Version 3.01

VESA APAJA

2018 University of Jyväskylä, Finland

## Contents

<b>1 History</b>	<b>4</b>
<b>2 Scaling and computational cost</b>	<b>6</b>
<b>3 Basic concepts</b>	<b>7</b>
3.1 Simple Monte Carlo . . . . .	7
3.2 Importance sampling . . . . .	9
3.3 Correlated samples and MC accuracy . . . . .	10
3.4 Sampling from a distribution . . . . .	11
3.4.1 Sampling the standard normal distribution . . . . .	16
3.5 Central Limit Theorem . . . . .	20
3.6 Detailed balance condition . . . . .	25
<b>4 Markov Chain Monte Carlo</b>	<b>27</b>
4.1 Metropolis–Hastings algorithm . . . . .	27
<b>5 Variational Monte Carlo</b>	<b>34</b>
5.1 Optimization of the trial wave function . . . . .	37
5.2 He atom wavefunction with e-e cusp . . . . .	42
<b>6 Diffusion Monte Carlo</b>	<b>46</b>
6.1 Short-time estimates of Green’s function . . . . .	49
6.2 A working DMC algorithm . . . . .	60
6.3 Mixed and pure estimators . . . . .	63
6.4 Fixed node and released node methods . . . . .	66
6.5 Excited states . . . . .	68
6.6 Second order DMC algorithms . . . . .	70
6.7 DMC Example: the ground state of a He atom . . . . .	73
<b>7 Path Integral Monte Carlo</b>	<b>77</b>
7.1 First ingredient: products of density matrices . . . . .	78
7.2 Second ingredient: the high-temperature density matrix . . . . .	80
7.3 Connection to path integral formulation of quantum mechanics . . . . .	81
7.4 Link action . . . . .	83
7.5 Improving the action . . . . .	83
7.6 Bose Symmetry . . . . .	84
7.7 Sampling paths . . . . .	85
7.8 Fermion paths: The sign problem . . . . .	86
7.9 The excitation spectrum and the dynamic structure function . . . . .	87
7.10 Fermion PIMC methods . . . . .	88

<b>8 The fermion sign problem</b>	<b>89</b>
<b>9 Error estimation</b>	<b>94</b>
9.1 Some definitions and clarifications . . . . .	94
9.2 Biased and unbiased estimators of variance . . . . .	95
9.3 Integrated autocorrelation time . . . . .	97
9.4 Block averaging . . . . .	98
9.5 Resampling methods . . . . .	99
9.5.1 Jackknife . . . . .	99
9.5.2 Bootstrap . . . . .	100
<b>10 Large-time-step propagators</b>	<b>104</b>
10.1 Propagators with fourth or higher order accuracy . . . . .	104
10.2 Propagators with no time step error . . . . .	110
<b>11 Appendix</b>	<b>111</b>
11.1 McMillan trial wave function for liquid $^4\text{He}$ . . . . .	111
11.2 Cusp conditions in Coulomb systems . . . . .	118

## 1 History

These are lecture notes about quantum Monte Carlo (QMC) methods. Here are some hallmarks of QMC<sup>1</sup>

- 1940's E. Fermi: Schrödinger equation can written as a diffusion equation; Physical principles of *Diffusion Monte Carlo (DMC)* discovered.
- 1942 A. A. Frost: evaluation of the energy of few simple molecules by picking few representative points in the configuration space; *Variational Monte Carlo (VMC)* is born.
- 1947 N. Metropolis and S. Ulam: Diffusion Monte Carlo developed into an algorithm; "... as suggested by Fermi ...".
- 1950's R. Feynman: Path integral formulation of quantum mechanics; Physical principles of *Path Integral Monte Carlo (PIMC)* discovered
- 1962 M. H Kalos: Solved the Schrödinger equation in the form of an integral equation: *Green's function Monte Carlo (GFMC)* is born.
- 1964 H. Conroy: Proposed, that points should be picked at random from the configuration space with probability proportional to  $\Psi_T^2$ , the square of the trial wave function. Application to  $H_2^+$ ,  $H^-$ ,  $HeH^{++}$ , He,  $H_2$ , and Li - the first application to a fermion system!
- 1965 W. L. McMillan: Energy of liquid  ${}^4He$ ; Applied the Metropolis algorithm to sample points with probability proportional to  $\Psi_T^2$ .
- 1971 R. C. Grim and R. G. Storer: Importance sampling.
- 1975 J. B. Anderson: First application of DMC to electronic systems
- 1986 D. M. Ceperley and E. L. Pollock: PIMC calculation of the properties of liquid  ${}^4He$  at finite temperatures.
- 1998 N.V. Prokofev, B. V. Svistunov, and I. S. Tupitsyn: Worm algorithm
- 2009 G. H. Booth, A. J. W. Thom, and A. Alavi: Fermion MC as a game of life in Slater determinant space

Some more recent developments are mentioned later in these lecture notes. QMC calculations published in July 2016 (highlighting by me):

---

<sup>1</sup>After J. B. Anderson in *Quantum Simulations of Complex Many-Body Systems : From Theory to Algorithms*, Editors J. Grotendorst, D. Marx, and A. Muramatsu.

- Quantum Monte Carlo Method for the Ground State of **Correlated Fermions**, by H Wang, M Iazzi, P Corboz, M Troyer
- *Ab initio* Quantum Monte Carlo simulation of the warm dense **electron gas** in the thermodynamic limit, by T Dornheim, S Groth, T Sjostrom, FD Malone ...
- Staircase of crystal phases of hard-core bosons on the **Kagome lattice**, by D Huerga, S Capponi, J Dukelsky, G Ortiz
- Determinant quantum Monte Carlo algorithm for simulating Hubbard models, by E Huang, E Nowadnick, Y Kung, S Johnston, B Moritz ...
- Hybrid Monte Carlo simulations of emergent magnetism in **graphene** in presence of hydrogen adatoms, by MV Ulybyshev
- A Fast Selected **Inversion Algorithm for Green's Function** Calculation in Many-Body Quantum Monte Carlo Simulations, by C Jiang, Z Bai, R Scalettar
- Impurities near an Antiferromagnetic-Singlet **Quantum Critical Point**, by T Mendes, N Costa, G Batrouni, N Curro ...
- **Jastrow correlation factor** for periodic systems, by TM Whitehead, MH Michael, GJ Conduit
- Microscopic study of static and dynamical properties of dilute one-dimensional **soft bosons**, by M Teruzzi, DE Galli, G Bertaina
- Dimensional modulation of spontaneous magnetic order in quasi-two-dimensional **quantum antiferromagnets**, by SC Furuya, M Dupont, S Capponi, N Laflorenci ...
- Computational Modelling as a Value Add in **Energy Storage Materials**, by RR Maphangwa, PE Ngeope
- J-freezing and Hund's rules in spin-orbit-coupled multiorbital **Hubbard models**, by AJ Kim, HO Jeschke, P Werner, R Valentí
- Level spectroscopy in a two-dimensional **quantum magnet**: linearly dispersing spinons at the deconfined quantum-critical point, by H Suwa, A Sen, AW Sandvik
- Communication: **Convergence of many-body wave-function expansions** using a plane-wave basis in the thermodynamic limit, by JJ Shepherd
- Do **positrons** measure atomic and molecular diameters?, by J Franz, K Fedus, GP Karwasz

- Doping evolution of spin and charge excitations in the **Hubbard model**, by SD Home, P Charges
- **Critical behavior** in the presence of an order-parameter pinning field, by FP Toldin, FF Assaad, S Wessel
- Charged fermions coupled to  $\mathbb{Z}_2$  gauge fields: Superfluidity, confinement and **emergent Dirac fermions**, by S Gazit, M Randeria, A Vishwanath
- A simple fermionic model of **deconfined phases and phase transitions**, by FF Assaad, T Grover
- Electron Correlation Effects in All-Metal **Aromatic Clusters**: A Quantum Monte Carlo Study, by J Higino Damasceno Jr, JN Teixeira Rabelo ...
- (Book) **Interacting Electrons**: Theory and Computational Approaches, by RM Martin, L Reining, DM Ceperley

and all this in just 20 days.

## 2 Scaling and computational cost

The computational cost of Diffusion Monte Carlo (DMC) is roughly an order of magnitude larger than the cost of Variational Monte Carlo of the same system.

In atomic and molecular physics the most accurate methods are the fixed-node diffusion Monte Carlo and the coupled cluster method on the level CCSD(T) (meaning the included coupled clusters contain singles, doubles, and perturbationally treated triplets). With the number of electrons  $N$ , the fixed node DMC scales as  $N^4$ , while CCSD(T) scales as  $N^7$ , so the latter is practical only for small systems. The computational cost for fixed node DMC increases as  $Z^{5.5-6.5}$  with the atomic number  $Z$ . The situation improves if one uses a *pseudopotential*, which is non-singular at the nucleus.<sup>2</sup>

The wave function near the nucleus oscillates very rapidly (reflecting the fact that electrons move rapidly). If one uses a plane-wave basis, the infinite basis is cut off at a prescribed energy, but these high-frequency oscillations cause the basis set to become too large for practical purposes. The goal of using the lowest possible cutoff energy for the plane-wave basis set led to the invention of ultra soft pseudopotentials by Vanderbilt in 1990.<sup>3</sup>

---

<sup>2</sup>M. Burkatzki, C. Filippi, and M. Dolg, *Energy-consistent pseudopotentials for quantum Monte Carlo calculations*, J. Chem. Phys. **126**, 234105 (2007) .

<sup>3</sup>Vanderbilt, D. *Soft self-consistent pseudopotentials in a generalized eigenvalue formalism*, Phys. Rev. **B41**, 7892-7895 (1990).

### 3 Basic concepts

Many-body theorists are interested in systems with many degrees of freedom. Often one encounters multi-dimensional integrals, like the partition function of  $N$  classical atoms,

$$Z \propto \int d\mathbf{r}_1 d\mathbf{r}_2 \dots d\mathbf{r}_N \exp[-\beta V(\mathbf{r}_1, \dots, \mathbf{r}_N)] , \quad (1)$$

where  $\beta = 1/(k_B T)$  and  $V(\mathbf{r}_1, \dots, \mathbf{r}_N)$  is the potential energy. If one discretises each coordinate with only ten points, and the machine could do  $10^7$  points per second, would the partition function for twenty particles take  $10^{53}$  seconds, some  $10^{34}$  times the age of the universe (at the moment you start running the program ...).

We *must* evaluate the integrand at some of the points, otherwise the result wouldn't contain any information of the integrand. So how to pick the points? Make a compromise: If one cannot evaluate the integrand in any decent number of discretization points per dimension, one might as well pick them at random from the multi-dimensional space.

#### 3.1 Simple Monte Carlo

How could one calculate the area of a unit circle with random numbers? First put a box around the circle, or more economically, a box around the first quadrant. If you take random coordinates  $x$  and  $y$  uniformly distributed between 0 and 1, mark this  $x \in U[0, 1]$  and  $y \in U[0, 1]$ <sup>4</sup>. The probability that the point  $(x, y)$  is inside the circle is

$$P(\text{hit circle}) = \frac{\text{Area of a quarter unit circle}}{\text{Area of a box}} = \frac{\pi}{4} . \quad (2)$$

You know that you've hit the circle, when  $x^2 + y^2 \leq 1$ , so that's it: start picking up points  $(x, y)$  and count how many times you hit the circle out of  $N$  tries. This is a very ineffective way of calculating  $\pi$ , and the more space one has that is outside the circle the worse it gets. This is a very simple example of *importance sampling*: The better your random picks hit the relevant region in space (inside the circle), the better the efficiency. After a one night run the result was  $\pi \approx 3.141592318254839$ , with only 6 correct decimals. By the way, this stone-throwing calculation of  $\pi$  is also a simple test for the (pseudo-)random number generator.

This  $\pi$ -problem was inefficient application of MC mostly because the dimensionality was too low, just two.

Next consider an alternative way to do a one-dimensional integral,

$$I = \int_0^1 dx f(x) . \quad (3)$$

---

<sup>4</sup>We assume that a method to generate (pseudo) random numbers  $x$ ,  $x \in U[0, 1]$  is available.

One can estimate this integral as the average of function  $f(x)$  in the integration range,

$$I \approx I_N = \frac{1}{N} \sum_{i=1}^N f(x_i) , \quad (4)$$

where  $x_i$  are random points evenly distributed in the range  $x_i \in [0, 1]$ . To estimate the error for arbitrary  $f$  we can assume, that it is a random variable; a sensible assumption since we don't want to tailor this for some specific  $f$ . The *variance* or the *square of the standard deviation* is then

$$\sigma_I^2 \approx \sigma_{I_N}^2 = \frac{1}{N} \sigma_f^2 \quad (5)$$

$$= \frac{1}{N} \left[ \frac{1}{N} \sum_{i=1}^N f(x_i)^2 - \left( \frac{1}{N} \sum_{i=1}^N f(x_i) \right)^2 \right] , \quad (6)$$

and it measures how much the random variable deviates from its mean, *i.e.*, from the estimate of the integral  $I$ . The inaccuracy  $\sigma_I$  is inversely proportional to the square root of the number of samples,

$$\sigma_I \sim \frac{1}{\sqrt{N}} . \quad (7)$$

The MC error converges slowly, but steadily. The trapezoid rule integration error diminishes as  $1/N^2$  in one dimension, so the comparison is very unfavorable to MC. This rises the question:

### When does MC integration become the most effective way to integrate?

If one has to evaluate the integrand  $N$  times to calculate a  $d$ -dimensional integral, then for each dimension one has  $\sim N^{1/d}$  points, whose distance is  $h \sim N^{-1/d}$ . The error for every integration cell of volume  $h^d$  is in the trapezoid rule  $\sim h^{d+2}$ , so the total error will be  $N$  times that,  $\sim N^{-2/d}$ . For high-dimensional integrals this error diminishes very slowly with increasing number of evaluation points  $N$ .

*The error in Monte Carlo is proportional to  $1/\sqrt{N}$  regardless of the dimension of space*

In a 4-dimensional space the trapezoid and the MC integration are equally effective, at higher dimensions MC wins. Why exactly does a naive, deterministic method, such as trapezoid or Simpson's rule, become ineffective at higher dimensions? Think about a 3D cube and fill it with a regular grid of  $N$  points. Looking at the 2D projection of these grid points on a square: you see only  $N^{2/3}$  points, because many points overlap. This means there are gaping holes in the space where you don't evaluate your function. One should pick points that try to fill the holes. This can be done deterministically, it's goes under the name *quasi-Monte Carlo methods*,

“quasi” because the points are not random, but form a clever, space-covering pattern. Also Monte Carlo random points do better than naive deterministic grid points, because projected random points don’t overlap and, as a result, the space is sampled more evenly.<sup>5</sup>

### 3.2 Importance sampling

Eq. (6) shows that our new integration method becomes better for flatter functions, it’s exact for a constant function. The integral of a constant function takes just one function evaluation anywhere, multiplied by the integration volume, and there is no error at all. So let’s try to make the integrand flatter. Define a normalized weight function, aka a probability distribution function (PDF)  $w$ ,

$$\int_{-\infty}^{\infty} dx w(x) = 1 \quad \text{normalization .} \quad (8)$$

Next we write the original integral in the equivalent form

$$I = \int_{-\infty}^{\infty} dx w(x) \frac{f(x)}{w(x)} \quad (9)$$

and change variables, the cumulative distribution function  $\text{cdf}(x)$  is

$$y := \text{cdf}(x) = \int_{-\infty}^x dx' w(x') . \quad (10)$$

Now we have

$$\frac{dy}{dx} = w(x) , \quad (11)$$

and  $\text{cdf}(x = -\infty) = 0$ ;  $\text{cdf}(x = \infty) = 1$ , so the integral is,

$$I = \int_0^1 dy \frac{f(x(y))}{w(x(y))} . \quad (12)$$

According to the above strategy this is estimated as the average of the argument evaluated at random points  $r_i \in U[0, 1]$ :

$$I \approx I_N = \frac{1}{N} \sum_{i=1}^N \frac{f(x(r_i))}{w(x(r_i))} . \quad (13)$$

If we can find a weight function  $w$  that approximated  $f$  well, then  $f/w$  is flatter than  $f$  and the variance is smaller. The applicability of this method relies on the assumptions, that

---

<sup>5</sup>Examples of deterministic vs. MC integrations are given in the blog of Yiannis Papadopoulos.

- (i) we know something useful about  $f$ , and we can look for a nice weight function  $w$  that approximates  $f$
- (ii) we can calculate  $x(r)$  for that weight function, *i.e.*, we know how to draw random numbers from the PDF  $w$ .

Since  $r_i \in U[0, 1]$ , points  $x_i = x(r_i)$  are distributed as  $dr(x)/dx = w(x)$ . Therefore more samples are taken from regions of space where  $w$  - and by construction also  $f$  - is large, and little effort is spent in regions where the weight is small. This is called *importance sampling*. Notice that importance-sampling method is problem specific.

However, sometimes the importance sampling distribution  $w$  can be improved as we collect data. This is done in the VEGAS code, which collects a histogram of values of  $f$  sampled so far, and updates  $w$  to do better sampling.<sup>6</sup>

### 3.3 Correlated samples and MC accuracy

The error in MC decreases as  $1/\sqrt{N}$  for  $N$  measurements. This means about 100 times more work to get one more significant figure to the result. This is quite normal for Monte Carlo methods, but actually the convergence is  $C/\sqrt{N}$ , and the factor  $C$  may be fatal to MC.

Samples may be correlated, meaning the chosen points are not quite random. This is the case if one uses the so-called *random walk* to generate points: the next point is a random, but small, step away from the previous one. It can be shown that for correlated sampled

$$\text{error in mean} = \sqrt{\frac{2\tau_{\text{int}}}{N}}\sigma , \quad (14)$$

where  $\sigma$  is the variance of  $N$  independent samples. The integrated autocorrelation time  $\tau_{\text{int}}$  describes how badly the samples are correlated. The bad news is that close to a critical point  $\tau_{\text{int}}$  diverges. This is known as *critical slowing down*, and it tends to make MC calculations slow near phase transitions.

The term "critical slowing down" can mean two things:

- Decreasing rate of recovery from small perturbations. It signals approaching criticality, such as an ecological disaster. Used as an early-warning mechanism.
- A Monte Carlo method samples the phase space inefficiently due to long-range correlations near criticality. This simply means that MC spends long time in very similar situations. A more clever algorithm does not suffer from critical slowing down. A typical example is the Ising model simulation, where a single-spin flip algorithm slows down near phase transition, but a cluster algorithm doesn't.

---

<sup>6</sup>See VEGAS algorithm

### 3.4 Sampling from a distribution

Without importance sampling MC is mostly pretty useless, so we'd better find a way how to generate random numbers that sample a given PDF  $w$ . Either analytically or numerically. First we need to establish a connection between a uniformly distributed variable  $r$  and  $x$  that has PDF  $w$ . Use again the cumulative distribution function,

$$y := \text{cdf}(x) := \int_{-\infty}^x dx' w(x') , \quad (15)$$

which gives

$$\frac{dy}{dx} = \frac{dcdf(x)}{dx} = w(x) . \quad (16)$$

Apparently,

$$\int_0^1 dr = \int_{-\infty}^{\infty} dx w(x) . \quad (17)$$

In MC, the left integral is evaluated by picking  $N$  random points  $r_i \in U[0, 1]$ . The right integral is evaluated by picking points  $x_i$  from distribution  $w$ . This proves that the values  $x$  in Eq. (15) have distribution  $w$ . An obvious solution is to invert  $r(x)$ , and solve  $x_i$  for a given  $r_i$ , but we shall see there are other ways.

#### A non-random method

Let's say we have evenly spaced grid points  $y_i$  given by

$$y_i = \frac{i}{N} = \int_0^{y_i} dx w(x) , \quad i = 0, 1, \dots, N . \quad (18)$$

The points  $x_i$  can be solved from the differential equation  $dy(x)/dx = w(x)$  using discretization

$$\frac{y_{i+1} - y_i}{x_{i+1} - x_i} \approx \frac{dy}{dx} = w(x_i) . \quad (19)$$

Since  $y_{i+1} - y_i = 1/N$ , we obtain the recurrence relation

$$x_{i+1} = x_i + \frac{1}{N w(x_i)} , \quad (20)$$

where the initial value  $x_0 = 0$  can be used. This samples  $w$  only approximately.

### Method based on inverse functions

#### A) Discrete distributions

Let's assume we want to sample integers  $k$ , where  $1 \leq k \leq N$ , with probability  $P_k$ .

1. Construct the cumulative table of probabilities,  $F_k = F_{k-1} + P_k$ .
2. Sample  $r \in U[0, 1]$ , find unique  $k$  so that  $F_{k-1} < r < F_k$ . Repeat step 2 as many times as needed.

#### B) Continuous distributions

This is sometimes called the *mapping method*.

1. Calculate the cumulative function of  $w(x)$

$$F(x) = \int_{-\infty}^x dx' w(x') \quad (21)$$

either analytically or numerically.

2. Sample  $r \in U[0, 1]$ , solve  $x$  from  $F(x) = r$ ; the solutions  $x$  sample  $w(x)$ .

Solving  $x$  from  $F(x) = r$  can be made quite fast by tabulating  $F(x)$ , but it's approximate, since the values  $x$  are picked from a limited set. A root-finding routine can solve  $x$  accurately.

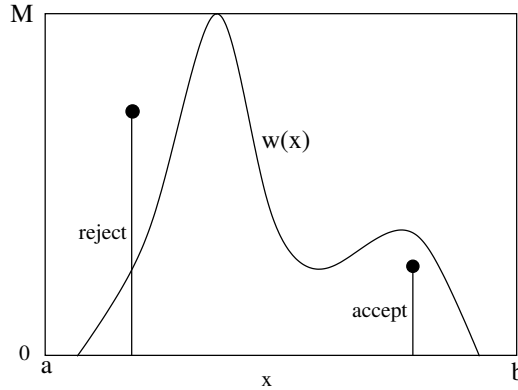


Figure 1: Illustration of the rejection method.

### Rejection method<sup>7</sup>

Also known as the hit and miss method, or the acceptance–rejection method. We saw that using inverse function you need to solve  $x$  from  $F(x) = r$ . If one solution takes 100 ms, solving  $10^8$  values takes 16 minutes – just to get the random numbers. Let's try something faster. This is essentially an application of the stone-throwing idea used earlier to compute  $\pi$ .

#### Special Case

Let's first assume we know that the distribution is limited from above,  $w(x) < M$ ,  $x \in [a, b]$ . A sequence of random numbers that sample  $w$  can be generated as follows:

1. Draw  $r_1 \in U[a, b]$  and  $r_2 \in U[0, M]$   
this picks a random point inside the box around  $w(x)$ , see Fig. 1
2. If  $w(r_1) \geq r_2$ , accept  $x = r_1$  as the desired random number, else discard both  $r_1$  and  $r_2$ . Go to 1.

This avoids solving  $x$  from  $F(x) = r$ , in the expense of throwing out some tries. But why does this work? Take a look at the identity

$$\begin{aligned} w(x) &= \int_0^M dr_2 \theta(w(x) - r_2) \\ &= \int_a^b dr_1 \int_0^M dr_2 \delta(x - r_1) \theta(w(r_1) - r_2) . \end{aligned} \quad (22)$$

The first equality states the fact that integrating the step function  $\theta$  (which is 1 if  $r_2 < w(x)$ ) to  $w(x)$  gives  $w(x)$ ;  $M$  is there just to make sure we cover the full range of values. See Fig. 2. The second line uses a Dirac delta to put *another* random variable to the argument. Apparently,

---

<sup>7</sup>John von Neumann in the late 1950's

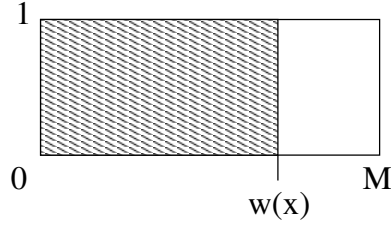


Figure 2: The shaded area is  $w(x)$ .

the algorithm integrates Eq. (22) using MC integration. Notice that we don't solve  $x$  from  $w(x) = r_2$ , thanks to the Dirac delta. Piece by piece, the identity as an algorithm is

$$w(x) = \underbrace{\int_a^b dr_1}_{\text{sample } r_1 \in U[a,b]} \underbrace{\int_0^M dr_2}_{\text{sample } r_2 \in U[0,M]} \underbrace{\delta(x - r_1)}_{\text{suggest } r_1 \text{ as } x} \underbrace{\theta(w(r_1) - r_2)}_{\text{accept, if } r_2 < w(r_1)} . \quad (23)$$

#### General Case

Sometimes we don't know  $M$  and don't want to use  $a$  and  $b$  either. Then we could sample  $r_1$  from some other, yet unspecified, PDF  $g(r_1)$  and find a condition when to accept this  $r_1$  as  $x$ . Copying the ideas in the special case,

$$\begin{aligned} g(x)h(x) &= g(x) \int_0^\infty dr_2 \theta(h(x) - r_2) \\ &= \int_0^\infty dr_1 g(r_1) \int_0^\infty dr_2 \delta(x - r_1) \theta(h(r_1) - r_2) , \end{aligned} \quad (24)$$

so if  $h(x) = w(x)/g(x)$  the integral would equal  $w(x)$ . The step function makes the integrand vanish for  $r_2 > \max[h(r_1)]$ , so if we could make  $h(r_1) \leq 1$  as a probability, then  $r_2 \leq 1$  and we could sample  $r_2 \in U[0, 1]$ . This can be achieved by an extra factor  $c$ : Define  $h(x) = cw(x)/g(x)$ , and

$$\begin{aligned} w(x) &= \frac{1}{c} h(x) g(x) \\ &= \frac{1}{c} \int_0^\infty dr_1 g(r_1) \int_0^1 dr_2 \delta(x - r_1) \theta(h(r_1) - r_2) . \end{aligned} \quad (25)$$

We are almost done, all we need is to find *some*  $c$  that makes  $h(x) \leq 1$ . If  $\max(h) < 1$ , then sampling  $r_2 \in U[0, 1]$  would waste some time trying to pick useless numbers between  $\max(h)$  and 1. The optimal choice is clearly

$$\max(h) = 1 , \quad (26)$$

which gives  $c = [\max(w/g)]^{-1} = \min(g/w)$ . Now we are ready to write down the algorithm:

1. Evaluate

$$c = \min \left( \frac{g}{w} \right) \quad (27)$$

2. Draw  $r_1 \in U[0, 1]$  and  $r_2$  from PDF  $g(x)$ .

3. If

$$c \frac{w(r_1)}{g(r_1)} \geq r_2 , \quad (28)$$

then accept  $x = r_1$  as the desired random number, else discard both  $r_1$  and  $r_2$ . Go to 2.

A trivial case would be  $g(x) = w(x)$ , which would mean that we already know how to sample  $w(x)$ . Then  $c = 1$  and all  $r_1$  would be accepted ( $1 \geq r_2$  is always valid): we say that the *acceptance ratio* is 1 in that case. If  $c$  is small, that is, in some region  $g(x) \ll w(x)$ , then much more trial  $r_1$ 's would be rejected and the algorithm would be ineffective. This problem is known as *under-sampling*, and it can even turn the code useless. In layman's terms, if one is nearly overlooking some region where  $w(x)$  is large, then  $w(x)$  is under-sampled. The function  $g(x)$  acts as an importance sampling function, and picking a bad one can be disastrous.

### 3.4.1 Sampling the standard normal distribution

The standard normal distribution  $Normal(x)$  is a Gaussian with mean zero and variance one,

$$Normal(x) = \frac{1}{\sqrt{2\pi}} e^{-x^2/2}. \quad (29)$$

This PDF is of special importance in MC, so we give few ways to sample random numbers  $x$  from it. A generalization to arbitrary mean and variance is easy. If you want to sample

$$Normal(y, \mu, \sigma) = \frac{1}{\sqrt{2\pi}\sigma} e^{-(y-\mu)^2/(2\sigma^2)}, \quad (30)$$

you obviously need to spread the PDF and shift it's mean to  $\mu$ :  $y = \sigma x + \mu$ . Sampling from a multivariate Gaussian is beyond the present scope.

- **Crude algorithm**

Draw  $N$  random numbers  $r_i \in U[0, 1]$  and calculate the sum

$$x = \sqrt{\frac{12}{N}} \sum_{i=1}^N \left(r_i - \frac{1}{2}\right) \quad (31)$$

As  $N$  increases this approaches the standard normal distribution, a consequence of the *Central Limit Theorem* (proved later). This gives a rather good  $Normal(x)$  already with small  $N$ . Values  $N = 6$  or  $N = 12$  can be quite useful, if only a crude normal distribution is sufficient. You can't get the large- $x$  tails right, though.

- **Box-Müller algorithm I**<sup>8</sup>

1. Draw  $r_1$  and  $r_2 \in U[0, 1]$
2. Evaluate  $\theta = 2\pi r_1$  and  $R = \sqrt{-2 \ln r_2}$
3.  $(x_1, x_2) = (R \cos(\theta), R \sin(\theta))$
4. Go to step 1.

You get *two* random numbers ( $x_1$  and  $x_2$ ) per round. The downside is that the four special functions are slow, so use this algorithm only if you need accurate values  $x$  from  $Normal(x)$ .

---

<sup>8</sup>G. Box and M. Müller, Ann. Math. Stat. 38 (1958) 610

- **Box-Müller algorithm II**

A modified version of the previous algorithm, uses the rejection method to avoid trig. functions.

1. Draw  $r_1$  and  $r_2 \in U[0, 1]$
2. Make  $R_1 = 2r_1 - 1$  and  $R_2 = 2r_2 - 1$ , they sample  $\in U[-1, 1]$
3. If  $R = R_1^2 + R_2^2 > 1$  reject the pair and go to step 1
4. Result:

$$(x_1, x_2) = \sqrt{\frac{-2 \ln R}{R}} (R_1, R_2) \quad (32)$$

5. Go to step 1

Again, we get two random samples per round. The acceptance ratio of this algorithm is  $\pi/4$ , the ratio of the area of a unit circle to the area of the 2-by-2 box around it.

- **Fernandéz–Rivero algorithm<sup>9</sup>**

A very fast algorithm. Highly recommended! This is actually a small Maxwell-Boltzmann gas simulation, with fictitious, energy-conserving collisions, carried out by the velocity exchange in step 5. The velocities become very fast normally distributed, and gives as results in step 8.

1. Initialise  $v_i = 1, i = 1, \dots, N$  ( $N$  is about 1024) and set  $j = 0$
2. Draw K (about 16) values  $\theta_k \in U[0, 2\pi]$ ; compute  $c_k = \cos(\theta_k)$  and  $s_k = \sin(\theta_k)$ .
3. Set  $j = (j + 1) \bmod N$ , draw  $i \in IU[0, N - 1]$  so that  $i \neq j$
4. Draw  $k \in IU[0, K - 1]$
5. Set  $\text{tmp} = c_k v_i + s_k v_j$  and  $v_j = -s_k v_i + c_k v_j$
6. Set  $v_i = \text{tmp}$
7. If still in thermalization go to step 3
8. Result:  $v_i$  and  $v_j$
9. Go to 3

Here  $IU[0, N]$  means random integer between 0 and  $N$ .

The Box-Müller and Fernandéz–Rivero algorithms are accurate also at the tail of  $Normal(x)$ , while the crude algorithm clearly can get only as far from the origin as  $N$  steps allow.

---

<sup>9</sup>J. F. Fernandéz and J. Rivero, Comp. in Phys. 10 (1996) 83-88.

### Proof of the Box-Müller algorithm

The algorithm is based on a common trick to integrate a Gaussian: the product of two Gaussians with Cartesian coordinates  $x$  and  $y$  can be most easily integrated in circular coordinates using

$$x^2 + y^2 = r^2 . \quad (33)$$

We start the proof from the end. The Box-Müller algorithm calculates the integral

$$\begin{aligned} & \int_0^1 dr_1 \int_0^1 dr_2 \delta(x_1 - \sqrt{-2 \ln r_1} \cos(2\pi r_2)) \delta(x_2 - \sqrt{-2 \ln r_1} \sin(2\pi r_2)) \\ &= \int_0^1 dr_1 \int_0^1 dr_2 \delta(r_1 - e^{-(x_1+x_2)^2/2}) \delta(r_2 - \frac{1}{2\pi} \arctan(\frac{x_2}{x_1})) \left| \frac{\partial(r_1, r_2)}{\partial(x_1, x_2)} \right| \\ &= \frac{1}{2\pi} e^{-(x_1^2+x_2^2)/2} = \frac{1}{\sqrt{2\pi}} e^{-x_1^2/2} \frac{1}{\sqrt{2\pi}} e^{-x_2^2/2} = \text{Normal}(x_1) \text{Normal}(x_2) . \end{aligned}$$

The key point is the Jacobian of the transformation, which is exactly the desired product of the two Gaussians. These algorithms are always *mappings* from one or more random numbers  $\in U[0, 1]$  to another distribution. The last line shows that both  $x_1$  and  $x_2$  are sampling the standard normal distribution, while the algorithm computes lhs integral using MC integration.

### Principle of the Fernández-Rivero algorithm

This algorithm has it's roots in physics, and it is apparently a simulation. As a first step, take a look at how exponentially distributed random numbers can be generated. Consider a collection of  $N$  classical particles, that can exchange energy with each other but not with the rest of the world. From statistical physics we know that this ensemble will equilibrate to a state, where the energies are distributed according to the Gibbs law,

$$P(E) \sim e^{-E/T} , \quad (34)$$

where  $T$  is the temperature. Let the  $N$ -dimensional table  $E$  hold the energies of the particles. Initialise this table to unity,  $E_i = 1$  for  $1 \leq i \leq N$ . Next introduce an interaction between the particles in such a way, that the total energy is conserved. Let the particles interact pairwise, pick two particles  $i$  and  $j$  at random. To conserve the total energy the sum  $E_i + E_j$  must be kept constant, mark  $S = E_i + E_j$ . Next let the interaction to transfer a random amount of energy from particle  $i$  to particle  $j$ . The algorithm is

1. Initialise  $E_i = 1$  for  $1 \leq i \leq N$  and set  $j = 0$
2. Set  $j = (j + 1) \bmod N$  and draw an integer  $i \neq j$  from  $i \in \text{int}[N] U[0, 1]$
3. Set  $S = E_i + E_j$
4. Draw  $r \in U[0, 1]$ , set  $E_i = rE_i$  and after that set  $E_j = S - E_i$

5. If still in thermalization go to step 2
6. Result: two random numbers  $E_i$  and  $E_j$
7. Go to step 2

According to Fernández and Rivero,  $N \sim 1000$  is enough for generations of about  $10^{15}$  exponentially distributed random numbers. The energies have to be thermalised before they become Gibbs distributed, so one has to run the algorithm about  $10 \times N$  times to let the dust settle. After that, each round produces two independent random numbers,  $E_i$  and  $E_j$ , distributed as  $w(E) = e^{-E}$ . The modulo operation can be done fast with logical `and` if  $N$  is a power of 2:  $N = 1024$  is just fine.

Normal distributed random numbers can be generated in a related fashion. From statistical mechanics we know that in equilibrium velocities have the Maxwell distribution, which is a Gaussian. This time we keep track of the velocities of the particles, and to conserve energy their squares must be conserved. Let the velocities of the interacting particles be  $v_i$  and  $v_j$ . Think of them as components of a two-dimensional vector, whose length squared  $v_i^2 + v_j^2$  must be conserved in the interaction. Thus the interaction should rotate the vector; To speed up the rotation one can compute a finite set of rotation matrices beforehand. Although plausible, the actual proof that the algorithm does what it promises is beyond the scope of these lecture notes

### 3.5 Central Limit Theorem

The Central Limit Theorem states that

*Given a distribution with a mean  $\mu$  and variance  $\sigma^2$ , the sampling distribution of the mean approaches a normal distribution with a mean  $\mu$  and a variance  $\sigma^2/N$  as the sample size  $N$  increases.*

This is almost magic: taking the mean value of variables  $x$  with almost *any* probability distribution function (PDF)  $f(x)$ ,

$$z = \frac{x_1 + x_2 + \dots + x_N}{N} \quad (35)$$

the sampling distribution  $g(z)$  of the mean value approaches a normal distribution! Even more amazingly, this seems to happen already for a rather small  $N$ .

What is exactly  $N$  and a "sampling distribution"? In principle, the number of samples  $x_i$  is infinite, but we are not going to add them all up to get the mean. So we *sample the mean* by taking a finite size specimen (of size  $N$ ) and gather the mean values of those  $N$  points to get an idea of the true mean value.

#### Proof:

We wish to find  $g(z)$  for large  $N$ . The PDF of  $N$  arbitrary values  $x_i$  is the product of the individual probabilities, you just add the constraint that their mean is  $z$  – a job for the Dirac delta –

$$g(z) = \int dx_1 dx_2 \dots dx_N f(x_1) f(x_2) \dots f(x_N) \delta\left(z - \frac{x_1 + x_2 + \dots + x_N}{N}\right). \quad (36)$$

Write the Dirac delta in integral form,

$$\delta(x) = \frac{1}{2\pi} \int dk e^{ikx}, \quad (37)$$

to get

$$g(z) = \frac{1}{2\pi} \int dk dx_1 dx_2 \dots dx_N f(x_1) f(x_2) \dots f(x_N) \quad (38)$$

$$\times \exp\left[ik\left(z - \frac{x_1 + x_2 + \dots + x_N}{N}\right)\right]$$

$$\dots \times \left[ \int dx_N f(x_N) \exp\left[ik\left(\frac{z - x_N}{N}\right)\right] \right]$$

$$= \frac{1}{2\pi} \int dk \left[ \int dx f(x) \exp\left[ik\left(\frac{z - x}{N}\right)\right] \right]^N. \quad (39)$$

For large  $N$  the value of  $(x_1 + x_2 + \dots + x_N)/N$  is going to be close to  $\mu$ , so it's a good idea to add and subtract it:

$$g(z) = \frac{1}{2\pi} \int dk \left[ \int dx f(x) \exp \left[ ik \left( \frac{z - \mu + \mu - x}{N} \right) \right] \right]^N \quad (40)$$

$$= \frac{1}{2\pi} \int dk e^{ik(z-\mu)} \underbrace{\left[ \int dx f(x) \exp \left[ ik \left( \frac{\mu - x}{N} \right) \right] \right]}_I^N. \quad (41)$$

The integral in the brackets can be expanded in powers of the small deviation  $\mu - x$ ,

$$I = \int dx f(x) \left[ 1 + \frac{ik(\mu - x)}{N} - \frac{k^2(\mu - x)^2}{2N^2} + \dots \right] \quad (42)$$

$$= 1 + ik \frac{\mu - \int dx f(x)x}{N} - \frac{k^2}{2N^2} \int dx f(x)(\mu - x)^2 + \dots \quad (43)$$

$$= 1 - \frac{k^2 \sigma^2}{2N^2} + \dots, \quad (44)$$

where the first order term (red) is zero by definition (see Eq. (48) below). For large  $N$ ,

$$g(z) \approx \frac{1}{2\pi} \int dk e^{ik(z-\mu)} \left[ 1 - \frac{k^2 \sigma^2}{2N^2} \right]^N = \frac{1}{2\pi} \int dk e^{ik(z-\mu)} \left[ 1 - \frac{x}{N} \right]^N, \quad x := \frac{k^2}{2/(\sigma/\sqrt{N})^2}, \quad (45)$$

and since

$$\left[ 1 - \frac{x}{N} \right]^N \approx e^{-x}, \text{ for large } N, \quad (46)$$

the integral is a Fourier transform of a Gaussian, and we get the result

**CENTRAL LIMIT THEOREM**

$$z := \frac{x_1 + x_2 + \dots + x_N}{N}$$

$$g(z) \approx \frac{1}{\sqrt{2\pi} \left[ \sigma/\sqrt{N} \right]} e^{-\frac{(z-\mu)^2}{2[\sigma/\sqrt{N}]^2}} \quad \text{distribution of } z.$$

(47)

In words: *with large  $N$ , the distribution of mean values is a normal distribution with variance  $\sigma/\sqrt{N}$ .* This is one way to see why MC results converge as  $\sim 1/\sqrt{N}$ . What is remarkable in this result is that the probability distribution  $f(x)$  of values  $x$  is present only as the two

momenta,

$$\mu = \int dx f(x)x \quad (48)$$

$$\sigma^2 = \int dx f(x)(x - \mu)^2 . \quad (49)$$

Figure 3 illustrates how fast the distribution of mean approaches the normal distribution. The underlying distribution  $f(x)$  is box-shaped, 1 between -0.5 and 0.5, zero elsewhere (that's  $x \in U[-0.5, 0.5]$ ). The average of two values,  $z = (x_1 + x_2)/2$ , is limited to  $-1 \leq z \leq 1$ , so the tails of the normal distribution are beyond reach. Still, the triangular shape already resembles  $Normal(z)$ . The average of 12 numbers is so close to  $Normal(z)$  that it's hard to see the difference. Still, the values are limited to  $-6 \leq z \leq 6$ , so the tails are wrong – this tail error is common to all distributions  $f(x)$  that have a limited domain.

### Cauchy distribution

Not all PDF's satisfy the Central Limit Theorem. As an example, consider the (standard) Cauchy distribution

$$w(x) = \frac{1}{\pi(1 + x^2)} , \quad (50)$$

which looks a bit like the standard normal distribution (see Fig. (4)). It's a PDF,

$$\int_{-\infty}^{\infty} w(x) = 1 . \quad (51)$$

However, the mean value

$$\mu = \int_{-\infty}^{\infty} xw(x) , \quad (52)$$

is a problem. The argument is antisymmetric, so contributions from  $x < 0$  and  $x > 0$  cancel exactly giving  $\mu = 0$ . However, the separate integrals for  $x < 0$  and  $x > 0$  diverge. If one samples  $N$  points  $x_1, \dots, x_N$  from the Cauchy distribution and computes their average, it cannot converge to any value because the points are not chosen symmetrically about  $x = 0$ : *the Cauchy distribution has no statistical mean*. The variance is even worse,

$$\int_{-\infty}^{\infty} x^2 w(x) = \infty . \quad (53)$$

The non-existence of these momenta pulls the carpet from under the central limit theorem. Even though you can sample the Cauchy distribution, and – with a great deal of wishful thinking – calculate the mean over a set of points, still no matter how many data points you collect, your statistical estimate for the mean is as "accurate" as with just one point!

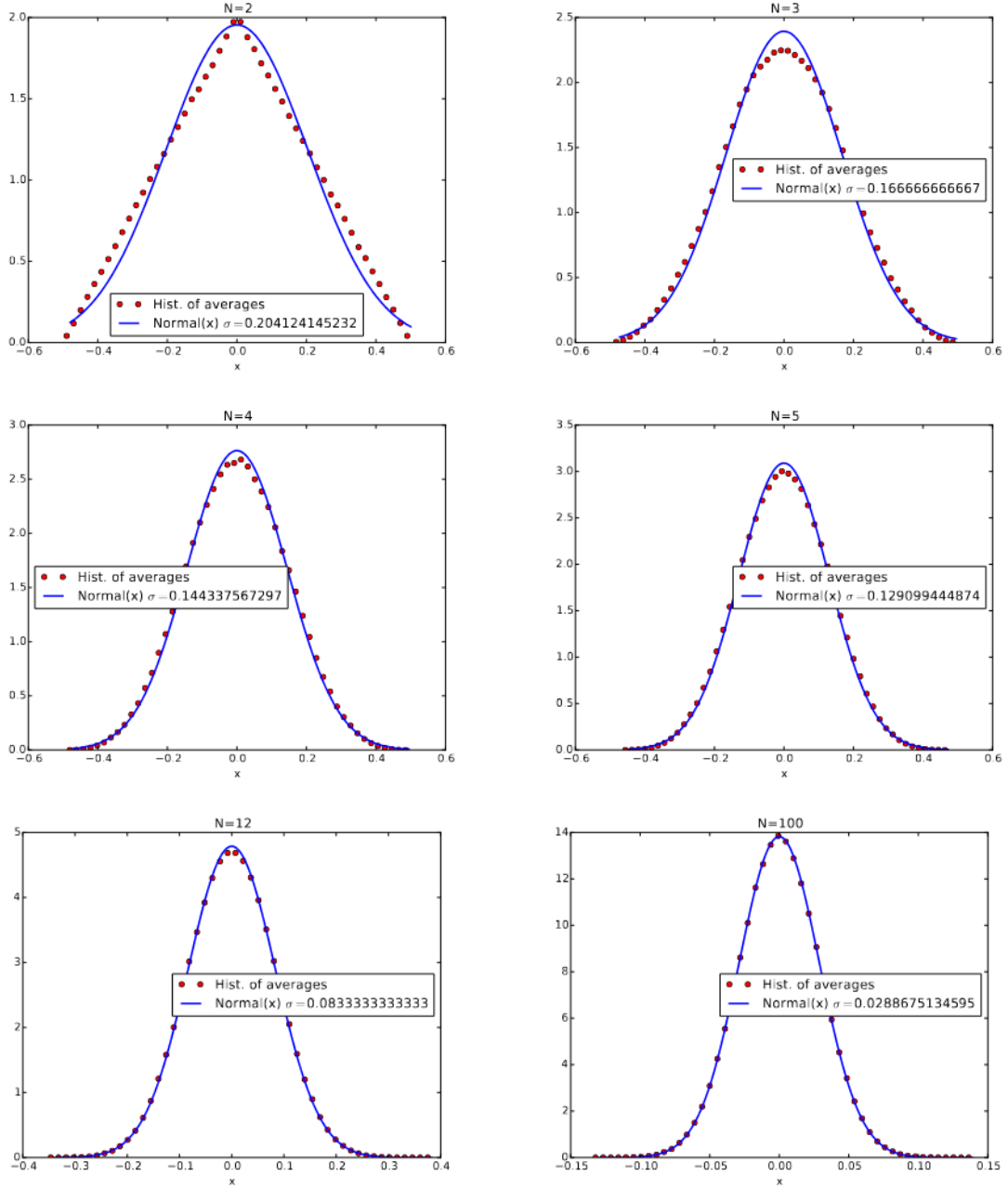


Figure 3: The distribution of the mean value of  $N$  random numbers  $\in U[-0.5, 0.5]$  for  $N = 2, 3, 4, 5, 12, 100$  (Eq. (31)) (red markers), compared with the normal distribution (solid blue line). The input distribution has variance  $\sigma_0^2 = 1/12$ , and the plotted normal distribution variance is  $\sigma^2 = \sigma_0^2/N$ .

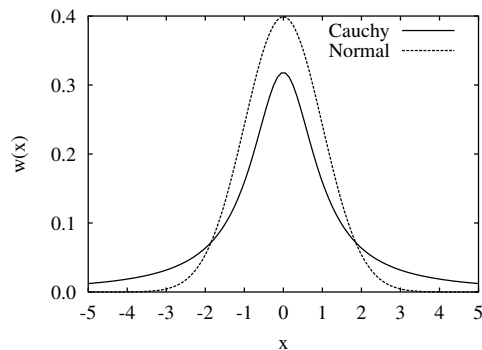


Figure 4: The standard Cauchy probability distribution compared with the standard normal distribution.

One often uses the Cauchy distribution as a test distribution to see how sensitive a method is to contributions from tails. Off-topic, the distribution of the ratio of two Gaussian-distributed random variables with  $\mu = 0$  is a Cauchy distribution, hence another name *normal ratio distribution*.

### 3.6 Detailed balance condition

The detailed balance condition is a sufficient, but not necessary, condition that the system reaches the equilibrium.

With the equilibrium I mean the correct equilibrium, it is the one where the states appear with correct weights  $\pi(S)$ ; There are numerous ways to reach a wrong “equilibrium”! To put it another way, we want to make certain that after repeating moves according to some transition probability  $P(S \rightarrow S')$  the asymptotic distribution of states  $S$  is  $\pi(S)$ . This is the usual starting premise: The weights of the states  $\pi(S)$  are known and the task is to construct the transition probability  $P(S \rightarrow S')$  that will lead to equilibrium. The detailed balance condition gives the first guideline to follow. What makes it so pleasing, is that *any* transition probability that satisfies the detailed balance condition with the weights  $\pi(S)$  is acceptable!

The detailed balance condition, known also as *microscopic reversibility*, states that

Detailed balance condition

$$P(S \rightarrow S')\pi(S) = P(S' \rightarrow S)\pi(S') . \quad (54)$$

where  $\pi(S)$  is the weight of state  $S$ . This equality assures that there is no net traffic between the states  $S$  and  $S'$ , but it does more than that.<sup>10</sup> The origin of the detailed balance condition can be traced to the so-called master equation, which states how the probability of a state  $\pi(S)$  varies as a function of the simulation time (treated as continuous) :

$$\frac{d\pi(S')}{dt} = \sum_S P(S \rightarrow S')\pi(S) - \sum_S P(S' \rightarrow S)\pi(S') , \quad (55)$$

where the terms sum the changes of getting to  $S'$  minus changes of getting out of  $S'$ . Perhaps the easiest way to interpret the terms in the sums is to think of them as “probability of being in the initial state times the transition rate from the initial to the final state”. The master equations is a continuity equation for the probability. It’s also characteristic to Markov processes, because the future depends only on the present state, not on the earlier history.

Now the connection between the detailed balance condition and the equilibrium of the system becomes more transparent. In equilibrium there are no net changes in probabilities,  $\frac{d\pi(S')}{dt} = 0$ , and the master equation reduces to

$$\sum_S P(S \rightarrow S')\pi(S) = \sum_S P(S' \rightarrow S)\pi(S') . \quad (56)$$

This has an infinite number of solutions, but one is exceptionally simple: Obviously this equality is valid if the terms in the sums are equal, term by term,  $P(S \rightarrow S')\pi(S) = P(S' \rightarrow S)\pi(S')$ . This is the detailed balance condition (54) - the two sums are in balance term by term:

---

<sup>10</sup>A bad simulation can get permanently stuck to state  $S$ , so there is definitely no net traffic between any states – but usually at finite temperatures this is not the *correct* equilibrium! Another form of false equilibria are *limit cycles*, which also result from irreversible changes made in a poor simulation.

*Balance every process between a pair of states,  
Transition  $S \rightarrow S'$  is in balance with the reverse transition  $S' \rightarrow S$ .*

Of course the two sums in (56) can give the same value even though the terms are not the same term by term: The detailed balance condition is not the *only* solution that is compatible with the equilibrium condition. With some imagination you may add a kind of running weight to the terms, so that once the sum is done the extras cancel. In short, Monte Carlo doesn't *need* detailed balance, but it's simple and safe.

Finally, to wrap up the discussion about detailed balance we need to show that after a repeated application of transitions with probability  $P(S \rightarrow S')$ , that satisfy the detailed balance condition, the asymptotical distribution is  $\pi(S')$ . We set out to prove that

$$\pi(S') = \sum_S \pi(S) P(S \rightarrow S') . \quad (57)$$

In matrix notation this reads  $\pi = \pi P$ , which states that  $\pi$  is the (left) eigenvector of transition matrix  $P$  with eigenvalue 1.

Proof<sup>11</sup>:

$$\begin{aligned} \sum_S \pi(S) P(S \rightarrow S') &= \sum_S \pi(S') P(S' \rightarrow S) \\ &= \pi(S') \sum_S P(S' \rightarrow S) = \pi(S') . \end{aligned} \quad (58)$$

The first equality follows from detailed balance, the last one from the fact that  $P$  is a *stochastic matrix*. This means that the sum of row elements of  $P$  is unity and all elements are non-negative: the probability that state  $S'$  is followed by *some* state  $S$  (includes the case where  $S'$  remains  $S'$ ) is one.

**Example: Transitions in a two-state system** Let the weights in a two-state system be  $\pi(1) = 5$  and  $\pi(2) = 3$ . The detailed balance conditions says

$$\frac{P(1 \rightarrow 2)}{P(2 \rightarrow 1)} = \frac{\pi(2)}{\pi(1)} = \frac{3}{5} . \quad (59)$$

Mark  $P_{12} = P(1 \rightarrow 2)$  and  $P_{21} = P(2 \rightarrow 1)$ . This fixes the ratio of the two off-diagonal elements of  $P$ , and using the fact that this is a stochastic matrix we get the missing elements:

$$P = \begin{pmatrix} P_{11} & P_{12} \\ P_{21} & P_{22} \end{pmatrix} = \begin{pmatrix} 1 - 3x & 3x \\ 5x & 1 - 5x \end{pmatrix} . \quad (60)$$

---

<sup>11</sup>This is not a rigorous proof, to give credit to the statement that this is asymptotically valid one would have to discuss the simulation time  $t$ .

Any  $x$  will do, as long as the elements are non-negative. A neat choice would be  $x = 1/5$ ,

$$P = \begin{pmatrix} 2/5 & 3/5 \\ 1 & 0 \end{pmatrix}. \quad (61)$$

First test that the distribution  $\pi$  is a left eigenvector with eigenvalue 1. Indeed,

$$\pi P = (5 \ 3) \begin{pmatrix} 2/5 & 3/5 \\ 1 & 0 \end{pmatrix} = (5 \ 3) = \pi. \quad (62)$$

Next, successive applications of  $P$  give

$$P^{10} \approx \frac{1}{8} \begin{pmatrix} 5.01614 & 2.978186 \\ 4.96977 & 3.03023 \end{pmatrix} \quad (63)$$

$$P^{20} \approx \frac{1}{8} \begin{pmatrix} 5.00011 & 2.99989 \\ 4.99982 & 3.00018 \end{pmatrix}, \quad (64)$$

so it really seems that the rows go asymptotically to  $\pi$  – the factor  $1/8$  is the normalization of  $\pi$ .

Another choice is interesting:  $x = 1/8$ . Then

$$P = \begin{pmatrix} 5/8 & 3/8 \\ 5/8 & 3/8 \end{pmatrix} = \frac{1}{8} \begin{pmatrix} 5 & 3 \\ 5 & 3 \end{pmatrix}, \quad (65)$$

and  $P^2 = P$ , meaning the matrix is *idempotent*, and shows the eigenvector  $\pi$  as rows.

## 4 Markov Chain Monte Carlo

### 4.1 Metropolis–Hastings algorithm

In year 1953 Metropolis *et al.*<sup>12</sup> published an algorithm, which can be used to sample an almost arbitrary, multidimensional distribution  $\pi(S)$ . Here  $S$  can be, for example, described by a set of particle coordinates  $\mathbf{R} = \{\mathbf{r}_1, \mathbf{r}_2, \dots, \mathbf{r}_N\}$  or a set of occupation numbers  $\{n_1, n_2, \dots\}$  of quantum mechanical states 1, 2, .... The algorithm generates the set of random numbers by means of a random walk. The sequence of points gone through is an example of a **Markov chain**, after the russian mathematician A. A. Markov (1856-1922). A Markov chain is defined as a process containing a finite number of states for which the probability of being in each state in the future depends only on the present state of the process.<sup>13</sup>

---

<sup>12</sup>N. Metropolis, N. Rosenbluth, A. W. Rosenbluth, A. H. Teller and E. Teller, *Equation of state calculations by fast computing machines*, J. Chem. Phys. **21** (1953) 1087-1092. An earlier form was published by Metropolis and Ulam 1949. Allegedly the algorithm was invented at a Los Alamos dinner party.

<sup>13</sup>Jeremy Kun's blog: *Markov Chain Monte Carlo Without all the B...s....*

It was Hastings<sup>14</sup> who generalised the algorithm to account for nonsymmetric transfer matrices, and showed how the asymmetry in proposals is compensated in the acceptance probabilities.

### The original Metropolis algorithm

Consider two states of the system,  $S$  and  $S'$ . In its original form the Metropolis algorithm samples the Boltzmann distribution, where the weight of the state  $S$  depends on its energy  $E(S)$  according to

$$\pi(S) = \frac{1}{Z} e^{-E(S)/T} . \quad k_B := 1 . \quad (66)$$

Metropolis *et al.* chose the acceptance probability from  $S$  to  $S'$  to be

$$A(S \rightarrow S') = \begin{cases} e^{-\Delta E/T}, & \text{if } \Delta E = E(S') - E(S) > 0 \quad \text{"uphill"} \\ 1, & \text{else} \quad \text{"downhill"} \end{cases} \quad (67)$$

Usually this is written in equivalently as

$$A(S \rightarrow S') = \min [1, e^{-\Delta E/T}] , \quad (68)$$

where *min* means "smaller of the two arguments". The detailed balance condition boils down to a very simple relation,

$$\frac{P(S \rightarrow S')}{P(S' \rightarrow S)} = \frac{T(S \rightarrow S')A(S \rightarrow S')}{T(S' \rightarrow S)A(S' \rightarrow S)} = \frac{\pi(S')}{\pi(S)} = e^{-\Delta E/T} . \quad (69)$$

The first two equalities go also under the name *Metropolis–Hastings* due to the explicit transfer matrix in the formula. The original Metropolis algorithm assumes a symmetric transfer matrix,  $T(S \rightarrow S') = T(S' \rightarrow S)$ , so the  $T$ 's cancel out from Eq. (69) and we might as well have written

$$P(S \rightarrow S') = \min [1, e^{-\Delta E/T}] . \quad (70)$$

If we are going uphill ( $E(S') > E(S)$ ), then

$$\frac{P(S \rightarrow S')}{P(S' \rightarrow S)} = \frac{e^{[E(S)-E(S')]/T}}{1} = e^{-\Delta E/T} , \quad (71)$$

and if we are going downhill then

$$\frac{P(S \rightarrow S')}{P(S' \rightarrow S)} = \frac{1}{e^{[E(S')-E(S)]/T}} = e^{-\Delta E/T} , \quad (72)$$

---

<sup>14</sup>W.K. Hastings, *Monte Carlo sampling methods using Markov chains and their applications*, Biometrika 57, 97-109 (1970). His PhD student Peskun derived the conditions for efficient sampling using Markov chains (Peskun ordering).

so the detailed balance condition is satisfied and this  $P(S \rightarrow S')$  leads asymptotically to the Boltzmann distribution.

Pay attention to the fact that in the detailed balance condition (69) the ratio does not involve the partition function  $Z$ , which is the normalization factor of the Boltzmann distribution. Thus we can construct the transition matrix without ever bothering to compute  $Z$ . A similar situation occurs in quantum Monte Carlo: There is no need to normalize the wave function explicitly. Great relief!

The algorithm is

- If  $e^{-\Delta E/T} > 1$  then  $P(S \rightarrow S') = 1$  and the move is always accepted.
- If  $e^{-\Delta E/T} < 1$  interpret it as a probability and compare it with a random number  $r \in U[0, 1]$ ; accept it if  $r < e^{-\Delta E/T}$ .

This means

1. Propose a move  $S \rightarrow S'$
2. If the energy decreases, accept the move: always go downhill
3. If the energy increases, accept the move with probability  $e^{-\Delta E/T}$ : go uphill if the temperature allows you. Go to 1.

### Off-lattice Metropolis algorithm for almost any $\pi(\mathbf{R})$

This is exactly what variational Monte Carlo is doing, just replace  $\pi(\mathbf{R})$  with the square of the trial wave function,  $|\varphi_T(\mathbf{R})|^2$ . Start with the "walker" at point  $\mathbf{R}$ . This represents one possible configuration or state of the system. Here is a Metropolis algorithm to sample the next point, and so on:

1. Pick randomly a trial point  $\mathbf{R}'$  from the neighbourhood of  $\mathbf{R}$ . You can choose, for example, a random point within some distance  $\delta$  of the original point.

2. calculate

$$ratio = \frac{\pi(\mathbf{R}')}{\pi(\mathbf{R})} \quad (73)$$

3. If  $ratio > 1$

accept  $\mathbf{R}'$  as the next point; set  $\mathbf{R} = \mathbf{R}'$  (move the walker)

else

Draw  $z \in U[0, 1]$ .

if  $ratio > z$

accept  $\mathbf{R}'$  as the next point

(in a program, set  $\mathbf{R} = \mathbf{R}'$ , because there is no need to store the old point).

else

reject  $\mathbf{R}'$ , the "next point" is the old point  $\mathbf{R}$ .

4. Go to 1.

Step 3 is the *Metropolis question*. A common mistake is to forget the last part of step 3 and not count rejected moves as old points. Obviously one must now and then use the same point more than once if the walker is in a region where  $\pi(\mathbf{R})$  is large to describe that the walker now and then refuses to step out of high-weight regions<sup>15</sup>

The free parameter  $\delta$  dictates the acceptance ratio and the effectiveness of sampling. The walker is supposed to move around the phase space where  $\pi(\mathbf{R})$  is nonzero within reasonable time. Hence there are two reasons why sampling can be ineffective:

- Walker tries to take *too long steps*; In a region with large  $\pi(\mathbf{R})$  most of the trial steps would be rejected.
- Walker tries to take *too short steps* and almost all of them are accepted.

In both cases the walker is not moving around as it should. A rule of thumb says that for most effective sampling **the acceptance ratio should be about 60 percent**.

---

<sup>15</sup>Random walkers are like drunkards; once the lost soul has landed in his favorite pub you may need more than one persuasion to make him leave for another, nice pub.

The other free parameter in the algorithm is the starting point of the walk. In principle it can be chosen freely, but it's better to start it from a point where  $\pi(\mathbf{R})$  is fairly large to make the walk *thermalize* (loose memory of its origin) faster.

The Metropolis algorithm can be used, for example, to evaluate expectation values

$$\langle f \rangle_w = \frac{\int d\mathbf{R} \pi(\mathbf{R}) f(\mathbf{R})}{\int d\mathbf{R} \pi(\mathbf{R})}. \quad (74)$$

One just takes the average value of  $f$  over the points produced by the random walk. The points in the random walk are not statistically independent, therefore the statistical error of the result is not given by Eq. (6).

### Example

Look again at the two-state system with weights  $\pi(1) = 5$  and  $\pi(2) = 3$ . Assume that the transfer matrix is symmetric; The Metropolis acceptance probability is the same as the transition probability,

$$P(S \rightarrow S') = A(S \rightarrow S') = \min \left[ 1, \frac{\pi(S')}{\pi(S)} \right]. \quad (75)$$

so the corresponding matrix is (don't use the above formula for  $S \rightarrow S'$ )

$$P = \begin{pmatrix} 2/5 & 3/5 \\ 1 & 0 \end{pmatrix}. \quad (76)$$

This happens to be the matrix from chosen in the previous example, the  $x = 1/5$  case of P given in Eq. (60).

### Example

One Markov chain generated by the stochastic matrix given above is shown in Fig. 5. It starts with state 1, moves to 2 with probability 3/5. Transition 2  $\rightarrow$  1 is always accepted (downhill). A change of state is always proposed, so the transfer matrix (proposal matrix) was

$$T = \begin{pmatrix} 0 & 1 \\ 1 & 0 \end{pmatrix}, \quad (77)$$

which is symmetric. The Metropolis choice of acceptances is the most effective, with

$$P(x = 1/5) = \begin{pmatrix} 2/5 & 3/5 \\ 1 & 0 \end{pmatrix}. \quad (78)$$

It's interesting to notice that earlier we found the idempotent matrix

$$P(x = 1/8) = \frac{1}{8} \begin{pmatrix} 5 & 3 \\ 5 & 3 \end{pmatrix}, \quad (79)$$

which shows the result immediately! How can Metropolis  $P(x = 1/5)$  beat this?

*The Metropolis acceptance is the most efficient in the sense that it moves between states most effectively, and the Markov chain converges fastest toward  $\pi$ .*

The choice  $1/8$  is less efficient if applied to a Markov chain, but yes, it shows the result immediately. Small stochastic system are often better solved as eigenvalue problems and not with Markov chains, but for large stochastic systems finding an eigenvalue solution may be a very slow process.

### Example

A three-state system has the stochastic matrix

$$P = \begin{pmatrix} 0.6 & 0.1 & 0.3 \\ 0.2 & 0.6 & 0.2 \\ 0.0 & 0.2 & 0.8 \end{pmatrix} \quad (80)$$

What is the underlying distribution? By random walk and counting the frequencies as in the previous example gives  $\pi = (0.2408, 0.4815, 0.8427)$  (normalized to 1), some three decimals have converged. In this case it's a lot faster to compute matrix powers,

$$P^{30} = \begin{pmatrix} 0.240771708282918 & 0.481543412582873 & 0.842700970860107 \\ 0.240771704899532 & 0.481543415038322 & 0.842700971788043 \\ 0.240771706755404 & 0.481543411654936 & 0.842700973315557 \end{pmatrix} \quad (81)$$

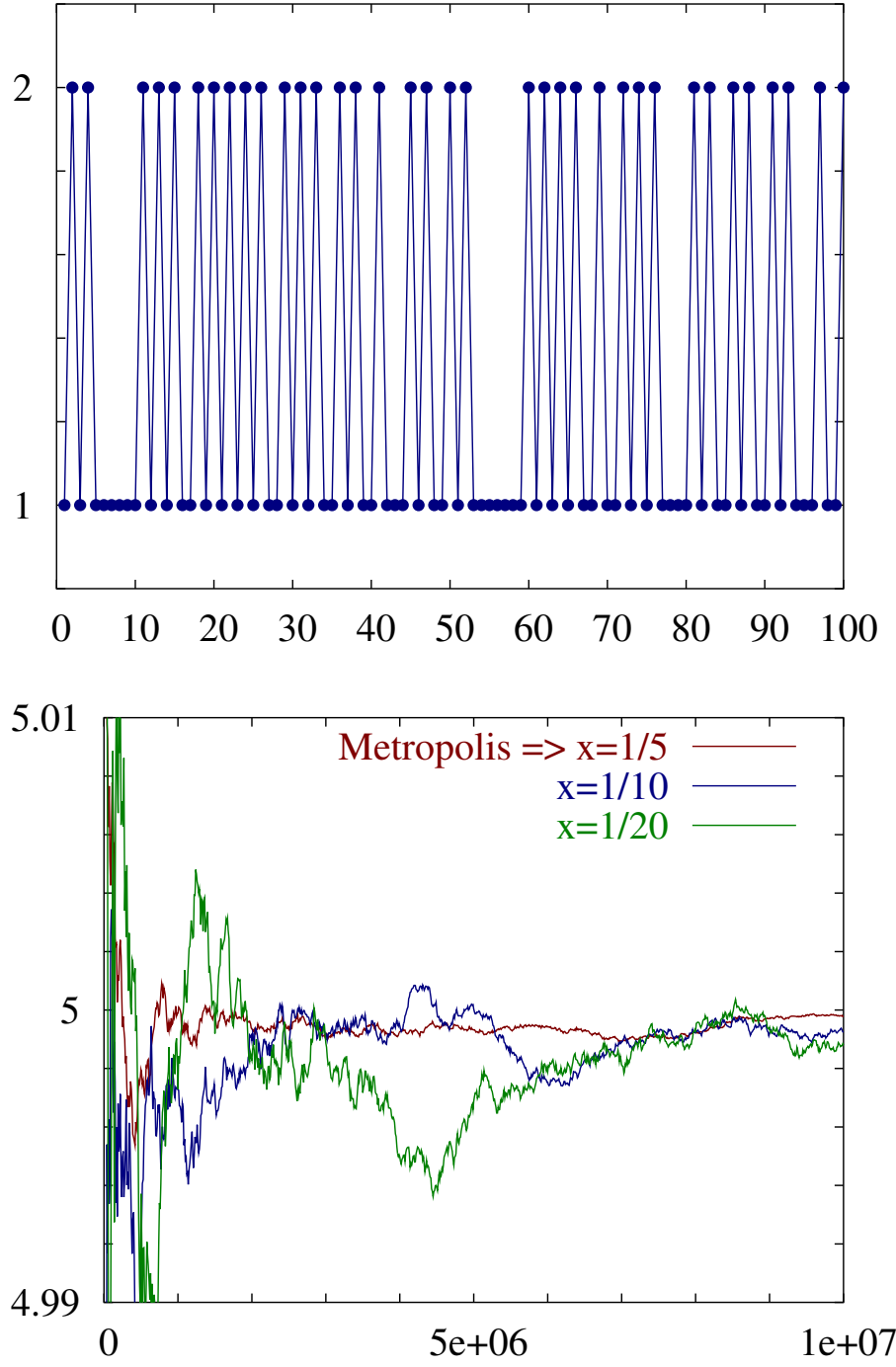


Figure 5: Upper figure: A Markov chain for the two-state system with  $\pi = (5, 3)$ , lines are quides to the eye. The frequencies states 1 and 2 occurred during the depicted simulation were 5.20 and 2.82, respectively. After  $10^8$  steps the frequencies were 5.00010832 and 2.99989176. Lower figure: The convergence toward  $\pi(2) = 5$  for three choices of  $x$  in equation (60) (three distinct transition matrices) gives a visual confirmation that the Metropolis matrix has smallest fluctuations.

## 5 Variational Monte Carlo

Eq. (74) can be readily applied to quantum many-body physics. The most straightforward application is the **variational Monte Carlo** (VMC), the simplest of **quantum Monte Carlo** (QMC) methods. If the method applies a Markov chain, then sometimes the name **Markov chain Monte Carlo** is also used.

Let  $\varphi_T(\mathbf{R})$  be any trial wave function,  $\mathbf{R} = (\mathbf{r}_1, \mathbf{r}_2, \dots, \mathbf{r}_N)$  is the set of  $d \times N$  coordinates of the  $N$  particles in the  $d$ -dimensional system. The energy in that state is

$$E_T = \frac{\langle \varphi_T | H | \varphi_T \rangle}{\langle \varphi_T | \varphi_T \rangle} = \frac{\int d\mathbf{R} \varphi_T^*(\mathbf{R}) H \varphi_T(\mathbf{R})}{\int d\mathbf{R} |\varphi_T(\mathbf{R})|^2} \quad (82)$$

$$= \frac{\int d\mathbf{R} |\varphi_T(\mathbf{R})|^2 [\varphi_T(\mathbf{R})^{-1} H \varphi_T(\mathbf{R})]}{\int d\mathbf{R} |\varphi_T(\mathbf{R})|^2} . \quad (83)$$

The highlighted quantity

$$w(\mathbf{R}) = \frac{|\varphi_T(\mathbf{R})|^2}{\int d\mathbf{R} |\varphi_T(\mathbf{R})|^2} \quad (84)$$

is a perfectly good PDF and the quantity we are averaging is the *local energy*,

$$E_L(\mathbf{R}) = \varphi_T^{-1}(\mathbf{R}) H \varphi_T(\mathbf{R}) \quad \text{Local Energy .} \quad (85)$$

The energy in state  $\varphi_T$  is

$$E_T = \int d\mathbf{R} w(\mathbf{R}) E_L(\mathbf{R}) \approx \frac{1}{M} \sum_{i=1}^M E_L(\mathbf{R}_i) , \quad (86)$$

the average of the local energy calculated over  $M$  points  $\mathbf{R}_i$  sampled from the distribution  $\varphi_T$ . One can use the Metropolis algorithm to pick up these points as a random walk

$$\mathbf{R}_1 \rightarrow \mathbf{R}_2 \rightarrow \dots \rightarrow \mathbf{R}_M . \quad (87)$$

According to the Rayleigh-Ritz variational principle the true ground state energy is

$$E_0 \leq E_T , \quad (88)$$

so by making a good guess for the trial wave function one can easily calculate the upper bound of the ground-state energy.

### Metropolis VMC algorithm

This is for a  $N$ -particle system with trial wave function  $\varphi_T(\mathbf{R})$ .

1. Pick up an initial configuration  $\mathbf{R}_1$ . For a smooth start, the wave function squared,  $|\varphi_T(\mathbf{R}_1)|^2$ , should not be too small. A lattice is usually a good starting configuration.
2. Choose the initial step size  $step$ .
3. Set  $i = 1$ .
4. Pick  $i$ :th particle.
5. Draw three random numbers  $d_x$ ,  $d_y$  and  $d_z \in U[-\frac{1}{2}, \frac{1}{2}]$  (this is just  $U[0, 1] - \frac{1}{2}$ ). These make the displacement vector  $\mathbf{d} = (d_x, d_y, d_z)$ .
6. Compute new attempted particle position  $\mathbf{r}'_i = \mathbf{r}_i + step \mathbf{d}$
7. Compute

$$ratio = \left| \frac{\varphi_T(\mathbf{R}')}{\varphi_T(\mathbf{R})} \right|^2$$

8. **Metropolis question:** If  $ratio > 1$  accept move. Else draw  $t \in U[0, 1]$  and if  $ratio > t$  accept move. These amount to accepting the move with probability

$$P = \min [1, ratio] .$$

If move was accepted set  $\mathbf{r}_i = \mathbf{r}'_i$ , else keep old  $\mathbf{r}_i$ .

9. Keep count  $N_{accept}$  on how many of the moves have been accepted out of  $N_{try}$  attempted moves.
10. Set  $i = i + 1$ . If  $i < N$  go to 4.
11. Control the step size: If  $100 * N_{accept}/N_{try} < 40$  set decrease  $step$ , if  $100 * N_{accept}/N_{try} > 60$  increase  $step$ .
12. If still in thermalization, go to 3.
13. Accumulate averages. Print out progress.
14. If still collecting data, go to 3

## Properties of VMC

- What goes in comes out: you only get the properties of the trial wave function  $\varphi_T(\mathbf{R})$ .
- Optimization of  $\varphi_T(\mathbf{R})$  is time consuming, but better  $\varphi_T(\mathbf{R})$  means lower variance and faster converge.
- You see almost immediately if the property you added to  $\varphi_T(\mathbf{R})$  has the desired effect.
  - Squeezed liquid: first get liquid properties right (such as atom-atom repulsion), then multiply with a constraint (atom-wall repulsion). Properties on top of properties,

$$\varphi_T(\mathbf{R}) = \varphi_{\text{atom-wall}}(\mathbf{R})\varphi_{\text{atom-atom}}(\mathbf{R}) . \quad (89)$$

The atom-atom part includes all many-body effects, the atom-wall part single particle effects. The latter can be solved very accurately, knowing the atom-wall potential.

- If  $|\varphi_T\rangle$  is the ground state, it has zero variance in VMC.  
Every  $|\varphi_T\rangle$  gives an upper limit to the energy (Rayleigh-Ritz variational principle).
- There is no way to know how close to the true ground state your  $|\varphi_T\rangle$  is.
- Integrated quantities with few degrees of freedom, such as energy, are easy to evaluate.  
Functions with more degrees of freedom, such as the pair distribution function, need more time.
- Human bias induces error: Humans favor simple wave functions over complicated ones:  
solid over liquid, and polarised over unpolarised.<sup>16</sup>
- Only ratios of weights matter  $\Rightarrow \int d\mathbf{R} |\varphi_T(\mathbf{R})|^2$  is irrelevant !  
Computation of the norm would be another error-prone task, so this is excellent. We sampled the trial wave function as a Markov chain, which moves from  $\mathbf{R}$  to  $\mathbf{R}'$  based on the ratio of weights, new vs. old.

---

<sup>16</sup>Humans also tend to pick simple passwords like 12345 and qwerty.

## 5.1 Optimization of the trial wave function

Optimization comes in two flavours,<sup>17</sup>

1. Energy optimization
2. Variance optimization

Both energy and variance "measure" the distance of the trial wave function from the eigenstate we want. As we shall see, they disagree. With this we can live with, just keep in mind this imperfection. The big problems are more on the technical side. The trial wave function usually has many parameters, and the optimization problem is non-linear. The non-linearity comes from the fact that each parameter tries to quantify a certain property of the wave function, and the properties are inter-related in a non-linear fashion. Sugar and honey don't taste the same, but both add sweetness, so you can't add honeyness to your cake as much as you want without getting to add negative amount of sugar to compensate the sweetness – there are limitations to a certain parametrization.

After a lengthy evaluation there will be some error in each energy, and from the energy-vs-parameter plot it will be very hard – if not impossible – to determine the location of the minimum accurately. In MC calculations, correlations of samples are often mentioned with a negative tone, but in optimization they can actually give us means to determine the location of the minimum, energy or variance. Let's introduce correlated sampling with a *positive* impact.

### Correlated sampling

Direct minimization may be too inaccurate due to statistical fluctuations of data. One can hope that there is some "systematics" behind the fluctuations and that the trial wave function with different parameters  $\alpha$  give rise to "similar" fluctuations. If this is the case, then the cause of our trouble with fluctuations is that using *different* configurations  $\mathbf{R}$  for different  $\alpha$  mixes this systematics. The idea of using *the same set of configurations*  $\{\mathbf{R}\}$  to evaluate the expectation values of a several version of the same quantity is known as correlated sampling. If the fluctuations are somehow systematic, then

*The differences of the correlated averages can be  
much more accurate than the averages themselves.*

Sometimes minute energy differences matter, like in dealing with  $^3\text{He}$  impurities in liquid  $^4\text{He}$ , or in pinpointing the Wigner crystallization or paramagnetic-to-ferromagnetic transitions in electron gas. Separate computation of electron gas and Wigner crystal energies as a function of density easily lead to large uncertainties in the Wigner crystallization density.

---

<sup>17</sup>See also Assaraf and Caffarel Phys. Rev. Lett. 83, 4682 (1999), and Umrigar and Filippi Phys. Rev. Lett. 94, 150210 (2005).

To elucidate correlated sampling, consider the expectation value of the local energy with different parameters  $\alpha$ . It can be written in the form

$$\langle E(\alpha) \rangle := \frac{\int d\mathbf{R} |\varphi_T(\mathbf{R}, \alpha)|^2 E_L(\mathbf{R}; \alpha)}{\int d\mathbf{R} |\varphi_T(\mathbf{R}, \alpha)|^2} = \frac{\int d\mathbf{R} |\varphi_T(\mathbf{R}, \alpha_0)|^2 \left[ \frac{|\varphi_T(\mathbf{R}, \alpha)|^2}{|\varphi_T(\mathbf{R}, \alpha_0)|^2} E_L(\mathbf{R}; \alpha) \right]}{\int d\mathbf{R} |\varphi_T(\mathbf{R}, \alpha_0)|^2 \frac{|\varphi_T(\mathbf{R}, \alpha)|^2}{|\varphi_T(\mathbf{R}, \alpha_0)|^2}}.$$

While these expressions are mathematically equivalent (unless dividing by zero), their stochastically evaluated MC values are not. Approximating the integrals as sums over  $M$  samples we get

$$w(\mathbf{R}_i, \alpha_0) := \frac{|\varphi_T(\mathbf{R}_i; \alpha_0)|^2}{\int d\mathbf{R} |\varphi_T(\mathbf{R}_i; \alpha_0)|^2} \quad (90)$$

$$\langle E(\alpha) \rangle \approx \frac{\sum_{i=1}^M |\varphi_T(\mathbf{R}_i; \alpha_0)|^2 \left[ \frac{|\varphi_T(\mathbf{R}_i, \alpha)|^2}{|\varphi_T(\mathbf{R}_i, \alpha_0)|^2} E_L(\mathbf{R}_i; \alpha) \right]}{\sum_{i=1}^M |\varphi_T(\mathbf{R}_i; \alpha_0)|^2 \left[ \frac{|\varphi_T(\mathbf{R}_i, \alpha)|^2}{|\varphi_T(\mathbf{R}_i, \alpha_0)|^2} \right]} \quad (91)$$

$$= \frac{\sum_{i=1}^M w(\mathbf{R}_i; \alpha_0) \left[ \frac{|\varphi_T(\mathbf{R}_i, \alpha)|^2}{|\varphi_T(\mathbf{R}_i, \alpha_0)|^2} E_L(\mathbf{R}_i; \alpha) \right]}{\sum_{i=1}^M w(\mathbf{R}_i; \alpha_0) \left[ \frac{|\varphi_T(\mathbf{R}_i, \alpha)|^2}{|\varphi_T(\mathbf{R}_i, \alpha_0)|^2} \right]} \quad (92)$$

The configurations  $\mathbf{R}_i$  are sampled from  $w(\mathbf{R}_i; \alpha_0)$ : In correlated sampling you re-use the same configurations for all  $\alpha$ , so the values  $\langle E(\alpha) \rangle$  will be correlated. Their variances are larger than for uncorrelated sampling, but - if we are lucky - the fluctuations may "cancel in the same direction", and the differences

$$\langle E(\alpha_1) \rangle - \langle E(\alpha_2) \rangle, \quad (93)$$

come out more accurate than the absolute values of either of them. This is a welcome property, for in optimization we just want to know if we are going upward or downward, not how high we are.

One general notion is very useful, namely that the fluctuations of  $\langle ab \rangle$  are usually much larger than those of  $\langle ab \rangle - \langle a \rangle \langle b \rangle$  ("covariance"). This is especially true if  $a$  and  $b$  are uncorrelated, in which case the covariance is zero. Umrigar and Filippi (a footnote) used this idea and *subtract* terms like  $\langle a \rangle \langle b \rangle$  that will vanish for an infinite sample to get expressions that contain only covariances.

## Objective functions

The zero variance property can be used as an optimization criteria in finding a better trial wave function. It is often a more stable process to optimize the variance of the energy, not the

energy itself. One possible quantity to minimise — the **objective function** — is<sup>18</sup>

$$\sigma_{\text{opt}}^2 = \frac{\sum_{i=1}^{N_{\text{opt}}} \left| \frac{\varphi_T(\mathbf{R}_i; \alpha)}{\varphi_T(\mathbf{R}_i; \alpha_0)} \right|^2 [E_L(\mathbf{R}_i) - E_{\text{guess}}]^2}{\sum_{i=1}^{N_{\text{opt}}} \left| \frac{\varphi_T(\mathbf{R}_i; \alpha)}{\varphi_T(\mathbf{R}_i; \alpha_0)} \right|^2}, \quad (94)$$

Instead of taking a new set of randomly picked configurations one is using the *same set of configurations*  $\mathbf{R}_i = \{\mathbf{R}_1, \mathbf{R}_2, \dots, \mathbf{R}_{N_{\text{opt}}}\}$ , which sample a *fixed*  $\varphi_T(\mathbf{R}; \alpha_0)$ . This is again correlated sampling.

Let us test the process for the hydrogen atom, where we can compute  $\sigma_{\text{opt}}^2$  exactly for the trial wave function in the limit  $N_{\text{opt}} \rightarrow \infty$  in (94). We use the trial wave function

$$\varphi_T(\mathbf{R}) = e^{-\alpha r}, \quad (95)$$

where  $r$  is the distance of the electron from the proton (at origin). The local energy in atomic units is

$$E_L(\mathbf{R}) = -\frac{1}{2}\alpha^2 + \frac{\alpha - 1}{r}, \quad (96)$$

so the exact ground-state energy is  $E_0 = -0.5$  (Hartrees) at  $\alpha = 1$ . Simple integration gives

$$\sigma_{\text{opt}}^2 = \frac{5}{4}\alpha^4 - 3\alpha^3 + \alpha^2(2 - E_{\text{guess}}) + 2\alpha E_{\text{guess}} + E_{\text{guess}}^2. \quad (97)$$

Figure 6 shows  $\sigma_{\text{opt}}^2$  as function of  $\alpha$  for few guessed energies  $E_{\text{guess}}$ . Notice that if  $E_{\text{guess}} > E_0$  there is another, lower minimum at low  $\alpha$ , and in this case the optimization process is unstable and even infinite number of configurations won't help!

In short, the process of finding the minimum of  $\sigma_{\text{opt}}^2$  can be *unstable* if  $E_{\text{guess}} > E_0$ , and the proposal by Umrigar *et al.* cited above should be applied with care. Even so, the variance  $\sigma_{\text{opt}}^2$  does have an absolute minimum at the exact ground state, because then  $E_L(\mathbf{R}) = E_0$  for all  $\mathbf{R}$  and

$$\begin{aligned} \sigma_{\text{opt}}^2 &\geq \frac{\sum_{i=1}^{N_{\text{opt}}} [E_0 - E_{\text{guess}}]^2 w(\mathbf{R}_i)}{\sum_{i=1}^{N_{\text{opt}}} w(\mathbf{R}_i)} \\ &= (E_0 - E_{\text{guess}})^2 \geq 0. \end{aligned} \quad (98)$$

Hence the limiting value  $\sigma_{\text{opt}}^2 = 0$  requires also  $E_{\text{guess}} = E_0$ . This can be seen also in the case of hydrogen in Fig. 6, where the zero value at  $\alpha = 1$  corresponds to exactly  $E_{\text{guess}} = E_0 = -0.5$ .

One point worth remembering is, that if your trial wave function has exactly the correct form with  $n$  unknown parameters, then you need just  $n$  independent configurations to find out

---

<sup>18</sup>For other objective functions and further discussion, see P. R. C. Kent, R. J. Needs, and G. Rajagopal, Phys. Rev. B59 (1999) 12344.

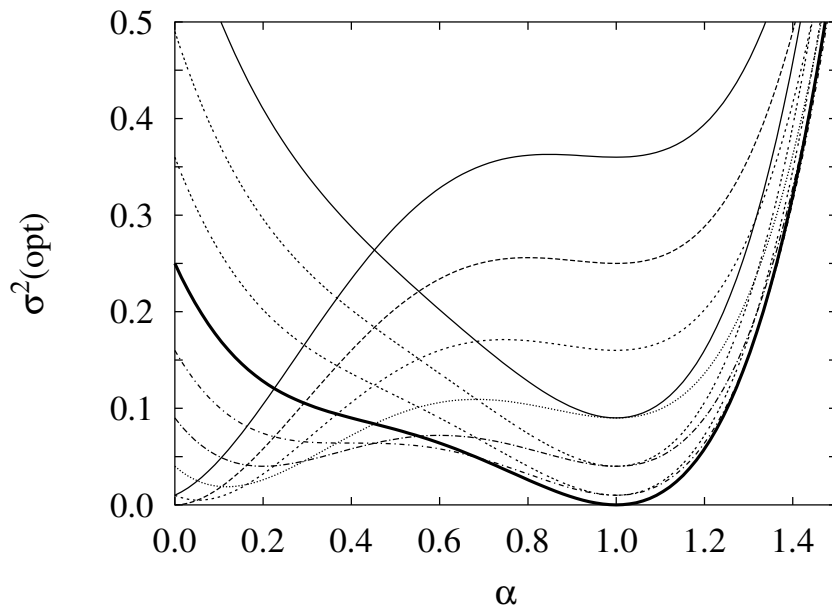


Figure 6: The *exact* objective function (94) in the limit  $N_{\text{opt}} \rightarrow \infty$  as a function of  $\alpha$  for a hydrogen atom with trial wave function (95). The guessed energies are  $E_{\text{guess}} = 0.1, 0.0, -0.1, \dots, -0.8$ , the curves for  $E_{\text{guess}} > E_0$  are those with another minimum at small  $\alpha$ . The bold line shows the case  $E_{\text{guess}} = E_0 = -0.5$ .

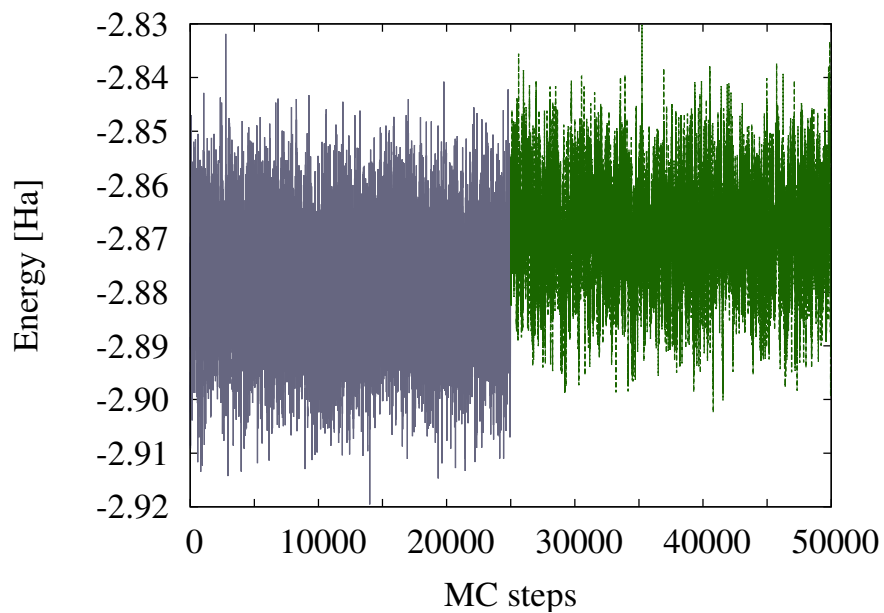


Figure 7: The figure illustrates the serious misconception that energy optimization and variance optimimization are equivalent ways to find the best parameters. The first 25000 steps are VMC data from energy optimised Padé-Jastrow wave function of He atom with just one parameter ( $a = 0.1437$ ): The energy is  $E = -2.878$  and the variance  $\sigma^2 = 0.11$ . The last 25000 step are variance optimised data ( $a = 0.3334$ ):  $E = -2.869$  and  $\sigma^2 = 0.08$ . So the higher energy result has lower variance and vice versa!

their values! Just solve the set of linear equations. With imperfect trial wave functions there is no guarantee that the parameters giving smallest variance of some form, like  $\sigma_{\text{opt}}^2$ , correspond to the best trial wave function. This can be seen by considering an optimization process, where one of the configurations happens to give a much larger contribution than the rest. In that case the variance would be close to zero, but the parameters would be very poor indeed! In some cases — one is the helium atom problem with two 1S orbitals — your optimization process may fail to converge to the “best” value. In that case you might try another objective function. If the potential energy diverges for some configurations, then you’d better take care of the cusp conditions (see appendix). See section 6.7 for more details about the He-atom problem.

Figure 7 shows how energy optimization and variance optimization may disagree about what state is closest to the true ground state. The fact that a lower energy state may have higher variance does not contradict the zero-variance property, it merely indicates that the search of the “best” wave function in the limited Hilbert space spanned by the possible trial wave functions has local minima in either energy or variance or both.

## 5.2 He atom wavefunction with e-e cusp

The 1S trial wave function satisfy the electron-nucleus Kato cusp condition (appendix), but not the electron-electron cusp condition, because there’s nothing that cancels the e-e coulomb potential singularity. One should add a  $r_{12} := |\mathbf{r}_1 - \mathbf{r}_2|$ -dependent part to the trial wave function. One popular choice is the Padé form,

$$\varphi_T := e^U = e^{U_{en} + U_{ee}} \quad (99)$$

$$U_{en} = -\alpha(r_1 + r_2) \quad \text{1S part} \quad (100)$$

$$U_{ee} = \begin{cases} \frac{r_{12}}{2(1+\beta r_{12})} & \text{parallel spins} \\ \frac{r_{12}}{4(1+\beta r_{12})} & \text{anti-parallel spins} \end{cases} \quad (101)$$

These  $U_{ee}$ ’s look a bit odd because the dimensions don’t match, but they are valid for dimensionless quantities in Hartree atomic units. Another popular choice is, credited to Ceperley and Alder,

$$U_{ee} = \frac{A}{r_{12}} (1 - e^{-r_{12}/F}) \quad (102)$$

$$F = \begin{cases} \sqrt{A} & \text{parallel spins} \\ \sqrt{2A} & \text{parallel spins} \end{cases} \quad (103)$$

The e-e cusp conditions for factor  $e^{-u(r)}$ , derived in the appendix, are

$$\left. \frac{du}{dr} \right|_{r=0} = \begin{cases} -\frac{1}{2} & \text{parallel spins} \\ -\frac{1}{4} & \text{anti-parallel spins} \end{cases}, \quad (104)$$

and both choices of  $U_{ee}$  satisfy them. For example,

$$u(r) = -\frac{r}{2(1+\beta r)} \quad (105)$$

$$\Rightarrow \frac{du}{dr} = -\frac{1}{2(1+\beta r)} + \frac{2\beta r}{(2(1+\beta r))^2} = \frac{-2(1+\beta r) + 2\beta r}{(2(1+\beta r))^2} = -\frac{2}{(2(1+\beta r))^2} \quad (106)$$

$$\rightarrow -\frac{1}{2}, \text{ as } r \rightarrow 0, \quad (107)$$

so the chosen form satisfies the e-e cusp condition.<sup>19</sup> The fact that the e-e cusp condition is satisfied can be seen below in the local energy, where the  $1/r_{12}$  singularities cancel.

For two electrons and  $Z$  protons in the nucleus (He atom has  $Z = 2$ ) the Hamiltonian is

$$\hat{\mathcal{H}} = -\frac{1}{2} \sum_{i=1}^2 \nabla_i^2 - \frac{Z}{r_1} - \frac{Z}{r_2} + \frac{1}{r_{12}} \quad (108)$$

in the Born-Oppenheimer approximation. The local energy is

$$E_L = \varphi_T^{-1} \hat{\mathcal{H}} \varphi_T = \underbrace{-\frac{1}{2} [(\nabla_1 U)^2 + (\nabla_2 U)^2 + \nabla_1^2 U + \nabla_2^2 U]}_{T_L} + \underbrace{\left[ -\frac{Z}{r_1} - \frac{Z}{r_2} + \frac{1}{r_{12}} \right]}_V. \quad (109)$$

For the local kinetic energy calculation we need some help results,

$$\nabla_1 r_1 = \frac{\mathbf{r}_1}{r_1} \quad \nabla_1 \cdot \mathbf{r}_1 = 3 \quad (\text{in 3 dimensions}) \quad (110)$$

$$\nabla_1 \cdot \frac{\mathbf{r}_1}{r_1} = \frac{3}{r_1} - \frac{1}{r_1^2} \mathbf{r}_1 \cdot \nabla_1 r_1 = \frac{2}{r_1} \quad (111)$$

$$\nabla_1 r_{12} = \frac{\mathbf{r}_{12}}{r_{12}} \quad (112)$$

$$\nabla_1 \cdot \mathbf{r}_{12} = \nabla_1 \cdot (\mathbf{r}_1 - \mathbf{r}_2) = 3 \quad (113)$$

$$\nabla_1 \cdot \left( \frac{\mathbf{r}_{12}}{r_{12}} \right) = \frac{3}{r_{12}} - \frac{1}{r_{12}^2} \mathbf{r}_{12} \cdot \nabla_1 r_{12} = \frac{2}{r_{12}}. \quad (114)$$

First,

$$\nabla_1 U = -\alpha \frac{\mathbf{r}_1}{r_1} + \left[ \frac{1}{2(1+\beta r_{12})} - \frac{\beta r_{12}}{2(1+\beta r_{12})^2} \right] \frac{\mathbf{r}_{12}}{r_{12}} = -\alpha \frac{\mathbf{r}_1}{r_1} + \frac{1}{2(1+\beta r_{12})^2} \frac{\mathbf{r}_{12}}{r_{12}}, \quad (115)$$

and from this we get

$$(\nabla_1 U)^2 = \alpha^2 + \frac{1}{4(1+\beta r_{12})^4} - \frac{\alpha}{(1+\beta r_{12})^2} \frac{\mathbf{r}_1}{r_1} \cdot \frac{\mathbf{r}_{12}}{r_{12}},$$

---

<sup>19</sup>The choice  $U_{ee} = \frac{r_{12}}{2}$  would also satisfy the e-e cusp condition, but the correlations would increase with increasing e-e distance unlike their Coulomb interaction.

so

$$(\nabla_1 U)^2 + (\nabla_2 U)^2 = 2\alpha^2 + \frac{1}{2(1+\beta r_{12})^4} - \frac{\alpha}{(1+\beta r_{12})^2} \frac{r_1+r_2}{r_{12}} \left(1 - \frac{\mathbf{r}_1 \cdot \mathbf{r}_2}{r_1 r_2}\right) , \quad (116)$$

and

$$\nabla_1^2 U = -2\alpha \frac{1}{r_1} - \frac{2\beta}{2(1+\beta r_{12})^3} + \frac{1}{2(1+\beta r_{12})^2} \frac{2}{r_{12}} , \quad (117)$$

so

$$\nabla_1^2 U + \nabla_2^2 U = -2\alpha \left(\frac{1}{r_1} + \frac{1}{r_2}\right) - \frac{2\beta}{(1+\beta r_{12})^3} + \frac{1}{(1+\beta r_{12})^2} \frac{2}{r_{12}} . \quad (118)$$

Now we can collect  $T_L$ ,

$$T_L = -\frac{1}{2}[(\nabla_1 U)^2 + (\nabla_2 U)^2 + \nabla_1^2 U + \nabla_2^2 U] \quad (119)$$

$$\begin{aligned} &= -\alpha^2 - \frac{1}{4(1+\beta r_{12})^4} + \frac{\alpha}{2(1+\beta r_{12})^2} \frac{r_1+r_2}{r_{12}} \left(1 - \frac{\mathbf{r}_1 \cdot \mathbf{r}_2}{r_1 r_2}\right) \\ &\quad + \alpha \left(\frac{1}{r_1} + \frac{1}{r_2}\right) + \frac{\beta}{(1+\beta r_{12})^3} - \frac{1}{(1+\beta r_{12})^2} \frac{1}{r_{12}} \\ &= -\alpha^2 + \alpha \left(\frac{1}{r_1} + \frac{1}{r_2}\right) \quad \text{the old 1S part} \end{aligned} \quad (120)$$

$$+ \frac{1}{2(1+\beta r_{12})^2} \left[ -\frac{1}{2(1+\beta r_{12})^2} + \frac{\alpha(r_1+r_2)}{r_{12}} \left(1 - \frac{\mathbf{r}_1 \cdot \mathbf{r}_2}{r_1 r_2}\right) + \frac{2\beta}{1+\beta r_{12}} - \frac{2}{r_{12}} \right] , \quad (121)$$

and the local energy is

$$\begin{aligned} E_L &= -\alpha^2 + (\alpha - Z) \left(\frac{1}{r_1} + \frac{1}{r_2}\right) + \frac{1}{r_{12}} \\ &\quad + \frac{1}{2(1+\beta r_{12})^2} \left[ -\frac{1}{2(1+\beta r_{12})^2} + \frac{\alpha(r_1+r_2)}{r_{12}} \left(1 - \frac{\mathbf{r}_1 \cdot \mathbf{r}_2}{r_1 r_2}\right) + \frac{2\beta}{1+\beta r_{12}} - \frac{2}{r_{12}} \right] \end{aligned} \quad (122)$$

At  $r_{12} \rightarrow 0$  the  $1/r_{12}$  singularities cancel and the e-e cusp condition is satisfied;  $\beta$  is a free parameter. Notice how choosing the denominator with the factor 2 in  $2(1+\beta r_{12})$  cancels the 2 in the singular term  $-2/r_{12}$ . The e-n cusp condition requires  $\alpha = Z$ . See the Python code `vmc-Heatom_cusp.py`.

The general case is also fairly similar. The wave function is

$$\varphi_T = e^U \quad (123)$$

$$U = \sum_i -\alpha r_i + \frac{1}{2} \sum_{i \neq j} \frac{r_{ij}}{(4|2)(1 + \beta r_{ij})} \quad (124)$$

$$\nabla_k U = -\alpha \frac{\mathbf{r}_k}{r_k} + \sum_{i(\neq k)} \frac{1}{(4|2)(1 + \beta r_{ki})^2} \frac{\mathbf{r}_{ki}}{r_{ki}} \quad (125)$$

$$\nabla_k^2 U = -\frac{2\alpha}{r_k} + \sum_{i(\neq k)} \frac{1}{(4|2)(1 + \beta r_{ki})^3} \frac{2}{r_{ki}}, \quad (126)$$

where 4 applies to anti-parallel and 2 to parallel spins of indices,  $i$  and  $j$ , or  $i$  and  $k$ , Collect,

$$T_L = -\frac{1}{2} \sum_k [(\nabla_k U)^2 + \nabla_k^2 U]. \quad (127)$$

In code it's easier to compute the vector  $\nabla_k U$  and square it and sum over  $k$ , avoiding a triple sum. In DMC  $\nabla_k U$  is needed anyhow for drift.

To conclude, optimization is not a black box that always produces the optimal parameters. But if it does, then you have the best possible trial wave function and your DMC code will be much more efficient.

## 6 Diffusion Monte Carlo

The Schrödinger equation in imaginary time turns into a diffusion equation. Diffusion is classical motion we surely can simulate. Replace  $it/\hbar$  with  $\tau$  to get the imaginary time Schrödinger equation,

$$-\frac{\partial|\Psi(\tau)\rangle}{\partial\tau}=\hat{\mathcal{H}}|\Psi(\tau)\rangle. \quad (128)$$

If the Hamiltonian is time independent, the formal solution is

$$|\Psi(\tau)\rangle=e^{-\hat{\mathcal{H}}\tau}|\Psi(0)\rangle \quad \text{projection}. \quad (129)$$

Starting from an initial guess  $|\Psi(0)\rangle$  one **projects** with the operator  $e^{-\hat{\mathcal{H}}\tau}$  to get  $|\Psi(\tau)\rangle$ .

What does this projection project? As so often in quantum mechanics, the eigenstate expansion reveals the details.<sup>20</sup> The eigenstates  $|\phi_i\rangle$  of  $\hat{\mathcal{H}}$  are solutions of

$$\hat{\mathcal{H}}|\phi_i\rangle=E_i|\phi_i\rangle, \quad E_0 < E_1 < E_2 < \dots. \quad (130)$$

We can expand any  $N$ -body state in the basis of eigenstates of  $\hat{\mathcal{H}}$ . Especially

$$|\Psi(0)\rangle=\sum_i c_i |\phi_i\rangle, \quad (131)$$

where the sum is over all eigenstates. We have then

$$|\Psi(\tau)\rangle=\sum_i c_i e^{-E_i\tau} |\phi_i\rangle. \quad (132)$$

This reveals that in imaginary time all states with  $E_i > 0$  decay exponentially, the ground state with energy  $E_0 \leq E_i$  has the slowest decay rate (for bound systems highest growth rate). Now you see what the replacement  $it/\hbar$  to  $\tau$  does: it changes oscillations to exponential decay/growth,

$$\sum_i c_i e^{-itE_i/\hbar} |\phi_i\rangle \text{ changes to } \sum_i c_i e^{-E_i\tau} |\phi_i\rangle \quad (133)$$

Write down the first terms of the sum, starting with the ground state 0, first excited state, etc.,

$$\begin{aligned} |\Psi(\tau)\rangle &= c_0 e^{-E_0\tau} |\phi_0\rangle + c_1 e^{-E_1\tau} |\phi_1\rangle + \dots \\ &= c_0 e^{-E_0\tau} \left[ |\phi_0\rangle + \frac{c_1}{c_0} e^{-(E_1-E_0)\tau} |\phi_1\rangle + \dots \right]. \end{aligned} \quad (134)$$

---

<sup>20</sup>The eigenstate expansion is remarkable. We have no way of knowing if we can ever solve the eigenstates, we just go ahead and use them!

If we project with the operator  $e^{-\tau\hat{\mathcal{H}}}$  to large  $\tau$ , meaning far to "future" in imaginary time, the factors  $e^{-(E_1-E_0)\tau}$  become exponentially small (for a non-degenerate ground state). The projection leaves only

$$|\Psi(\tau)\rangle \rightarrow c_0 e^{-E_0\tau} |\phi_0\rangle \quad \text{as } \tau \rightarrow \infty . \quad (135)$$

The factor  $c_0 e^{-E_0\tau}$  is just a number, which goes to the normalization of the wave function. What we have now is a procedure that will **project out all excited state contributions from an initial wave function**. There are a couple of snags:

1. You have to project to a large  $\tau$  to kill the first excited state, it only decays as  $e^{-(E_1-E_0)\tau}$ . In practise you keep on projecting until nothing changes and you hope you have reached the bottom.
2. If your initial wave function is orthogonal to the ground state, you have  $c_0 = 0$ . Then the first term is zero and you may have overlap with the first excited state, so the bottom is at the first excited state instead. This may actually be desirable, if you wanted to find  $E_1$ , but new problems arise, as we shall see.
3. The evolution is numerically unstable, since also the amplitude of the ground state decays. This is easy to solve, and we do it promptly.

We can stabilise the evolution by subtracting a trial or reference energy  $E_T$  from all energies. This merely shifts the energy scale; the energy-shifted equation

$$-\frac{\partial|\Psi(\tau)\rangle}{\partial\tau} = (\hat{\mathcal{H}} - E_T)|\Psi(\tau)\rangle \quad (136)$$

has the solution

$$|\Psi(\tau)\rangle = e^{-(\hat{\mathcal{H}}-E_T)\tau}|\Psi(0)\rangle = \sum_i c_i e^{-(E_i-E_T)\tau} |\phi_i\rangle . \quad (137)$$

Now all states with energy above  $E_T$  will decay, and those with energy below  $E_T$  are amplified in (imaginary) time. This means that if we choose  $E_T \approx E_0$ , the asymptotic state that survives is proportional to the ground state  $|\phi_0\rangle$ . We can then start with whatever state  $|\Psi(0)\rangle$  and it will evolve into the ground state, *provided it's not orthogonal to it; a snag mentioned above*. In the course of the evolution  $E_T$  is updated toward  $E_0$ , which is known more and more accurately.

Now we know in principle what the final outcome is. We still have to conceive a method to evolve  $\Psi(\mathbf{R}, 0)$  in practise, since we have neither the eigenvalues nor the eigenfunctions. We start again from Eq. (137). The operator responsible for the time evolution is Green's function

$$\hat{G}(\tau) = e^{-(\hat{\mathcal{H}}-E_T)\tau} , \quad (138)$$

which satisfies the operator equation

$$-\frac{\partial \hat{G}(\tau)}{\partial \tau} = (\hat{\mathcal{H}} - E_T) \hat{G} . \quad (139)$$

Numerics can't handle abstract operators (same way abstract vectors are intangible), so we have to fix a representation in some space. We can pick any complete basis, a convenient one is the sets of all  $N$ -body coordinates  $\{|\mathbf{R}\rangle\}$ . It's complete,

$$\int d\mathbf{R} |\mathbf{R}\rangle \langle \mathbf{R}| = \mathbb{1} \quad , \text{ the unit operator,} \quad (140)$$

and it's continuous – "the sum over all states" is  $\int d\mathbf{R}$  – and orthonormal,

$$\langle \mathbf{R}' | \mathbf{R} \rangle = \delta(\mathbf{R}' - \mathbf{R}) \quad (\text{Dirac delta}) . \quad (141)$$

We already used the basis  $\{|\mathbf{R}\rangle\}$ , the wave function in coordinate space is a projection of the state vector to it:

$$\Psi(\mathbf{R}; \tau) := \langle \mathbf{R} | \Psi(\tau) \rangle \quad \text{definition .} \quad (142)$$

The unit operator can be inserted to many places,

$$|\Psi(\tau)\rangle = \mathbb{1} |\Psi(\tau)\rangle = \int d\mathbf{R} |\mathbf{R}\rangle \langle \mathbf{R}| \Psi(\tau) = \int d\mathbf{R} |\mathbf{R}\rangle \Psi(\mathbf{R}; \tau) . \quad (143)$$

The coordinate space representation of  $\hat{G}$  is a matrix,

$$\hat{G} = \mathbb{1} \hat{G} \mathbb{1} = \left[ \int d\mathbf{R}' |\mathbf{R}'\rangle \langle \mathbf{R}'| \right] \hat{G} \left[ \int d\mathbf{R} |\mathbf{R}\rangle \langle \mathbf{R}| \right] = \int d\mathbf{R} d\mathbf{R}' |\mathbf{R}\rangle \langle \mathbf{R}'| \langle \mathbf{R}' | \hat{G} | \mathbf{R} \rangle , \quad (144)$$

with matrix elements

$$\langle \mathbf{R}' | \hat{G}(\tau) | \mathbf{R} \rangle = \langle \mathbf{R}' | e^{-(\hat{\mathcal{H}} - E_T)\tau} | \mathbf{R} \rangle := G(\mathbf{R}', \mathbf{R}; \tau) . \quad (145)$$

The many-body Hamiltonian is often of the form

$$\hat{\mathcal{H}} = \hat{\mathcal{T}} + \hat{\mathcal{V}} \quad (146)$$

$$\hat{\mathcal{T}}\Psi(\mathbf{R}; \tau) = -D \nabla_{\mathbf{R}}^2 \Psi(\mathbf{R}; \tau) \quad \text{kinetic operator} \quad (147)$$

$$\hat{\mathcal{V}}\Psi(\mathbf{R}; \tau) = V(\mathbf{R}) \quad \text{potential operator ,} \quad (148)$$

with the notations  $\nabla_{\mathbf{R}}^2 = \sum_{i=1}^N \nabla_i^2$  (sum over all  $N$  particles) and  $D = \hbar^2/(2m)$ <sup>21</sup>. Green's function is the solution of the equation

$$-\frac{\partial}{\partial \tau} G(\mathbf{R}', \mathbf{R}; \tau) = [\hat{\mathcal{H}} - E_T] G(\mathbf{R}', \mathbf{R}; \tau) = [-D \nabla_{\mathbf{R}}^2 + V(\mathbf{R}) - E_T] G(\mathbf{R}', \mathbf{R}; \tau) . \quad (149)$$

Remembering that

$$\langle \mathbf{R} | \hat{A} | \Psi \rangle = \hat{A} \langle \mathbf{R} | \Psi \rangle = \hat{A} \Psi(\mathbf{R}) , \quad (150)$$

the coordinate representation the calculation goes like this:

$$-\frac{\partial}{\partial \tau} G(\mathbf{R}', \mathbf{R}; \tau) = -\frac{\partial}{\partial \tau} \langle \mathbf{R}' | e^{-\tau(\hat{\mathcal{H}} - E_T)} | \mathbf{R} \rangle = \langle \mathbf{R}' | (\hat{\mathcal{H}} - E_T) e^{-\tau(\hat{\mathcal{H}} - E_T)} | \mathbf{R} \rangle \quad (151)$$

$$= [\hat{\mathcal{H}} - E_T] \langle \mathbf{R}' | e^{-\tau(\hat{\mathcal{H}} - E_T)} | \mathbf{R} \rangle = [\hat{\mathcal{H}} - E_T] G(\mathbf{R}', \mathbf{R}; \tau) . \quad (152)$$

## 6.1 Short-time estimates of Green's function

At first glance Eq. (149) doesn't look any more promising than the original Schrödinger equation (128). But for *short time intervals*  $\tau$  we may solve it approximately. A theorem by Trotter<sup>22</sup> says, that while the kinetic and the potential parts  $T$  and  $V$  of the Hamiltonian do not commute,

$$[\hat{\mathcal{T}}, \hat{V}] \neq 0 \Leftrightarrow \hat{\mathcal{T}} \hat{V} \neq \hat{V} \hat{\mathcal{T}} \quad (153)$$

$$\text{obvious because } \nabla_{\mathbf{R}}^2 [V(\mathbf{R}) \Psi(\mathbf{R})] \neq V(\mathbf{R}) \nabla_{\mathbf{R}}^2 \Psi(\mathbf{R}) \text{ for arbitrary } \Psi(\mathbf{R}) , \quad (154)$$

we may ignore this for a very brief moment, and evolve from time 0 to  $\tau$ , where  $\tau$  is small.

The reason why we would like to separate  $\hat{\mathcal{T}}$  and  $\hat{V}$  is that we can deal with either "kinetic evolution"  $G_T(\tau)$  (diffusion) or "potential evolution"  $G_V(\tau)$  (an amplitude factor), but not with both happening "simultaneously". We can expand  $\hat{G}$  as

$$G(\tau) = e^{-(\hat{\mathcal{H}} - E_T)\tau} = e^{-(\hat{\mathcal{T}} + \hat{V} - E_T)\tau} = \underbrace{e^{-\hat{\mathcal{T}}\tau}}_{G_T(\tau)} \underbrace{e^{-(\hat{V} - E_T)\tau}}_{G_V(\tau)} + \mathcal{O}(\tau^2) . \quad (155)$$

The operator  $\hat{V}$  is diagonal in coordinate space (doesn't move particles),

$$\langle \mathbf{R}' | \hat{V} | \mathbf{R} \rangle = V(\mathbf{R}) \delta(\mathbf{R}' - \mathbf{R}) , \quad (156)$$

---

<sup>21</sup>" $D$ " for "diffusion constant".

<sup>22</sup>H. F. Trotter, Proc. Am. Math. Soc. **10** (1959) 545.

so

$$G_V(\mathbf{R}', \mathbf{R}; \tau) = e^{-(V(\mathbf{R}) - E_T)\tau} \delta(\mathbf{R}' - \mathbf{R}) . \quad (157)$$

Operate on a wave function with  $\hat{G}_V(\tau)$ ,

$$\hat{G}_V(\tau) \Psi(\mathbf{R}, \tau) = e^{-(\hat{V} - E_T)\tau} \Psi(\mathbf{R}, \tau) = e^{-(V(\mathbf{R}) - E_T)\tau} \Psi(\mathbf{R}, \tau) , \quad (158)$$

so potential-induced evolution in coordinate space only multiplies the amplitude by a factor  $e^{-(V(\mathbf{R}) - E_T)\tau}$ . In other words,  $G_V(\tau)$  satisfies the *rate equation*

$$\frac{\partial G_V(\mathbf{R}', \mathbf{R}, \tau)}{\partial \tau} = -(V(\mathbf{R}) - E_T) G_V(\mathbf{R}', \mathbf{R}, \tau) . \quad (159)$$

The kinetic evolution is not diagonal in coordinate space, because it takes the derivative  $\nabla_{\mathbf{R}}^2$ . However, in momentum space  $G_T(\tau)$  is diagonal, because of momentum conservation.<sup>23</sup> Define the momentum space by specifying it's relation to coordinate space,

$$\langle \mathbf{R} | \mathbf{K} \rangle = \frac{1}{\sqrt{\Omega}} e^{-i\mathbf{K} \cdot \mathbf{R}} \quad \text{definition of momentum space} , \quad (160)$$

where  $\Omega$  is the (normalization) volume. Next we can prove that  $\{|\mathbf{K}\rangle\}$  is complete,

$$\int d\mathbf{K} |\mathbf{K}\rangle \langle \mathbf{K}| = \mathbb{1} \quad (\text{continuum}) \quad (161)$$

$$\sum_{\mathbf{K}} |\mathbf{K}\rangle \langle \mathbf{K}| = \mathbb{1} \quad (\text{discrete}) . \quad (162)$$

---

<sup>23</sup>Conversely, in momentum space  $G_V(\tau)$  is not diagonal, because the potential changes particle momenta.

### Completeness of $\{|\mathbf{K}\rangle\}$

Momentum states  $|\mathbf{K}\rangle := |\mathbf{k}_1, \dots, \mathbf{k}_N\rangle$  are eigenstates of the kinetic operator,

$$\hat{\mathcal{T}}|\mathbf{K}\rangle = \sum_{i=1}^N -\frac{\hbar^2}{2m_i} \nabla_i^2 |\mathbf{K}\rangle = \sum_{i=1}^N -\frac{\hbar^2}{2m_i} |\mathbf{K}|^2 |\mathbf{K}\rangle , \quad (163)$$

and the set of all eigenstates is complete. Dirac delta can be expressed as (using notation of discrete momentum space)

$$\delta(\mathbf{R} - \mathbf{R}') = \frac{1}{\Omega} \sum_{\mathbf{K}} e^{-i\mathbf{K}\cdot(\mathbf{R}-\mathbf{R}')} , \quad (164)$$

which is here understood as the product of  $d$ -dimensional Dirac deltas,

$$\delta(\mathbf{R} - \mathbf{R}') = \prod_{i=1}^N \delta^d(\mathbf{r}_i - \mathbf{r}'_i) \quad (165)$$

$$\delta^3(\mathbf{r}_i - \mathbf{r}'_i) = \delta(x_i - x'_i)\delta(y_i - y'_i)\delta(z_i - z'_i) \text{ in 3 dimensions .} \quad (166)$$

The completeness of  $\{|\mathbf{K}\rangle\}$  and the completeness of  $\{|\mathbf{R}\rangle\}$  are related,

$$\begin{aligned} \sum_{\mathbf{K}} |\mathbf{K}\rangle\langle\mathbf{K}| &= \sum_{\mathbf{K}} \mathbb{1} |\mathbf{K}\rangle\langle\mathbf{K}| \mathbb{1} \\ &= \sum_{\mathbf{K}} \int d\mathbf{R} |\mathbf{R}\rangle\langle\mathbf{R}| |\mathbf{K}\rangle\langle\mathbf{K}| \int d\mathbf{R}' |\mathbf{R}'\rangle\langle\mathbf{R}'| \\ &= \frac{1}{\Omega} \sum_{\mathbf{K}} \int d\mathbf{R} |\mathbf{R}\rangle e^{-i\mathbf{K}\cdot\mathbf{R}} \int d\mathbf{R}' e^{i\mathbf{K}\cdot\mathbf{R}'} \langle\mathbf{R}'| \\ &= \int d\mathbf{R} d\mathbf{R}' |\mathbf{R}\rangle\langle\mathbf{R}'| \left[ \frac{1}{\Omega} \sum_{\mathbf{K}} e^{-i\mathbf{K}\cdot(\mathbf{R}-\mathbf{R}')} \right] \\ &= \int d\mathbf{R} d\mathbf{R}' |\mathbf{R}\rangle\langle\mathbf{R}'| \delta(\mathbf{R} - \mathbf{R}') = \int d\mathbf{R} |\mathbf{R}\rangle\langle\mathbf{R}| = \mathbb{1} . \end{aligned} \quad (167)$$

An elegant way to derive the matrix elements of the kinetic evolution is to use eigenfunction expansion —this is the house rule of finding any Green's function in physics. The eigenfunctions of  $\hat{T}$  are plane waves, and the eigenvalues are kinetic energies. With  $K = |\mathbf{K}|$  in a box with side  $L$  (remember  $\mathbf{K}$  is a  $3N$ -dimensional vector),

$$\hat{T}\phi_{\mathbf{K}}(\mathbf{R}) = (-D\nabla_{\mathbf{R}}^2)\phi_{\mathbf{K}}(\mathbf{R}) = DK^2\phi_{\mathbf{K}}(\mathbf{R}) \quad (168)$$

$$\phi_{\mathbf{K}}(\mathbf{R}) = \langle \mathbf{R} | \mathbf{K} \rangle = \frac{1}{\sqrt{L^{3N}}} e^{-i\mathbf{K}\cdot\mathbf{R}}, \quad (169)$$

one gets (use completeness of  $\{\mathbf{K}\}$ )

$$G_T(\mathbf{R}', \mathbf{R}; \tau) := \langle \mathbf{R}' | e^{-\tau\hat{T}} | \mathbf{R} \rangle = \sum_{\mathbf{K}} \langle \mathbf{R}' | e^{-\tau\hat{T}} | \mathbf{K} \rangle \langle \mathbf{K} | \mathbf{R} \rangle \quad (170)$$

$$= \sum_{\mathbf{K}} \langle \mathbf{R}' | e^{-\tau DK^2} | \mathbf{K} \rangle \phi_{\mathbf{K}}^*(\mathbf{R}) = \sum_{\mathbf{K}} \phi_{\mathbf{K}}(\mathbf{R}') \phi_{\mathbf{K}}^*(\mathbf{R}) e^{-\tau DK^2} \quad (171)$$

$$= \frac{1}{L^{3N}} \sum_{\mathbf{K}} e^{-i\mathbf{K}\cdot(\mathbf{R}'-\mathbf{R})} e^{-\tau DK^2}. \quad (172)$$

The momentum values are  $2\pi/L$  apart, and for large  $L$  the sum can be converted to an integral,

$$\sum_{\mathbf{K}} \approx \frac{L^{3N}}{(2\pi)^{3N}} \int d\mathbf{K} \quad (173)$$

$$\frac{1}{L^{3N}} \sum_{\mathbf{K}} e^{-i\mathbf{K}\cdot(\mathbf{R}'-\mathbf{R})} e^{-\tau DK^2} \approx \frac{1}{(2\pi)^{3N}} \int d\mathbf{K} e^{-i\mathbf{K}\cdot(\mathbf{R}'-\mathbf{R})} e^{-\tau DK^2}, \quad (174)$$

where the integral is a Fourier transform of a Gaussian, leading to the nice result

$$G_T(\mathbf{R}', \mathbf{R}; \tau) = (4\pi D\tau)^{-3N/2} e^{-\frac{(\mathbf{R}-\mathbf{R}')^2}{4D\tau}}. \quad (175)$$

This is usually an excellent approximation, so I left out the " $\approx$ ". In DMC there is practically never any need to fall back to the sum (172). We'll soon see that in Path Integral Monte Carlo (PIMC)  $\tau$  is replaced by  $\beta$ , and pushing to a too low temperature eventually makes the integral approximation invalid. In other words, at a low enough temperature the deBroglie wave length of particles becomes larger than the box and one must evaluate the sum in Eq. (172).

The kinetic Green's function  $G_T$  corresponds to a  $3N$ -dimensional Gaussian spreading during time  $\tau$ , because  $G_T(\tau)$  satisfies the *diffusion equation*

$$\frac{\partial G_T(\mathbf{R}', \mathbf{R}; \tau)}{\partial \tau} = -D\nabla_{\mathbf{R}}^2 G_T(\mathbf{R}', \mathbf{R}; \tau). \quad (176)$$

To summarise, the short-time Green's function with error  $\mathcal{O}(\tau^2)$  is

$$G(\mathbf{R}', \mathbf{R}; \tau) = (4\pi D\tau)^{-3N/2} e^{-\frac{(\mathbf{R}-\mathbf{R}')^2}{4D\tau}} e^{-(V(\mathbf{R})-E_T)\tau} \quad \text{"primitive approximation"}. \quad (177)$$

**Free particle diffusion: MC evaluation of integrals with  $G_T(\mathbf{R}', \mathbf{R}; \tau)$** 

We know how the sample random numbers that have the normal (Gaussian) distribution  $\frac{1}{\sqrt{2\pi}}e^{-x^2/2}$  (see the Box-Müller or the Fernández-Rivero algorithm in section 3.4). Then MC estimate with  $M$  samples is

$$\frac{1}{\sqrt{2\pi}} \int_{-\infty}^{\infty} dx e^{-x^2/2} f(x) \approx \frac{1}{M} \sum_{i=1}^M f(x_i) \quad , \quad x_i \text{ sampled from } \frac{1}{\sqrt{2\pi}}e^{-x^2/2}. \quad (178)$$

If numbers  $\eta$  have the distribution  $\frac{1}{\sqrt{2\pi}}e^{-x^2/2}$ , then obviously numbers  $\eta\sigma$  have the distribution  $\frac{1}{\sqrt{2\pi}\sigma^2}e^{-x^2/(2\sigma^2)}$ . In  $G_T(\mathbf{R}', \mathbf{R}; \tau)$  the exponent is a product of  $N$  one-body Gaussians in 3 dimensions,

$$G_T(\mathbf{R}', \mathbf{R}; \tau) = (4\pi D\tau)^{-3N/2} e^{-\frac{(\mathbf{R}-\mathbf{R}')^2}{4D\tau}} = (4\pi D\tau)^{-3N/2} \prod_{i=1}^N e^{-\frac{(\mathbf{r}_i-\mathbf{r}'_i)^2}{4D\tau}} \quad (179)$$

$$= (4\pi D\tau)^{-3N/2} \prod_{i=1}^N \left[ e^{-\frac{(x_i-x'_i)^2}{4D\tau}} e^{-\frac{(y_i-y'_i)^2}{4D\tau}} e^{-\frac{(z_i-z'_i)^2}{4D\tau}} \right] \quad (180)$$

$$= (4\pi D\tau)^{-3N/2} \prod_{i=1}^N \prod_{d=x,y,z} e^{-\frac{(d_i-d'_i)^2}{4D\tau}}. \quad (181)$$

Hence we can write  $G_T$  as product of independent one-dimensional Gaussians. This is hardly surprising because this is free particle diffusion, so each particle diffuse independently to three directions. The value of  $\sigma$  can be found by comparing the exponents,

$$2\sigma^2 = 4D\tau \Rightarrow \sigma = \sqrt{2D\tau}. \quad (182)$$

Evolving the state from 0 to  $\tau$  with only the kinetic operator is

$$|\Psi(\tau)\rangle = G_T(\tau)|\Psi(0)\rangle = e^{-\tau\hat{T}}|\Psi(0)\rangle, \quad (183)$$

which in coordinate space is (use  $\int d\mathbf{R}|\mathbf{R}\rangle\langle\mathbf{R}| = \mathbb{1}$  and  $\langle\mathbf{R}'|\tau\rangle := \psi(\mathbf{R}'; \tau)$ )

$$\psi(\mathbf{R}'; \tau) = \langle\mathbf{R}'|e^{-\tau\hat{T}}|0\rangle = \int d\mathbf{R}\langle\mathbf{R}'|e^{-\tau\hat{T}}|\mathbf{R}\rangle\langle\mathbf{R}|0\rangle = \int d\mathbf{R}G_T(\mathbf{R}', \mathbf{R}; \tau)\psi(\mathbf{R}; 0). \quad (184)$$

The goal is to sample points  $\mathbf{R}'$  from  $\psi(\mathbf{R}'; \tau)$ , which is known only via the integral equation. Assuming we can sample points  $\mathbf{R}$  from  $\psi(\mathbf{R}; 0)$ , then after time  $\tau$  they will be at  $\mathbf{R}'$  given by

$$\mathbf{R}' = \mathbf{R} + \boldsymbol{\eta}\sqrt{2D\tau}, \quad (185)$$

where  $\boldsymbol{\eta}$  is a  $3N$ -dimensional vector of Gaussian-distributed random numbers. Just move a particle in  $x$  direction as

$$x' = x + \eta\sqrt{2D\tau} \quad , \quad (\eta \text{ is a Gaussian-distributed random number}) \quad (186)$$

and repeat for  $y$  and  $z$  directions; do this for all particles, one by one. This is the most efficient way to evaluate the integral  $\int d\mathbf{R}G_T(\mathbf{R}', \mathbf{R}; \tau)\psi(\mathbf{R}; 0)$  using MC.

**Special case:  $\tau \rightarrow 0$  limit**

In the limit  $\tau \rightarrow 0$  the Gaussian becomes narrower and approaches a Dirac delta, so this approximate  $G$  satisfies the boundary condition

$$G(\mathbf{R}', \mathbf{R}, 0) = \langle \mathbf{R}' | e^{-0 \hat{\mathcal{H}}} | \mathbf{R} \rangle = \langle \mathbf{R}' | \mathbb{1} | \mathbf{R} \rangle = \langle \mathbf{R}' | \mathbf{R} \rangle = \delta(\mathbf{R}' - \mathbf{R}) . \quad (187)$$

This is a natural requirement for the time evolution, since  $\tau = 0$  evolution shouldn't evolve anything. Specifically,

$$|\Psi(\tau)\rangle = e^{-\tau(\hat{\mathcal{H}} - E_T)} |\Psi(0)\rangle \rightarrow |\Psi(0)\rangle \text{ as } \tau \rightarrow 0 . \quad (188)$$

Ideally  $\tau$  should be so small, that the approximation to Green's function is more accurate than the statistical uncertainty. In practise one calculates the desired quantities with several values of  $\tau$  in multiple MC runs, and in the end extrapolates the result to  $\tau = 0$ . Later Fig. 11 will demonstrate this procedure for a set of He-atom results.

**With  $G(\tau)$  accurate to second order, the energy is accurate only to first order**

In one dimension the small- $\tau$  expansion of Green's function can be easily found with the aid of a sufficiently smooth function  $f(x)$ <sup>24</sup>. The Taylor expansion of  $f(x)$  around  $x = 0$  gives ( $f^{(n)}(x)$  stands for the  $n$ th derivative at  $x$ )

$$\begin{aligned} \int_{-\infty}^{\infty} dx \frac{1}{\sqrt{4\pi D\tau}} e^{-\frac{x^2}{4D\tau}} f(x) &= \int_{-\infty}^{\infty} dx \frac{1}{\sqrt{4\pi D\tau}} e^{-\frac{x^2}{4D\tau}} \sum_{n=0}^{\infty} \frac{x^n}{n!} f^{(n)}(0) \\ &= \sum_{n=0}^{\infty} f^{(n)}(0) \int_{-\infty}^{\infty} dx \frac{1}{\sqrt{4\pi D\tau}} e^{-\frac{x^2}{4D\tau}} \frac{x^n}{n!}. \end{aligned} \quad (189)$$

From symmetry one sees immediately that only even  $n$  contribute. The formula

$$\int_{-\infty}^{\infty} dx \frac{1}{\sqrt{4\pi D\tau}} e^{-\frac{x^2}{4D\tau}} \frac{x^{2n}}{(2n)!} = \frac{(D\tau)^n}{n!} \quad (190)$$

gives

$$\int_{-\infty}^{\infty} dx \frac{1}{\sqrt{4\pi D\tau}} e^{-\frac{x^2}{4D\tau}} f(x) = \sum_{n=0}^{\infty} f^{(2n)}(0) \frac{(D\tau)^n}{n!} \quad (191)$$

$$= \int_{-\infty}^{\infty} dx \delta(x) \sum_{n=0}^{\infty} f^{(2n)}(x) \frac{(D\tau)^n}{n!}. \quad (192)$$

where the integral form was recovered using Dirac delta. After partial integrations that shift the derivatives from  $f^{(2n)}$  to the Dirac delta in each term one finds, by comparing the factors of  $f(x)$  in the integrals, that

$$G_T(\tau) = \frac{1}{\sqrt{4\pi D\tau}} e^{-\frac{(x-x')^2}{4D\tau}} = \delta(x - x') + D\tau \delta''(x - x') + \mathcal{O}(\tau^2). \quad (193)$$

Combined with  $G_V$ , the time evolution of the wave function is

$$\Psi(x, \tau) = \Psi(x, 0) + [E_T - V(x)]\tau\Psi(x, 0) + D\tau\Psi''(x, 0) + \mathcal{O}(\tau^2), \quad (194)$$

so after stability has been reached,  $\Psi(x, \tau) = \Psi(x, 0)$ , we are left with the first-order terms that give back the Schrödinger equation

$$-D\Psi''(x, 0) + V(x)\Psi(x, 0) = E_T\Psi(x, 0) + \mathcal{O}(\tau). \quad (195)$$

In the zero- $\tau$  limit  $E_T$  is one of the eigenvalues of the Hamiltonian. A second order Green's function gives energies that are correct only to first order in  $\tau$ .

---

<sup>24</sup>R. Guardiola, *Lecture Notes in Physics: Microscopic Quantum Many-Body Theories and Their Applications*, Eds. J. Navarro and A. Polls, (Springer Verlag, Berlin 1998); Valencia lecture notes 1997.

### Representation of the many-body wave function

We need to figure out how to represent the many-body wave function  $\Psi(\mathbf{R}, 0)$  numerically. There are  $N$  particles somewhere in the continuous space  $3N$  dimension space. Choosing a single  $\mathbf{R}_1$  doesn't represent  $\Psi(\mathbf{R}, 0)$  well, the particles could be elsewhere. We take the Monte Carlo way and state that since we cannot possibly keep an infinite number of positions, we take a "representative" sample and represent  $\Psi(\mathbf{R}, 0)$  as an *ensemble of  $N_C$  configurations*  $\{\mathbf{R}_1, \mathbf{R}_2, \dots, \mathbf{R}_{N_C}\}$ . Each  $\mathbf{R}_i$  contains  $N$  **walkers**, which represent quantum particles. The evolution evolves the  $N_C$  configurations. In each of these  $N_C$  configurations we have  $N$  walkers (see Fig. 8).

Green's function (177) evolves the system via two processes:

#### Basic DMC algorithm with only branching and diffusion

1. Branching due to  $G_V(\tau)$ : The wave function  $\Psi(\mathbf{R}, 0)$  is multiplied by the factor  $e^{-(V(\mathbf{R}) - E_T)\tau}$ . So we calculate  $V(\mathbf{R})$  for each configuration and see whether this factor is more or less than one, and create/destroy configurations accordingly. Walkers are not moving.
2. Diffusion due to  $G_T(\tau)$ : Move walkers from  $\mathbf{R} \rightarrow \mathbf{R}'$  diffusively, in other words move each walker according to

$$r'_i = r_i + \eta \sqrt{2D\tau} ,$$

where  $\eta$  is a d-dimensional Gaussian random variable with zero mean and unit variance.

In practise this algorithm is never used, because it has one big problem. Often the potential is not bound from above. Walkers can easily diffuse into positions where the potential practically blows up. In step 1 we would need to create/destroy *very many* configurations and thus their total number would fluctuate wildly. This is the DMC version of the large variance problem we encountered earlier in crude Monte Carlo. We need importance sampling to keep walkers away from the infinities of the potential, and to concentrate our efforts to regions of moderate  $V(\mathbf{R})$ .

#### Importance sampling in DMC

Instead of  $\Psi(\mathbf{R}; \tau)$ , we seek to evolve

$$f(\mathbf{R}; \tau) = \varphi_T(\mathbf{R})\Psi(\mathbf{R}; \tau) , \quad (196)$$

where  $\varphi_T(\mathbf{R})$  is a time-independent trial wave function used for importance sampling. We know the evolution of  $\Psi(\mathbf{R}; \tau)$ , it's given by the imaginary-time Schrödinger equation (136). So use

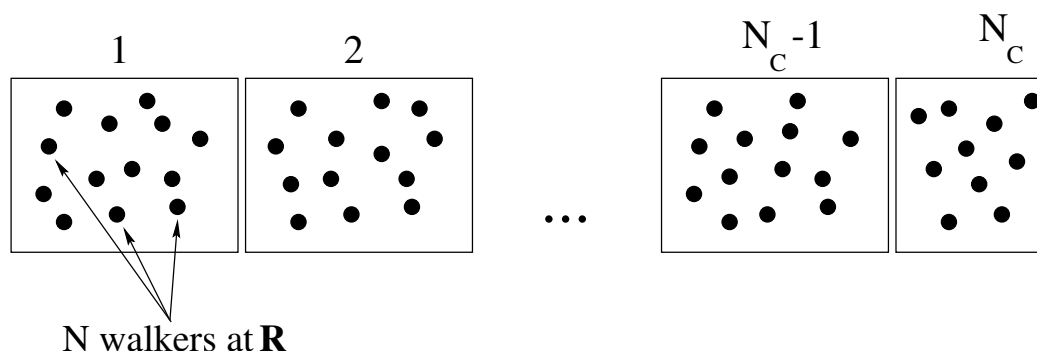


Figure 8: The wave function is represented by an ensemble of configurations.

that to find out how  $f(\mathbf{R}; \tau)$  evolves <sup>25</sup>:

$$-\frac{\partial \Psi(\mathbf{R}; \tau)}{\partial \tau} = (\hat{\mathcal{H}} - E_T) \Psi(\mathbf{R}; \tau) \quad (197)$$

$$\Leftrightarrow -\frac{1}{\varphi_T(\mathbf{R})} \frac{\partial f(\mathbf{R}; \tau)}{\partial \tau} = [-D\nabla_{\mathbf{R}}^2 + V(\mathbf{R}) - E_T] \frac{f(\mathbf{R}; \tau)}{\varphi_T(\mathbf{R})} \quad (198)$$

$$\Leftrightarrow -\frac{\partial f(\mathbf{R}; \tau)}{\partial \tau} = -D\varphi_T(\mathbf{R})\nabla_{\mathbf{R}}^2 \left[ \frac{f(\mathbf{R}; \tau)}{\varphi_T(\mathbf{R})} \right] + [V(\mathbf{R}) - E_T] f(\mathbf{R}; \tau) \quad (199)$$

$$\begin{aligned} \Leftrightarrow -\frac{\partial f(\mathbf{R}; \tau)}{\partial \tau} &= -D\nabla_{\mathbf{R}}^2 f(\mathbf{R}; \tau) + 2D \frac{\nabla_{\mathbf{R}}\varphi_T(\mathbf{R})}{\varphi_T(\mathbf{R})} \cdot \nabla_{\mathbf{R}} f(\mathbf{R}; \tau) \\ &\quad - 2D \left( \frac{\nabla_{\mathbf{R}}\varphi_T(\mathbf{R})}{\varphi_T(\mathbf{R})} \right)^2 f(\mathbf{R}; \tau) + D \frac{\nabla_{\mathbf{R}}^2\varphi_T(\mathbf{R})}{\varphi_T(\mathbf{R})} f(\mathbf{R}; \tau) \\ &\quad + [V(\mathbf{R}) - E_T] f(\mathbf{R}; \tau) \end{aligned} \quad (200)$$

$$\begin{aligned} &= -D\nabla_{\mathbf{R}}^2 f(\mathbf{R}; \tau) + D\nabla_{\mathbf{R}} \cdot [F(\mathbf{R})f(\mathbf{R}; \tau)] \\ &\quad \left[ -D \frac{\nabla_{\mathbf{R}}^2\varphi_T(\mathbf{R})}{\varphi_T(\mathbf{R})} + V(\mathbf{R}) - E_T \right] f(\mathbf{R}; \tau), \end{aligned} \quad (201)$$

so finally we have

$$-\frac{\partial f(\mathbf{R}; \tau)}{\partial \tau} = -D\nabla_{\mathbf{R}}^2 f(\mathbf{R}; \tau) + D\nabla_{\mathbf{R}} \cdot [F(\mathbf{R})f(\mathbf{R}; \tau)] + [E_L(\mathbf{R}) - E_T] f(\mathbf{R}; \tau). \quad (202)$$

Here we have defined the *drift force* (or *drift velocity, quantum force*)

$$\mathbf{F}(\mathbf{R}) := \nabla_{\mathbf{R}} \ln |\varphi_T(\mathbf{R})|^2 = 2 \frac{\nabla_{\mathbf{R}}\varphi_T(\mathbf{R})}{\varphi_T(\mathbf{R})}, \quad (203)$$

and the *local energy* (this was used also in VMC)

$$E_L(\mathbf{R}) := \varphi_T(\mathbf{R})^{-1} \hat{\mathcal{H}} \varphi_T(\mathbf{R}). \quad (204)$$

Notice that these are calculated from the *trial state*  $\varphi_T(\mathbf{R})$ , so the expressions for  $\mathbf{F}(\mathbf{R})$  and  $E_L(\mathbf{R})$  are usually derived in analytic form before starting the DMC time evolution. In the appendix we show how to evaluate the local energy and the drift force for the McMillan trial wave function designed for two- or three-dimensional liquid <sup>4</sup>He. The first term in Eq. (202) is the usual diffusion term. The drift force guides the diffusion process to regions where  $\varphi_T(\mathbf{R})$  is large (direction of gradient).

Green's function corresponding to Eq. (202) is a modification of Eq. (177). One possible solution is

$$G(\mathbf{R}', \mathbf{R}; \tau) = (4\pi D\tau)^{-3N/2} e^{-\frac{(\mathbf{R}-\mathbf{R}'-\mathbf{F}(\mathbf{R})D\tau)^2}{4D\tau}} e^{-\tau(E_L(\mathbf{R})-E_T)} + \mathcal{O}(\tau^2). \quad (205)$$

---

<sup>25</sup>We exclude points where  $\varphi(\mathbf{R}) = 0$ , particles simply can't get there.

This is not unique: Should we drift the walkers before or after we've diffused them ( $\mathbf{F}(\mathbf{R})$  or  $\mathbf{F}(\mathbf{R}')$ )? This is once again a non-commutativity problem, drift and diffusion don't commute. Sometimes one uses  $\frac{1}{2}[\mathbf{F}(\mathbf{R}) + \mathbf{F}(\mathbf{R}')]^2$  and similarly in the local energy  $\frac{1}{2}[E_L(\mathbf{R}) + E_L(\mathbf{R}')]$ . We'll talk about modifications later.

Notice that (205) has no explicit dependence on  $V(\mathbf{R})$ ; It's up to our trial wave function  $\varphi_T(\mathbf{R})$  to lead to a drift force which guides the walkers to positions where  $E_L(\mathbf{R})$  has low values and where  $V(\mathbf{R})$  is not blowing up.

## 6.2 A working DMC algorithm

The Diffusion Monte Carlo (DMC) algorithm corresponding to Green's function (205) has now **drift, diffusion and branching**. Here is one possible procedure<sup>26</sup>:

1. Initialise many ( $\sim 100 - 500$ ) configurations, where walkers are distributed according to  $|\varphi_T(\mathbf{R})|^2$ . We don't want them all destroyed in the branching process, so we need to generate as diverse a set as possible. You can pick from a VMC run that samples  $|\varphi_T(\mathbf{R})|^2$  positions  $\mathbf{R}$  now and then to a **zeroth generation of configurations**. The total number of configurations in a generation is its **population**.

2. In each configuration of the present generation, move the  $i^{th}$  walker with

$$\mathbf{r}_i^{\text{new}} = \mathbf{r}_i + D\tau \mathbf{F}(\mathbf{R}) + \boldsymbol{\eta}\sqrt{2D\tau}, \quad (206)$$

where  $\boldsymbol{\eta}$  is a 3-dimensional Gaussian random vector.

3. Calculate a weight for the move,

$$\textit{ratio} = \frac{|\varphi_T(\mathbf{R}')|^2 G(\mathbf{R}', \mathbf{R}; \tau)}{|\varphi_T(\mathbf{R})|^2 G(\mathbf{R}, \mathbf{R}', \tau)}, \quad (207)$$

and accept the move  $\mathbf{R} \rightarrow \mathbf{R}'$  with probability  $\min[1, \textit{ratio}]$  ("Metropolis question")<sup>27</sup>.

4. Take each configuration in turn and make  $N_{\text{copies}}$  copies of it,

$$N_{\text{copies}} = \text{int}[e^{-\tau(E_L(\mathbf{R}) - E_T)} + \xi] \quad \xi \in U[0, 1], \quad (208)$$

5. Estimate the ground-state energy  $E_0$  by taking the average of the local energies of *current* generation.

6. Keep the population healthy by adjusting the trial energy  $E_T$ . One way is to use a feedback mechanism,

$$E_T = E_0 + \kappa \ln \frac{N_{C\text{target}}}{N_C}, \quad (209)$$

where  $E_0$  is the best guess for the ground-state energy we have so far,  $N_{C\text{target}}$  is the population we'd like to have, and  $N_C$  is the one we have now. The positive parameter  $\kappa$  should have the smallest value that does the job.

7. go back to step 2

---

<sup>26</sup>P. Reynolds, D. Ceperley, B. Alder, W. Lester Jr, J. Chem. Phys. **77(11)**, 5593 (1982).

<sup>27</sup>Green's function in the *ratio* is the transfer matrix in the Metropolis-Hastings detailed balance formula, Eq. (69)

Step 3 with acceptance/rejection guarantees that the algorithm satisfies the detailed balance condition. Moreover, it is the only way to make sure that we really are sampling the correct distribution at finite  $\tau$ . This accept-reject test is easy to convert back to VMC by leaving out the  $G$ 's - a very useful property. Sometimes this acceptance/rejection step is left out, the rational being that the acceptance has to be very close to 100 percent. Another reason is that acceptance/rejection may lead to a new problem of "persistent configurations", configurations that get stuck. These lead to erroneous energy vs.  $\tau$  results and to wrong extrapolations to zero  $\tau$ .

Step 4: We want to have *on average*  $e^{-\tau(E_L(\mathbf{R})-E_T)}$  copies of the configuration  $\mathbf{R}$ . This number not an integer and we treat the remainder as a probability: if it's bigger than  $\xi$ , round the number upward. In math,

$$\langle e^{-\tau(E_L(\mathbf{R})-E_T)} \rangle = \langle \text{int} [e^{-\tau(E_L(\mathbf{R})-E_T)} + \xi] \rangle . \quad (210)$$

In case  $N_{\text{copies}} = 0$  that configuration is killed; This is one reason why we start with large  $N_C$ . Another reason is that a small number of configurations introduces *bias* to the result, because the wave function is poorly represented.

**Bias** means that something is causing non-randomness.

The source of bias may be statistical (e.g. a bad pseudo-random number generator) or systematic (non-random choices made somewhere or the algorithm is imperfect).

One way to avoid replicating is **reweighting**. Instead of actually making copies or killing configurations, we give them a weight, which describes essentially the relative number of descendants that configuration would have had in the replicating algorithm up to that moment. We give that weight to all quantities measured from that configuration. In a reweighting-DMC one computes

$$\begin{aligned} w_i &= w_i e^{-(E_L(\mathbf{R}_i)-E_T)\tau} \quad \text{update weight} \\ E &= E + w_i E_L(\mathbf{R}_i) \quad \text{weighted contribution of a configuration} \end{aligned}$$

This method will be applied in section 6.7 to a  ${}^4\text{He}$  atom. Reweighting is known to lead to slightly larger variances than replicating.

The problem with reweighting is that the cumulative weights tend to either decrease toward zero or to increase without limit. A configuration that has a tiny weight is useless to the computation and one with extremely high weight will dominate over all other configurations leading to poor statistics. Hence in a longer DMC run one has to **renormalize the weights** in some fashion, which is not causing serious bias. You cannot simply split half configurations whose weight exceeds a fixed value, say 2. A rule of thumb is that unless every configuration has some chance to be split your algorithm is badly biased. You can choose the configurations to be split by favouring the high-weight ones. This can be done, for example, by a wheel of fortune depicted in Fig. 9, where the chance that you hit a high-weight configuration is large.

Pick up at random any other configuration and replace it with the chosen configuration and let both configurations now carry half of the weight the chosen configuration had before splitting.

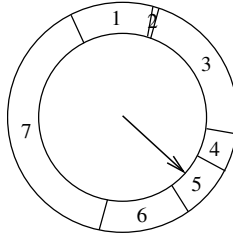


Figure 9: A way to choose a configuration, so that every one has a chance, but higher-weight ones are more probable. The lengths of the angular segments are the weights of the configurations. The angle of the pointer is chosen at random.

Commonly one starts with just one configuration, runs VMC for a while and picks up the  $N_C$  representative configurations. These too are run for a while using only VMC to get a good estimate for the energy of the trial wave function,

$$E_{\text{VMC}} = \langle \varphi_T | H | \varphi_T \rangle . \quad (211)$$

VMC steps are much faster to do than DMC steps, because the Gaussian step  $\eta$  can be much larger:  $\tau$  can be much larger, because VMC doesn't have to worry about any Green's function: no short time estimates are used.

The DMC evolution needs to be run for a while to let the excited states die out. The estimate  $E_0$  will be fluctuating around a fixed value and your subsequent generations will (hopefully) be sampling the distribution  $f(\mathbf{R}; \tau) = \varphi_T(\mathbf{R})\Psi(\mathbf{R}; \tau)$ . It's imaginary time to start collecting data for ground-state averages.

### 6.3 Mixed and pure estimators

Let's take a closer look at how averages are calculated using an importance sampling DMC algorithm. We need to be cautious, because the algorithm is *not* sampling the ground state directly, but the product state  $f(\tau) = \varphi_T \Psi(\tau)$  that approaches  $\varphi_T \phi_0$  as  $\tau \rightarrow \infty$ .

At time  $\tau$  the average of the local energy  $E_L(\tau)$  is (I'll drop the  $\mathbf{R}$ 's in the arguments to simplify notation)

$$\begin{aligned} E_{\text{mixed}} &= \frac{\int d\mathbf{R} f(\tau) E_L}{\int d\mathbf{R} f(\tau)} = \frac{\int d\mathbf{R} f(\tau) [\varphi_T^{-1} H \varphi_T]}{\int d\mathbf{R} f(\tau)} \\ &\rightarrow \frac{\int d\mathbf{R} \phi_0 H \varphi_T}{\int d\mathbf{R} \phi_0 \varphi_T}. \end{aligned} \quad (212)$$

This called a **mixed estimator**, because it is *not* the expectation value  $\langle \phi_0 | H | \phi_0 \rangle$ , but the mixed matrix element  $\langle \varphi_T | H | \phi_0 \rangle$ . We still get the correct ground-state energy directly out of importance sampling DMC, because

$$E_{\text{mixed}} = \frac{\int d\mathbf{R} \phi_0 \sum_i a_i E_i \phi_i}{\int d\mathbf{R} \phi_0 \sum_i a_i \phi_i} = E_0,$$

where the last step follows from orthogonality of the energy eigenstates. So the mean value of  $E_L$  is the ground-state energy also if importance sampling is used. What about the variance? We have

$$\begin{aligned} \sigma_E^2 &= \langle E_L^2 \rangle - E_0^2 = \frac{\int d\mathbf{R} f(\tau) E_L^2}{\int d\mathbf{R} f(\tau)} - E_0^2 \\ &\rightarrow \frac{\int d\mathbf{R} \varphi_T \phi_0 [\varphi_T^{-1} \hat{\mathcal{H}} \varphi_T] [\varphi_T^{-1} \hat{\mathcal{H}} \varphi_T]}{\int d\mathbf{R} \varphi_T \phi_0} - E_0^2 \\ &= \frac{\int d\mathbf{R} \phi_0 (\hat{\mathcal{H}} \varphi_T) \varphi_T^{-1} (\hat{\mathcal{H}} \varphi_T)}{\int d\mathbf{R} \varphi_T \phi_0} - E_0^2 \\ &= \frac{\int d\mathbf{R} \phi_0 (\sum_i a_i E_i \phi_i)^2 (\sum_i a_i \phi_i)^{-1}}{a_0} - E_0^2. \end{aligned} \quad (213)$$

If we have the perfect trial wave function ( $\varphi_T = \phi_0$ ;  $a_i = 0$  for  $i \neq 0$ ) , then  $\sigma_E^2 = 0$ . Same thing happens if you are evaluating the energy of an excited state and use exactly the correct wave function as  $\varphi_T$ . This is the famous **zero variance property**:

*The variance in the DMC energy will vanish for a trial wave function, which coincides with any eigenstate of the Hamiltonian.*

This is valid also for VMC. For a trial wave function that is an exact eigenstate this is trivial: The local energy will be just a constant, so no matter how you move your walkers you will — of course — always get that constant as the energy.

*The better the trial wave function, the smaller the error bars.*

Let's see what happens if you try to evaluate a quantity  $\hat{A}$  that does *not* commute with the Hamiltonian. Then you get also

$$\begin{aligned} A_{\text{mixed}} &= \frac{\int d\mathbf{R} f(\tau) [\varphi_T^{-1} \hat{A} \varphi_T]}{\int d\mathbf{R} f(\tau)} \\ &= \frac{\int d\mathbf{R} \phi_0 \hat{A} \varphi_T}{\int d\mathbf{R} \phi_0 \varphi_T} = \frac{\int d\mathbf{R} \phi_0 \hat{A} \sum_i a_i \phi_i}{a_0}, \end{aligned} \quad (214)$$

but this is where the road ends, because  $\phi_i$ 's are not eigenstates of  $\hat{A}$ . In this situation one commonly uses the so-called **extrapolated estimator**

$$\langle \phi_0 | A | \phi_0 \rangle \approx 2\langle \varphi_T | \hat{A} | \phi_0 \rangle - \langle \varphi_T | A | \varphi_T \rangle, \quad (215)$$

which assumes that the mixed estimator is “halfway” between the true ground-state and the VMC expectation values. Then one does a kind of linear extrapolation. More rigorously, one makes a (functional) Taylor expansion of the DMC and VMC estimators in terms of  $\Delta = \phi_0 - \varphi_T$ ,

$$\begin{aligned} \langle \phi_0 | \hat{A} | \varphi_T \rangle &= \langle \phi_0 | \hat{A} | \phi_0 \rangle + \int d\mathbf{R} \psi_0 [\langle \phi_0 | \hat{A} | \phi_0 \rangle - \hat{A}] \Delta + \mathcal{O}(\Delta^2) \\ \langle \varphi_T | \hat{A} | \varphi_T \rangle &= \langle \phi_0 | \hat{A} | \phi_0 \rangle + 2 \int d\mathbf{R} \psi_0 [\langle \phi_0 | \hat{A} | \phi_0 \rangle - \hat{A}] \Delta + \mathcal{O}(\Delta^2), \end{aligned} \quad (216)$$

so a combination of these gives

$$\langle \phi_0 | \hat{A} | \phi_0 \rangle = 2\langle \phi_0 | \hat{A} | \varphi_T \rangle - \langle \varphi_T | \hat{A} | \varphi_T \rangle + \mathcal{O}(\Delta^2). \quad (217)$$

Extrapolated estimators are needed very frequently, you cannot even determine the kinetic and potential energies directly:  $\hat{\mathcal{H}}$  commutes neither with  $\hat{\mathcal{T}}$  nor with  $\hat{\mathcal{V}}$ .

There is also a way to get more accurate ground-state expectation values for quantities that don't commute with  $\hat{\mathcal{H}}$ , known as **pure estimators**. A pure estimator means any estimator that is unbiased, *i.e.*, not affected by the choice of the trial wave function. The total energy in DMC is independent of  $\varphi_T$ , so it *is* already a pure estimator. But quantities that don't commute with the Hamiltonian (kinetic energy, potential energy, spatial distributions etc.) need special attention. I'm not going to describe the method in any detail, just mention that one needs to keep account of how long the configurations in the DMC run survive and how many descendants they have<sup>28</sup>.

---

<sup>28</sup>See, for example, Jordi Boronat's work in the 90's, published in Phys. Rev. B.

### Growth estimator

In DMC, the ground state energy can be obtained at least from two sources: (i) as the average of local energies,  $\langle E_L \rangle$  as in VMC or (ii) from the so-called growth estimator. The latter is based on the notion, that after the excited states have died out, the population (number of configurations) evolves during time  $\tau$  according to the equation

$$N(\tau) = e^{(E_0 - E_T)\tau} N(0) . \quad (218)$$

Solving for  $E_0$  one finds

$$E_0 = E_T + \frac{1}{\tau} \ln \frac{N(\tau)}{N(0)} . \quad (219)$$

This looks like the population control equation (209), just inverted to give  $E_0$ . Indeed, one has to refrain from adjusting the population manually during the evaluation period in Eq. (219). In practical application of the growth estimator it is profitable to have populations  $N(\tau)$  and  $N(0)$  evaluated at as distinct times as possible. The relation to the local energy is clear, since the population changes via branching, which is controlled by the local energy. The growth estimator is unpopular due to the large fluctuations in the population during a simulation, resulting in a large variance.

### The significance of branching in the DMC algorithm

In the importance sampling algorithm the total energy is the average over local energies evaluated at points  $\mathbf{R}$  generated by the DMC algorithm,

$$E_0 = \langle E_L \rangle_{\mathbf{R}} = \langle \varphi_T^{-1} \hat{\mathcal{H}} \varphi_T \rangle_{\mathbf{R}} \quad \text{with importance sampling .} \quad (220)$$

The functional form of  $E_L$  is completely determined by the trial wave function. The reason why averaging over  $E_L$  in DMC does give the true ground-state energy is that the configurations  $\mathbf{R}$  where one evaluates  $E_L(\mathbf{R})$  are biased due to branching.<sup>29</sup>

To bring in the significance of branching even more dramatically, let's do a most simple importance sampling and set  $\varphi_T = 1$  — a perfectly admissible choice for bosons. Now we get zero drift,

$$\mathbf{F}(\mathbf{R}) = 2 \frac{\nabla \varphi_T(\mathbf{R})}{\varphi_T(\mathbf{R})} = 2 \frac{\nabla(1)}{1} = 0 , \quad (221)$$

and the ground state energy is

$$E_0 = \langle E_L \rangle_{\mathbf{R}} = \langle 1^{-1} \hat{\mathcal{H}} 1 \rangle_{\mathbf{R}} = \langle -D \nabla_{\mathbf{R}}^2(1) + V(\mathbf{R}) \rangle_{\mathbf{R}} = \langle V(\mathbf{R}) \rangle_{\mathbf{R}} ! \quad (222)$$

Now branching has a huge job in biasing the positions  $\mathbf{R}$  so that the average of potentials  $V(\mathbf{R})$  gives the total ground-state energy. Essentially we get the correct ground-state energy by computing the value of the *potential energy* at well-chosen points ! Conversely, if  $\varphi_T(\mathbf{R})$  is perfect (an eigenstate), there is no branching at all.<sup>30</sup>

---

<sup>29</sup>Of course, reweighting can be used to achieve the same effect.

<sup>30</sup>If  $\varphi_T = 1$ , the only energy measure available is the potential energy. You have to get every energy-related

## 6.4 Fixed node and released node methods

The ground state of a many-body Bose system can always be chosen to be real and positive, so the quantity  $f(\mathbf{R}) = \varphi_T(\mathbf{R})\phi_0(\mathbf{R})$  can be safely interpreted as density in the diffusion process. Excited states and Fermi systems are more problematic, because the exact wave function has nodes (zeros)<sup>31</sup>. The negative areas themselves are not bothering us, because one can define

$$\phi(\mathbf{R}) = \phi^+(\mathbf{R}) - \phi^-(\mathbf{R}) , \quad (223)$$

where both  $\phi^+$  and  $\phi^-$  are positive and use them as densities. The Schrödinger equation can be written separately for both parts. Similar decomposition is done for the trial wave function, too. Eq. (223) is trivially satisfied by, for example,

$$\phi^\pm(\mathbf{R}) = \frac{1}{2} [| \phi(\mathbf{R}) | \pm \phi(\mathbf{R})] . \quad (224)$$

Now that I mentioned Fermi systems, it would seem appropriate to give an example of what the trial wave function might look like. The Slater-Jastrow wave function is given by

$$\varphi_T(\mathbf{R}) = \det(A_\uparrow) \det(A \downarrow) e^{U(\mathbf{R})} , \quad (225)$$

where  $A_\uparrow$  and  $A \downarrow$  are Slater matrices made of spin up and spin down single-particle orbitals; the Slater matrix is

$$A = \begin{pmatrix} \varphi_1(\mathbf{r}_1) & \varphi_1(\mathbf{r}_2) & \dots & \varphi_1(\mathbf{r}_N) \\ \varphi_2(\mathbf{r}_1) & \varphi_2(\mathbf{r}_2) & \dots & \varphi_2(\mathbf{r}_N) \\ \vdots & \vdots & \ddots & \vdots \\ \varphi_N(\mathbf{r}_1) & \varphi_N(\mathbf{r}_2) & \dots & \varphi_N(\mathbf{r}_N) \end{pmatrix} . \quad (226)$$

Orbitals  $\varphi_i$  can be, *e.g.*, plane waves or molecular orbitals. The term  $e^{U(\mathbf{R})}$  is the Jastrow factor (see the appendix for details).

The problem is that we usually have very little or no idea where the nodes of  $\phi$  are. The trial wave function is supposed to approximate the true solution, so we can choose one which has nodes. But this choice is forced upon the final solution:

$$\varphi_T(\mathbf{R}_0) = 0 \Rightarrow f(\mathbf{R}_0, \tau) = \varphi_T(\mathbf{R}_0)\psi(\mathbf{R}_0, \tau) = 0 , \quad (227)$$

and no amount of imaginary time evolution will make the zeroes to change a bit. If, as usual, the nodes of  $\varphi_T$  and  $\phi$  do not coincide, then near the nodes we would be badly undersampling  $\phi$ ; the result will certainly be biased and unreliable. Anyhow, this is exactly what is done in the **fixed node method**<sup>32</sup>.

---

quantity out of  $V(\mathbf{R})$ .

<sup>31</sup>We really need to impose those nodes somehow, without them the Bose case will converge to the ground state and the Fermi case will not obey the Pauli principle and cease to be a Fermi case.

<sup>32</sup>This section relies heavily on Jordi Boronat's section in Valencia lecture notes (1997).

One can see how the walkers avoid the nodes by looking at the drift force  $\mathbf{F}(\mathbf{R})$ , see Fig. 10. The drift is away from the nodes (nodal surfaces); At the nodes  $\mathbf{F}(\mathbf{R})$  is infinite and walkers shouldn't be able to cross nodal surfaces. Due to the finite time step  $\tau$  some walkers do cross, and usually one just deletes such spurious configurations from the set. This is not the best way, and in literature it's argued that it would be better just to reject moves that would cross a nodal surface. Of course, if the nodes of  $\varphi_T$  happened to coincide with the exact ones, then

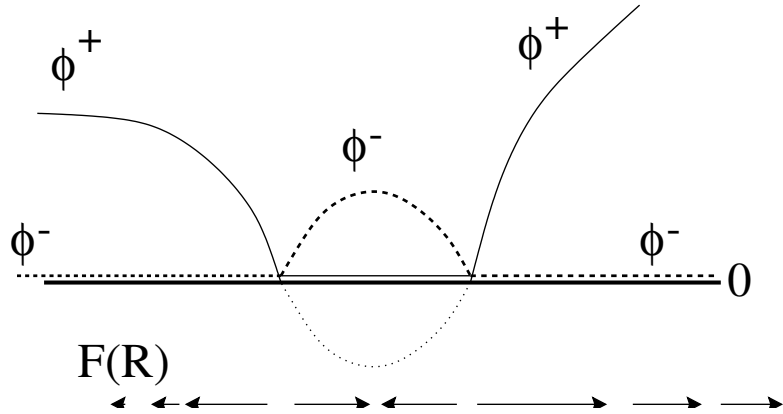


Figure 10: The drift force near the nodes of the wave function (trial or exact) and the decomposition proposed in Eq.(224).

$\phi$  would also be correctly sampled in the fixed node DMC. Until recently it was believed, that with the fixed-node DMC one always gets a variational upper bound for the exact eigenvalues. However, Foulkes, Hood and Needs<sup>33</sup> showed that this is true only if the state in question is non-degenerate or has only accidental degeneracy.

Many of the shortcomings of the fixed node method has been known ever since it was first applied, and something had to be done to somehow let the nodes of  $\varphi_T$  move towards the true nodes of  $\phi$  as the computation progresses. In the **released node method** one lets the walkers to cross nodal surfaces. One assigns a “colour” (red/blue) or a sign ( $\pm 1$ ) to each walker, which keeps track of whether the walker has crossed the nodal surface odd or even times. Each walker crossing a nodal surface “pulls” the surface with it to some extent. Only to some extent, because a single walker has only statistical significance, and a red walker in the midsts of blue ones does not mean the true nodal surface makes a wild loop to engulf that solitary walker. Thus we need to restrict the effect of a single walker, and usually it is done by letting the walker carry its original colour only for a finite “lifetime”  $\tau_r$ . Just like a hot chicken cooling in a box of icy chickens.

Next one must let the walkers to cross nodal surfaces, not only spuriously but in honest. One way is to use a slightly modified trial function, such as

$$\varphi'_T(\mathbf{R}) = \sqrt{|\varphi_T(\mathbf{R})|^2 + a^2} . \quad (228)$$

---

<sup>33</sup>W. M. C. Foulkes, R. Q. Hood and R. J. Needs, Phys. Rev. B **60**, 4558 (1999).

With proper value of  $a$  this approaches  $\varphi_T$  far away from the nodes. Parameter  $a$  controls the amount of flow across nodal surfaces, and for larger  $a$  we take shorter lifetime  $\tau_r$  and vice versa.

The fact that we have tinkered with our trial wave function can be compensated by attaching to each walker a weight

$$W(\mathbf{R}) = \sigma(\mathbf{R}) \frac{|\varphi_T(\mathbf{R})|}{\varphi'_T(\mathbf{R})} , \quad (229)$$

where the sign carried by the walker,  $\sigma(\mathbf{R})$ , is  $+1$  ( $-1$ ) for even (odd) number of crossings. It can be shown that using  $\varphi'_T(\mathbf{R})$  affects only the variance, and not the mean of the total energy. The released node energy has also the lifetime  $\tau_r$  as a parameter, and it's customary to define

$$E_{RN}(\tau_r) = \frac{\sum_{\tau \leq \tau_r} E_L(\mathbf{R}) W(\mathbf{R})}{\sum_{\tau \leq \tau_r} W(\mathbf{R})} , \quad (230)$$

where the sums are over walkers that have survived and have lifetime less than  $\tau_r$ . We are interested in the asymptotic region of large  $\tau_r$ , and one usually plots the sequence of energies for  $\tau_r^1 < \tau_r^2 < \dots < \tau_r^{\max}$ , which reveals the systematic error in the released-node energy.

## 6.5 Excited states

Here we take a closer look at how excited-state eigenvalues could be obtained from a DMC run. The list is by no means complete, the question has no satisfactory solution and is under constant research.

**Using orthogonality**  $\langle \varphi_T | \phi_0 \rangle = 0$  If the trial wave function is orthogonal to the ground state, the DMC process stabilises to an excited state with proper choice of the trial energy  $E_T$ . In the large- $\tau$  limit all high-energy states have died out and we are left with the two lowest ones. According to (223) we have

$$\Psi(\tau \rightarrow \infty) = \phi = \phi^+ - \phi^- , \quad (231)$$

where the two components are

$$\phi^\pm = c_0 \phi_0 e^{(E_1 - E_0)\tau} \pm c_1 \phi_1 . \quad (232)$$

This form reveals where the problem lies. The difference  $(\phi^+ - \phi^-)$  depends only on the first excited state, so the expectation value of the local energy will be stabilising to  $E_1$ . The variance, however, depends on  $(\Psi H)^2$ , so the orthogonality  $\langle \varphi_T | \phi_0 \rangle = 0$  does not eliminate the ground state contribution from the variance. And that contribution is increasing exponentially, as (232) shows. The strategy is then to achieve a quick decay to the first excited state before the ground-state “noise” overwhelms the signal. This is happening only if our trial state is very close to the true first excited state.

**Using decay curves** In principle, we could extract excited-state information from the decay curves. By fitting

$$E(\tau) = \frac{\sum c_i a_i e^{-(E_i - E_T)\tau} E_i}{\sum c_i a_i e^{-(E_i - E_T)\tau}} \quad (233)$$

to the DMC energy we could get  $E_i$ . However, this has turned out to be impractical, because  $E(\tau)$  depends on two exponentially decaying functions and the data is dominated by statistical noise. It would be more easy to fit, instead, the expectation value of the Green's function, which has only one exponent function:

$$I(\tau) = \langle \varphi_T | e^{-(H - E_T)\tau} | \varphi_T \rangle . \quad (234)$$

This function can be sampled during the random walk by evaluating the **cumulative branching weight**

$$I(\tau) = \langle \varphi_T | \prod_{k=0}^N e^{-(E_L - E_T)\tau} | \varphi_T \rangle . \quad (235)$$

The time dependence is simply

$$I(\tau) = \sum a_i^2 e^{-(E_i - E_T)\tau} , \quad (236)$$

which is much easier to fit. But again, the data is governed by statistical noise<sup>34</sup>. Fitting to exponentially decaying curves is an inverse Laplace transform - a perfectly stable task in the absence of statistical noise. If the data is noisy, the Laplace problem can be regularised by the use of a statistical **maximum entropy method**, in which prior knowledge is used to bias the inversion<sup>35</sup>. One faces a similar situation in path integral Monte Carlo (PIMC) calculations of the dynamic structure function, where the numerical inaccuracy shows up as rounded peaks in  $S(k, \omega)$ <sup>36</sup>

**Using the zero variance property** One way to search for the excited states owes to the fact that they are eigenstates of the Hamiltonian, which means that they have lower (zero) variance than other energies. In theory, one could take a sweep through the energies above the ground-state energy and look for minima in the variance. Unfortunately, statistical noise deems this method prohibitively expensive<sup>37</sup>.

**Matrix Monte Carlo method by Ceperley and Bernu**<sup>38</sup> Take  $m$  states, which hopefully have large overlap with the first  $m$  excited states of the system. Then McDonald's theorem

---

<sup>34</sup>D. Ceperley and B. Bernu. J. Chem. Phys. , 89 (1988) 6316.

<sup>35</sup>M. Caffarel and D. Ceperley, J. Chem. Phys. 97 (1992) 8415.

<sup>36</sup>M. Boninsegni and D. Ceperley, J. Low Temp. Phys. 104 (1996) 339.

<sup>37</sup>A. J. Williamson, PhD thesis, Cavendish Laboratory, September 1996.

<sup>38</sup>D. M. Ceperley and B. J. Bernu, J. Chem. Phys. 89 (1988) 6316.

states, that if you simultaneously diagonalise both the overlap matrix and the Hamiltonian, then the  $n$ th eigenvalue is an upper limit to the exact energy of the  $n$ th state. One can then use the DMC states  $f(\tau)$  to construct these matrices, and it can be shown that the eigenvalues approach the exact ones exponentially fast. Unfortunately, also the statistical noise increases exponentially fast. The method has been applied to small molecules and two-dimensional electron gas. There is a nice, short introduction to the method in the Valencia lecture notes by J. Boronat.

## 6.6 Second order DMC algorithms

A DMC algorithms is said to be first order, if the timestep error in the total energy is linear,  $E(\tau) = E_0 + a\tau$ . It would be desirable to find a second order algorithm,  $E(\tau) = E_0 + b\tau^2$ , so that larger timesteps could be used, possibly without any  $\tau \rightarrow 0$  extrapolations. This section will follow closely the discussion given by Chin<sup>39</sup>.

In section 6.1 we made a short-timestep approximation to the Green's function. To begin with, the Campbell-Baker-Hausdorff formula states that

$$e^A e^B = e^{A+B+\frac{1}{2}[A,B]+\frac{1}{12}[A-B,[A,B]]+\dots}. \quad (237)$$

This shows that the exact Green's function<sup>40</sup>

$$G = e^{-(H-E_T)\tau} = e^{-(T+V-E_T)\tau} \quad (238)$$

can be approximated as

$$G \approx e^{-(H'-E_T)\tau}, \quad (239)$$

where

$$H' = H - \frac{1}{2}\tau[H, V] + \frac{1}{12}\tau^2[H - 2V, [H, V]] + \dots. \quad (240)$$

But this is just the exact Hamiltonian  $H$  plus a small perturbation, and one can formally compute the result of the DMC calculation. Keeping only the first two terms in (240) leads to the short-time approximation to the Green's function derived earlier in these lecture notes. The ground state of that  $H'$  is

$$|\phi'_0\rangle = |\phi_0\rangle + \frac{1}{2}\tau V|\phi_0\rangle + \dots. \quad (241)$$

The first order term in (240) vanishes between eigenstates,

$$\langle\phi_i|[H, V]|\phi_i\rangle = 0, \quad (242)$$

---

<sup>39</sup>S. A. Chin, Phys. Rev. **A42** (1990) 6991.

<sup>40</sup>Chin thinks of the Hamiltonian as a matrix, hence  $G$  is a *transfer matrix*.

so although the eigenstates are first order in  $\tau$ , the eigenvalues are quadratic in  $\tau$ :

$$E'_0 = E_0 - \frac{1}{24}\tau^2\langle\phi_0|[V,[H,V]]|\phi_0\rangle + \dots . \quad (243)$$

This means that *without* importance sampling the primitive approximation to the Green's function (as it will be called in the PIMC section 7) is already quadratic. Still, the energy (243) is not showing the  $\tau$ -dependence of the energy that really comes out from an importance sampling DMC code. If this surprises you, remember that if one introduces a trial wave function one is not sampling  $|\phi_0|^2$ , but  $\phi_0\varphi_T$ . Hence the energy that is the average local energy over the distribution  $\phi_0\varphi_T$  behaves as

$$\begin{aligned} E_{DMC} &:= \frac{\langle\phi_0|H|\varphi_T\rangle}{\langle\phi_0|\varphi_T\rangle} \\ &= E_0 + \frac{1}{2}\tau\frac{\langle\phi_0|[H,V]|\varphi_T\rangle}{\langle\phi_0|\varphi_T\rangle} + \dots , \end{aligned} \quad (244)$$

which is just first order.

Quadratic  $E_{DMC}$  can be rather easily found by looking at the Campbell-Baker-Hausdorff formula. The undesired first order term will cancel if one takes a product of operators at half the timestep and another set with reversed order. One such approximate Green's function would be

$$G \approx e^{-\frac{1}{2}\tau V}e^{-\frac{1}{2}\tau T}e^{-\frac{1}{2}\tau T}e^{-\frac{1}{2}\tau V}, \quad (245)$$

which approximates the Hamiltonian

$$H' = H + \frac{1}{24}\tau^2[(2H - V), [H, V]] + \dots , \quad (246)$$

and the corresponding importance sampled DMC energy is

$$E_{DMC} = E_0 + \frac{1}{24}\tau^2 \left[ \langle\phi_0|\Delta H|\phi_0\rangle - \frac{\langle\phi_0|\Delta H|\phi_0\rangle}{\langle\phi_0|\phi_0\rangle} \right], \quad (247)$$

where

$$\Delta H = [(2H - V), [H, V]]. \quad (248)$$

Now we have at hand an approximate Green's function that leads to a quadratic DMC energy. However, the implementation of the Langevin algorithm that is used to solve the underlying Fokker-Planck equation can still turn the code first order. I will not discuss the subject at length, for more details see Chin's 1990 article. I just remind you what was noted below Eq. (205), that the way one combines the *deterministic* drift force to the *stochastic* Gaussian move is not unique. It is easy to imagine that a non-symmetrical way of doing this will give

rise to a first order DMC algorithm. The recipe is similar as in the Green's function: take intermediate steps, very much like in solving differential equations using Runge-Kutta and the kind.

At first glance it would seem that developing an even higher order DMC algorithm is an easy task. But Suzuki showed 1991<sup>41</sup>, that in the expansion

$$e^{(T+V)\tau} = \prod_{i=1}^N e^{a_i T \tau} e^{b_i V \tau} \quad (249)$$

one can go only up to second order without having some of the coefficients  $a_i$  and  $b_i$  negative. But a negative  $a_i$  would mean diffusion backwards in time, which is impossible to simulate!

Suzuki's "no-go theorem" means only that higher than second order algorithms must be based on a different kind of operator splitting than the one in Eq. (249).

Expansion of the Green's function is not just a Monte Carlo task. Recently Auer, Krotscheck and Chin published an application of fourth order algorithm (error  $\mathcal{O}(\tau^4)$ ) to solve non-trivial, three-dimensional Schrödinger equations<sup>42</sup>

**Second order algorithm** The following five stage algorithm will give a second order energy convergence. In the following  $r(k, i)$  is the  $k$ th coordinate of  $i$ th walker in configuration  $j$  (not marked):

1. Take a half-size timestep with a Gaussian of variance  $D\tau$ :

```
r(k, i) = r(k, i) + sqrt(D*tau)*gauss()
```

2. Compute the drift force using the new coordinates,  $\mathbf{F}(\mathbf{R})$ .
3. Move walkers according to that drift for half a timestep; keep the old configuration  $\mathbf{R}$  in memory for later use:

```
rp(k, i) = r(k, i) + 0.5d0*D*tau*F(k, i)
```

This gives you the configuration  $\mathbf{R}'$ .

4. Compute the drift force  $\mathbf{F}(\mathbf{R}')$ ; I call it  $\mathbf{FRP}$ .
5. In configuration  $\mathbf{R}$  (not in  $\mathbf{R}'!$ ), take a half-size Gaussian step and move walkers full step with drift force  $\mathbf{F}(\mathbf{R}')$ :

```
rp(k, i) = r(k, i)+D*tau*FRP(k, i)+sqrt(D*tau)*gauss()
```

---

<sup>41</sup>M. Suzuki, J. Math. Phys. 32, 400 (1991).

<sup>42</sup>J. Auer, E. Krotscheck, and S. A. Chin, J. Chem. Phys. 115 (2001) 6841.

This gives you a new configuration  $\mathbf{R}'$ , which is not the same as in step 3! That old  $\mathbf{R}'$  is not needed any more, and I make use of the memory space.

This algorithm is Eq. (25) in Chin's article, where it was given in the form

$$y_i = x_i + \sqrt{\Delta t/2} \xi_i \quad (250)$$

$$x'_i = y_i + \Delta t G_i((\mathbf{y} + \frac{1}{2}\Delta t \mathbf{G}(\mathbf{y})) + \sqrt{\Delta t/2} \xi_i), \quad (251)$$

where  $\xi$  is Gaussian random number with unit variance (as our  $\eta$  before). In the algorithm  $x_i$  and  $y_i$  are both  $\mathbf{R}$ , because  $x_i$  is not needed later and it's unnecessary to keep it in store. Also  $G$  is *half* our drift force and  $D = 1/2$ . After these changes one recovers the algorithm given above.

After these steps you have a new trial configuration  $\mathbf{R}'$  that you can accept or discard (use the modified Metropolis question with the Green's functions). These steps are done for each coordinate, each walker and in the outmost loop, for each configuration in the present generation. Only after all the steps are done you have the next generation ready.

## 6.7 DMC Example: the ground state of a He atom

The He atom can be used to show how DMC works in practise. The He ion is in the origin (with infinite mass in the present approximation) and the coordinates of the two electrons are  $\mathbf{r}_1$  and  $\mathbf{r}_2$ . Their spins are assumed to be antiparallel. If  $\nabla_i$  operates on the  $i$ th particle, the Schrödinger equation for bound states of helium in atomic units reads<sup>43</sup>

$$\left[ -\frac{1}{2}\nabla_1^2 - \frac{1}{2}\nabla_2^2 - \frac{2}{r_1} - \frac{2}{r_2} + \frac{1}{r_{12}} \right] \varphi(\mathbf{r}_1, \mathbf{r}_2) = E\varphi(\mathbf{r}_1, \mathbf{r}_2), \quad (252)$$

where  $r_{12} = |\mathbf{r}_1 - \mathbf{r}_2|$  is the distance between the electrons.

Next you need to write down the trial wave function and find the expression for the local energy. A simple choice would be the product of two 1S hydrogen orbitals,

$$\varphi_T(\mathbf{r}_1, \mathbf{r}_2) = e^{-\alpha r_1} e^{-\alpha r_2}, \quad (253)$$

which gives the local energy

$$\begin{aligned} E_L &= \varphi_T(\mathbf{r}_1, \mathbf{r}_2)^{-1} H \varphi_T(\mathbf{r}_1, \mathbf{r}_2) \\ &= e^{\alpha r_1} e^{\alpha r_2} \left[ -\frac{1}{2}\nabla_1^2 - \frac{1}{2}\nabla_2^2 - \underbrace{\frac{2}{r_1} + \frac{2}{r_2}}_{\text{kinetic part}} + \underbrace{\frac{1}{r_{12}}}_{\text{potential part}} \right] (e^{-\alpha r_1} e^{-\alpha r_2}) \\ &= -\alpha^2 + \underbrace{\frac{\alpha}{r_1} + \frac{\alpha}{r_2}}_{\text{kinetic part}} - \underbrace{\frac{2}{r_1} - \frac{2}{r_2}}_{\text{potential part}} + \frac{1}{r_{12}}. \end{aligned} \quad (254)$$

---

<sup>43</sup>Atomic units: energy in Hartrees (1 Ha = 2 Ry), distance in Bohr radia.

Notice that the “kinetic part” is *not* the kinetic energy of the trial state: The “kinetic part” can be negative for some choices of  $r_1$  and  $r_2$ ! It has only a statistical meaning, the averages give the kinetic and the potential energy, but one has to remember that since  $[H, T] \neq 0$  and  $[H, V] \neq 0$ , one gets by straightforward averaging only their mixed estimates. The “kinetic part” is an approximate energy contribution brought into the local energy by the use of a trial wave function, and it’s sole purpose is to try to cancel potential energy fluctuations when  $r_1$ ,  $r_2$  and  $r_{12}$  are changing. In real world large negative potential energy is compensated by large positive kinetic energy.

Variance optimization is tricky, because this 1S-orbital trial state is so far from the true ground state of He. For example, this trial wave function won’t keep the electrons apart. Minimum energy will be reached with  $\alpha = 1.6875$ , but the variance is at minimum at a slightly higher value. This value depends on the (fixed) set of configurations you happen to be using for optimization: If the set has many electrons near the origin, the variance optimization will try to make the Coulomb terms cancel as well as it can and at the same time try to minimise the energy, hence  $\alpha$  would be between 1.6875 and 2.0. On the other hand, if your configurations happen to be such that the potential energies are moderate, then the Coulomb cancellation will seem less acute and the optimal value of  $\alpha$  would be closer to 1.6875.

I applied the reweighting algorithm with the wheel-of-fortune type of weight renormalization. All attempted moves were accepted, so the algorithm did not rigorously satisfy the detailed balance condition. As is evident from Fig. 11, characteristic to the used algorithm is that the **timestep error** is linear for small  $\tau$ , but for larger time steps this linearity breaks down. Not shown in the figure is that a long computation with  $\alpha = 1.6875$  has large jumps in the variance due to electrons coming too close to the nucleus. Although this parameter gives the lowest trial-state energy, it is not the most stable when it comes to energy variance. Fig. 11 also shows the results for  $\alpha = 2$ , with some very large timesteps. The energy fluctuations are now in better control, as Fig. 12 shows. The negative spikes are characteristic to the  $\alpha = 1.6875$ -calculation, and even larger ones occur now and then causing sudden jumps to the energy variance. Smaller positive spikes are seen in the  $\alpha = 2.0$  data; they originate from the  $1/r_{12}$  electron repulsion, but they are less catastrophic to the variance.

The kinetic and potential energies of the trial state with  $\alpha = 2.0$  are  $\langle \varphi_T | T | \varphi_T \rangle = 4.0007 \pm 0.0009$  and  $\langle \varphi_T | V | \varphi_T \rangle = -6.7507 \pm 0.0008$ , respectively. The DMC calculation gave, after extrapolation to zero timestep,  $\langle \phi_0 | T | \varphi_T \rangle = 3.375$  and  $\langle \phi_0 | V | \varphi_T \rangle = -6.280$  (no error analysis was made). Hence the extrapolated estimators are  $E_{kin} = 2.750$  and  $E_{pot} = -5.809$  (unknown error). The total energy computed from these is  $-3.059$  with much larger error bars than in the total energy computed directly (-2.90465 in the present simulation vs. the exact value -2.903724). Deviations between the trial state energies and the DMC values give some measure to how close the trial state is to the true ground state: quite far in the present case. For the record, the total energy of the trial state was  $E_{trial} = -2.7500 \pm 0.0002$  from the same simulation. As always, the total energy comes out more accurately than the kinetic or the potential energy. Part of the potential energy fluctuations has been cancelled by the kinetic energy fluctuations.

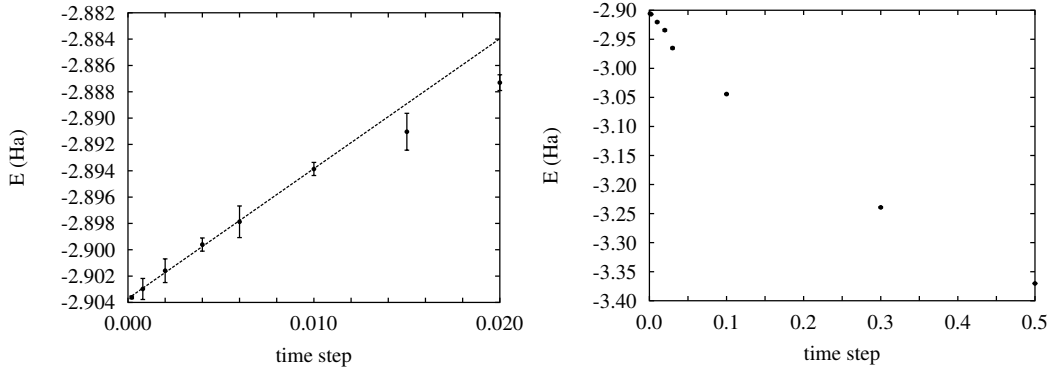


Figure 11: The dependence of the calculated total energy of a He atom of the time step in DMC. The error bars are obtained via **block averaging**. The upper panel show the results for  $\alpha = 1.6875$ , the lower for  $\alpha = 2.0$ . The extrapolated zero time step result from the upper panel data is -2.90374 Ha (four correct desimals).

Fig. 13 shows the DMC energy as a function of the time step obtained using the quadratic DMC algorithm given earlier. The error bars show the statistical error estimated using block averaging. The computation was continued until the  $\sigma$  of all data was 0.0005, therefore the small-time-step results have larger error bars. The least square fit shown in the figure is  $f(\tau) = -2.90286 - 2.1263 \tau^2$ , the horizontal line is the exact energy -2.903724. The shown results are obtained after a set of short runs, and the error bars are too large for serious use. However, the overall quadratic behaviour of the time-step error is evident.

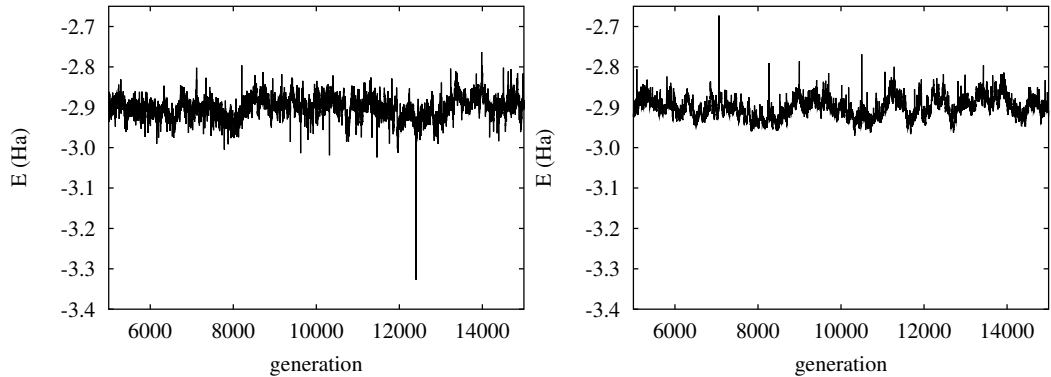


Figure 12: Plots of the local energy averages taken over 2000 configurations during over a set of generations for  $\alpha = 1.6875$  (upper panel) and  $\alpha = 2.0$  (lower panel). The time step was 0.001. The plot shows only a tiny fraction of the data collected for the results given in Fig. 11.

**T A B L E 9.2**  
Ground-State Energy of a Helium Atom<sup>a</sup>

Method	Energy/E <sub>h</sub>	Ionization energy/E <sub>h</sub>	Ionization energy/kJ·mol <sup>-1</sup>
<i>Perturbation calculations</i>			
Complete neglect of the interelectronic repulsion term	-4.0000	2.000	5250
First-order perturbation theory	-2.7500	0.7500	1969
Second-order perturbation theory	-2.9077	0.9077	2383
Thirteenth-order perturbation theory <sup>b</sup>	-2.903 724 33	0.903 724 33	2373
<i>Variational calculations</i>			
(1s) <sup>2</sup> with $\zeta = 1.6875$	-2.8477	0.8477	2226
Eckart, Equation 9.13 <sup>c</sup>	-2.8757	0.8757	2299
Hartree–Fock <sup>d</sup>	-2.861 68	0.8617	2262
Hylleraas, <sup>e</sup> 10 parameters	-2.903 63	0.903 63	2372
Pekeris, <sup>f</sup> 1078 parameters	-2.903 724 375	0.903 724 375	2373
<i>Experimental value</i>	-2.9033	0.9033	2373

a. These are nonrelativistic, fixed-nucleus approximation energies. Corrections for nuclear motion and relativistic corrections can be estimated to be  $10^{-4}E_h$ .

b. Scheer, C. W., Knight, R. E. Two-Electron Atoms III. A Sixth-Order Perturbation Study of the 1<sup>1</sup>S Ground State. *Rev. Mod. Phys.*, **35**, 426 (1963).

c. Eckart, C. E. The Theory and Calculation of Screening Constants. *Phys. Rev.*, **36**, 878 (1930).

d. Clementi, E., Roetti, C. Roothaan–Hartree–Fock atomic wavefunctions: Basis functions and their coefficients for ground and certain excited states of neutral and ionized atoms,  $Z \leq 54$ . *At. Data Nucl. Data Tables*, **14** (3–4), 177 (1974).

e. Hylleraas, E. A. Neue Berechnung der Energie des Heliums in Grundzustande, sowie des tiefsten Terms von Ortho-Helium. *Z. Physik*, **54**, 347 (1929).

f. Pekeris, C. L. 1<sup>1</sup>S and 2<sup>3</sup>S States of Helium. *Phys. Rev.*, **115**, 1216 (1959).

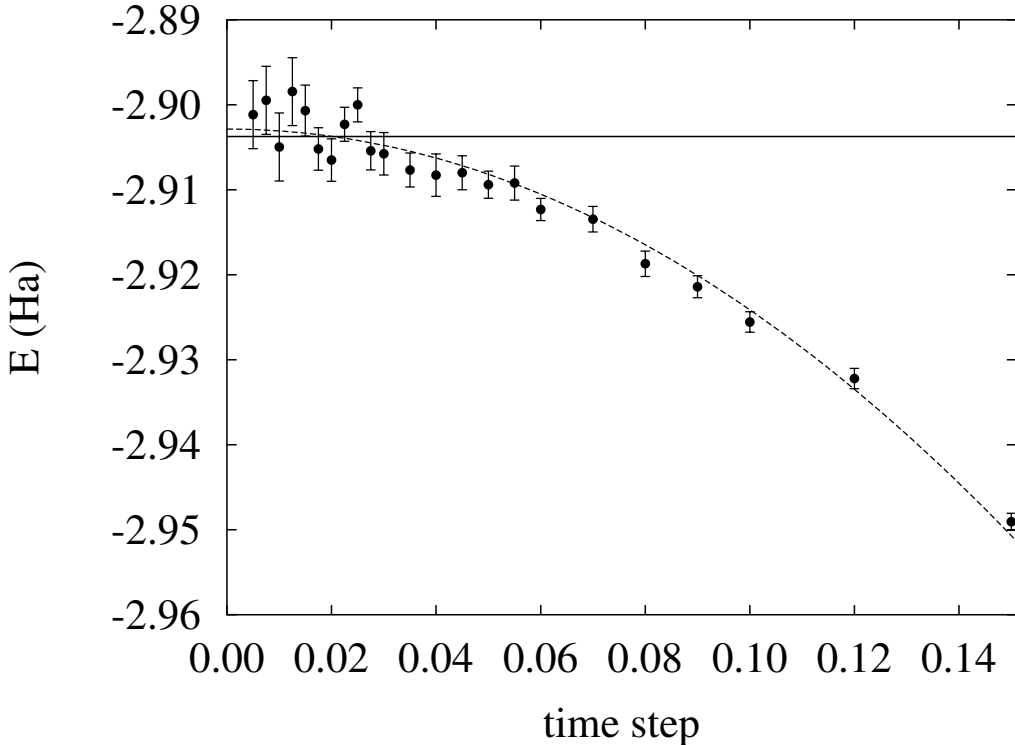


Figure 13: Time-step error in the quadratic DMC code, with a trial state that has 2S orbital states.

## 7 Path Integral Monte Carlo

Path Integral Monte Carlo (PIMC) is a Monte Carlo application of Feynman’s path integral formulation of quantum mechanics. It is very powerful and leads to in principle exact results at *finite temperature*. I shall be talking about bosons in equilibrium, but some remarks on fermion will be made in the end. The main reference to ideas presented in this section are from the review article by David Ceperley<sup>44</sup>

Our task is to sample the coordinate space so, that the energy eigenstates are visited according to the Maxwell–Boltzmann probability  $e^{-\beta E_N}$ . The basic quantity at finite temperature  $T$  is the (thermal) **density operator**,

$$\hat{\rho}(\beta) := e^{-\beta \hat{H}} \quad (255)$$

$$\beta := \frac{1}{k_B T} . \quad (256)$$

<sup>44</sup>D. Ceperley, *Path integrals in the theory of condensed helium*, Rev. Mod. Phys. **67** (1995) 279.

In coordinate space representation ( $|\mathbf{R}\rangle = \sum_n \phi_n(\mathbf{R})|\phi_n\rangle$ ) this is the **density matrix**,

$$\rho(\mathbf{R}, \mathbf{R}'; \beta) := \langle \mathbf{R}|e^{-\beta H}|\mathbf{R}'\rangle = \sum_n \phi_n(\mathbf{R})^* \phi_n(\mathbf{R}') e^{-\beta E_n}, \quad (257)$$

where the sum is over all states  $n$  and  $\phi_n(\mathbf{r})$  are the eigenfunctions of the Hamiltonian with energy  $E_n$ . Since these eigenstates are unknown for  $N$ -body systems, we must find a more practical way to compute the density matrix. But let's first list what we can do with the density matrix.

All static properties of the system can be computed from the density matrix. The expectation value of an arbitrary operator  $\hat{A}$  is

$$\langle \hat{A} \rangle := Z(\beta)^{-1} \sum_n \langle \phi_n | \hat{A} | \phi_n \rangle e^{-\beta E_n} \quad (258)$$

$$= Z(\beta)^{-1} \int d\mathbf{R} d\mathbf{R}' \rho(\mathbf{R}, \mathbf{R}'; \beta) \langle \mathbf{R} | \hat{A} | \mathbf{R}' \rangle, \quad (259)$$

where the normalization is the **partition function**,

$$Z(\beta) = \sum_n e^{-\beta E_n} = \sum_n \langle n | e^{-\beta H} | n \rangle \quad (260)$$

$$= \int d\mathbf{R} \langle \mathbf{R} | e^{-\beta H} | \mathbf{R} \rangle = \int d\mathbf{R} \rho(\mathbf{R}, \mathbf{R}; \beta). \quad (261)$$

Notice, how  $Z$  depends only on the *diagonal* part of the density matrix: there's only one  $\mathbf{R}$ . From statistical physics we know that

$$F = -k_B T \ln Z \quad \text{Helmholtz free energy} \quad (262)$$

$$\langle E \rangle = -\frac{\partial}{\partial \beta} \ln Z \quad \text{internal energy}, \quad (263)$$

and from these we get the pressure,

$$P = - \left( \frac{\partial F}{\partial V} \right)_{N,T} \quad (264)$$

## 7.1 First ingredient: products of density matrices

From the PIMC point of view the single most important property of the density operators is that the product of two density operators is also a density operator:

$$\hat{\rho}(\beta_1)\rho(\beta_2) = e^{-\beta_1 \hat{H}} e^{-\beta_2 \hat{H}} = e^{-(\beta_1 + \beta_2) \hat{H}} = \hat{\rho}(\beta_1 + \beta_2), \quad (265)$$

or in terms of temperatures,

$$\hat{\rho}(T_1)\hat{\rho}(T_2) = \hat{\rho}\left(\frac{T_1 T_2}{T_1 + T_2}\right). \quad (266)$$

If we take, for example,  $M$  temperatures  $T_1 = T_2 = \dots = T_M = T$ , then (265) states that

$$\hat{\rho}(T)\hat{\rho}(T)\dots\hat{\rho}(T) = \hat{\rho}(T)^M = \hat{\rho}\left(\frac{T}{M}\right), \quad (267)$$

so the product property makes it possible to express a low temperature density operator (rhs) as a product of higher temperature density operators. In coordinate space (265) is a convolution integral

$$\rho(\mathbf{R}_1, \mathbf{R}_3, \beta_1 + \beta_2) = \int d\mathbf{R}_2 \rho(\mathbf{R}_1, \mathbf{R}_2, \beta_1) \rho(\mathbf{R}_2, \mathbf{R}_3, \beta_2). \quad (268)$$

Let us define the **time step**  $\tau$ , <sup>45</sup>

$$\tau := \frac{\beta}{M}. \quad (269)$$

The density matrix can be divided into a  $M$ -segment, discrete **path**:

$$\begin{aligned} \rho(\mathbf{R}_0, \mathbf{R}_M; \beta) &= \int d\mathbf{R}_1 d\mathbf{R}_2 \dots d\mathbf{R}_{M-1} \rho(\mathbf{R}_0, \mathbf{R}_1; \tau) \rho(\mathbf{R}_1, \mathbf{R}_2; \tau) \\ &\quad \dots \rho(\mathbf{R}_{M-2}, \mathbf{R}_{M-1}; \tau) \rho(\mathbf{R}_{M-1}, \mathbf{R}_M; \tau). \end{aligned} \quad (270)$$

This is a multidimensional integral, exactly what Monte Carlo can do well.

Decomposing the partition function (260) into  $M$  path segments gives

$$Z = \int d\mathbf{R} \langle \mathbf{R} | e^{-\beta \hat{\mathcal{H}}} | \mathbf{R} \rangle \quad (271)$$

$$\begin{aligned} &= \int d\mathbf{R} d\mathbf{R}_1 \dots d\mathbf{R}_{M-1} \langle \mathbf{R} | e^{-\tau \hat{\mathcal{H}}} | \mathbf{R}_1 \rangle \langle \mathbf{R}_1 | e^{-\tau \hat{\mathcal{H}}} | \mathbf{R}_2 \rangle \\ &\quad \dots \langle \mathbf{R}_{M-2} | e^{-\tau \hat{\mathcal{H}}} | \mathbf{R}_{M-1} \rangle \langle \mathbf{R}_{M-1} | e^{-\tau \hat{\mathcal{H}}} | \mathbf{R} \rangle. \end{aligned} \quad (272)$$

So the partition function is a *path integral over all closed loops*. If  $\hat{A}$  is diagonal in coordinate space, the thermal average is computed as a trace

$$\langle A \rangle = Z^{-1} \int d\mathbf{R} d\mathbf{R}_1 \dots d\mathbf{R}_M \rho(\mathbf{R}, \mathbf{R}_1; \tau) \rho(\mathbf{R}_1, \mathbf{R}_2; \tau) \dots \rho(\mathbf{R}_M, \mathbf{R}; \tau) \langle \mathbf{R} | A | \mathbf{R} \rangle. \quad (273)$$

There is a clear analogy to classical polymers, each particle being one polymer. The above trace corresponds to a **ring polymer**. The lower the temperature, the longer the polymer.

---

<sup>45</sup>The time evolution of a state is given by the operator  $e^{-i\hat{\mathcal{H}}t/\hbar}$ , while now we are interested in  $e^{-\beta \hat{\mathcal{H}}}$ . The relation of these is  $t \sim -i\hbar\beta$ , which gives the idea to call  $\beta/M$  a "time step".

## 7.2 Second ingredient: the high-temperature density matrix

We wouldn't be any much wiser if we couldn't evaluate the individual segments of the paths. It turns out, however, that the density matrix at high temperature can be found, at least approximately. With  $\hat{\mathcal{H}} = \hat{\mathcal{T}} + \hat{\mathcal{V}}$  we have

$$\begin{aligned} e^{-\tau\hat{\mathcal{H}}} &= e^{-\tau(\hat{\mathcal{T}}+\hat{\mathcal{V}})} = e^{-\tau\hat{\mathcal{T}}}e^{-\tau\hat{\mathcal{V}}}e^{\frac{\tau^2}{2}[\hat{\mathcal{V}},\hat{\mathcal{T}}]} \\ &\approx e^{-\tau\hat{\mathcal{T}}}e^{-\tau\hat{\mathcal{V}}} \text{ for small } \tau . \end{aligned} \quad (274)$$

The last line is called the **primitive approximation**. In coordinate space it is

$$\rho(\mathbf{R}_0, \mathbf{R}_2; \tau) \approx \int d\mathbf{R}_1 \langle \mathbf{R}_0 | e^{-\tau\hat{\mathcal{T}}} | \mathbf{R}_1 \rangle \langle \mathbf{R}_1 | e^{-\tau\hat{\mathcal{V}}} | \mathbf{R}_2 \rangle . \quad (275)$$

Now you should hear a bell ringing: *but we've done this already!* Indeed, in section 6.1 we evaluated exactly the matrix elements of the kinetic and potential operators and called them Green's functions. I just copy the results here:

$$\langle \mathbf{R}_1 | e^{-\tau\hat{\mathcal{T}}} | \mathbf{R}_2 \rangle = (4\pi\lambda\tau)^{-3N/2} e^{-\frac{(\mathbf{R}_1 - \mathbf{R}_2)^2}{4\lambda\tau}} , \quad (276)$$

and

$$\langle \mathbf{R}_1 | e^{-\tau\hat{\mathcal{V}}} | \mathbf{R}_2 \rangle = e^{-\tau V(\mathbf{R}_1)} \delta(\mathbf{R}_1 - \mathbf{R}_2) . \quad (277)$$

Here  $\lambda = \frac{\hbar^2}{2m}$  replaces the diffusion constant  $D$ . The spreading of these Gaussians is given by the **thermal (de Broglie) wavelength**,

$$\lambda_{\text{deB}} = \sqrt{\frac{2\pi\hbar^2}{mk_B T}} . \quad (278)$$

If you take a look at the derivations of these formulae, you notice that something could go wrong because of the finite size of the simulations system. The  $k$ -space is not actually continuous, and in (174) we approximated the  $k$ -space sums with integrals. This is accurate only if

$$\lambda_{\text{deB}}\tau \ll L^2 \quad (279)$$

in a simulation box with sides  $L$ . If this condition is not met, the Gaussian (276) will reach across the simulation box, leading to spurious effects.

Using the primitive approximation Eq. (270) can be put into following form:

$$\begin{aligned} \rho(\mathbf{R}_0, \mathbf{R}_M; \beta) &\approx \int d\mathbf{R}_1 d\mathbf{R}_2 \dots d\mathbf{R}_{M-1} (4\pi\lambda\tau)^{-3NM/2} \\ &\times \exp \left[ -\sum_{m=1}^M \left( \frac{(\mathbf{R}_{m-1} - \mathbf{R}_m)^2}{4\lambda\tau} + \tau V(\mathbf{R}_m) \right) \right] . \end{aligned} \quad (280)$$

### 7.3 Connection to path integral formulation of quantum mechanics

From Eq. (280) we can easily get to Feynman's path integral formulation of quantum mechanics. First, shift from the thermal Green's function to a dynamic Green's function used in DMC by replacing  $\lambda \rightarrow D = \hbar^2/(2m)$ . Next, shift back to real time and take the limit  $M \rightarrow \infty$  in (280). Then

$$\begin{aligned} \frac{(\mathbf{R}_{m-1} - \mathbf{R}_m)^2}{4\lambda\tau} &\sim \frac{(\mathbf{R}_{m-1} - \mathbf{R}_m)^2}{4\frac{\hbar^2}{2m}\frac{i\Delta t}{\hbar M}} \\ &\rightarrow -\frac{i}{\hbar}\frac{1}{2}m\left(\frac{d\mathbf{R}}{dt}\right)^2 dt , \text{ as } M \rightarrow \infty , \end{aligned} \quad (281)$$

so the exponent term in (280) corresponds to

$$\exp\left\{\frac{i}{\hbar}\int dt \left[\frac{1}{2}m\left(\frac{d\mathbf{R}}{dt}\right)^2 - V(\mathbf{R})\right]\right\} = \exp\left\{\frac{i}{\hbar}S(\mathbf{R}, t)\right\} , \quad (282)$$

where  $S = \int dt L$  is the **classical action**, time integral of the Lagrangian  $L$ . We recover the famous Feynman-Kac formula of quantum mechanics,

$$\langle x', t' | x, t \rangle = \int \mathcal{D}e^{\frac{i}{\hbar}S[x(t)]} , \quad (283)$$

which states that the probability amplitude of a point particle to get from point  $(x, t)$  to point  $(x', t')$  is obtained by integrating over all possible paths between the points, attaching to each path a weight  $e^{\frac{i}{\hbar}S}$ . The measure  $\mathcal{D}$  is just a commonly used shorthand for “all paths and proper normalization”. The normalization, by the way, is in many cases the tricky part!

Fig. 15 shows two possible paths from point  $(x, t)$  to point  $(x', t')$ . Time is discretised to **time slices** of finite width, like in a simulation.

Eq. (283) is not only the most straightforward connection between classical and quantum mechanics, it is also an excellent starting point of the whole quantum mechanics of point-like particles (quantum field theory gives the rest). The classical limit (Ehrenfest's theorem) is easy to derive. For  $\hbar \rightarrow 0$  the integrand oscillates very rapidly and only paths with stationary  $S$  will contribute: we get  $\delta S = 0$ , the classical least action principle. Schrödinger equation follows, too, by considering a case where one makes a small variation to the path keeping the starting point  $(x, t)$  fixed. The path-integral formulation of quantum mechanics has been reviewed by its inventor, Richard Feynman<sup>46</sup>

**Visualization of paths** Paths can be visualised by drawing world-line plots that resemble Minkowski diagrams used in special relativity (see Ceperley's review for examples). One must

---

<sup>46</sup>R. P. Feynman, *Space-time approach to non-relativistic quantum mechanics*, Rev. Mod. Phys. **20** (1948) 367.

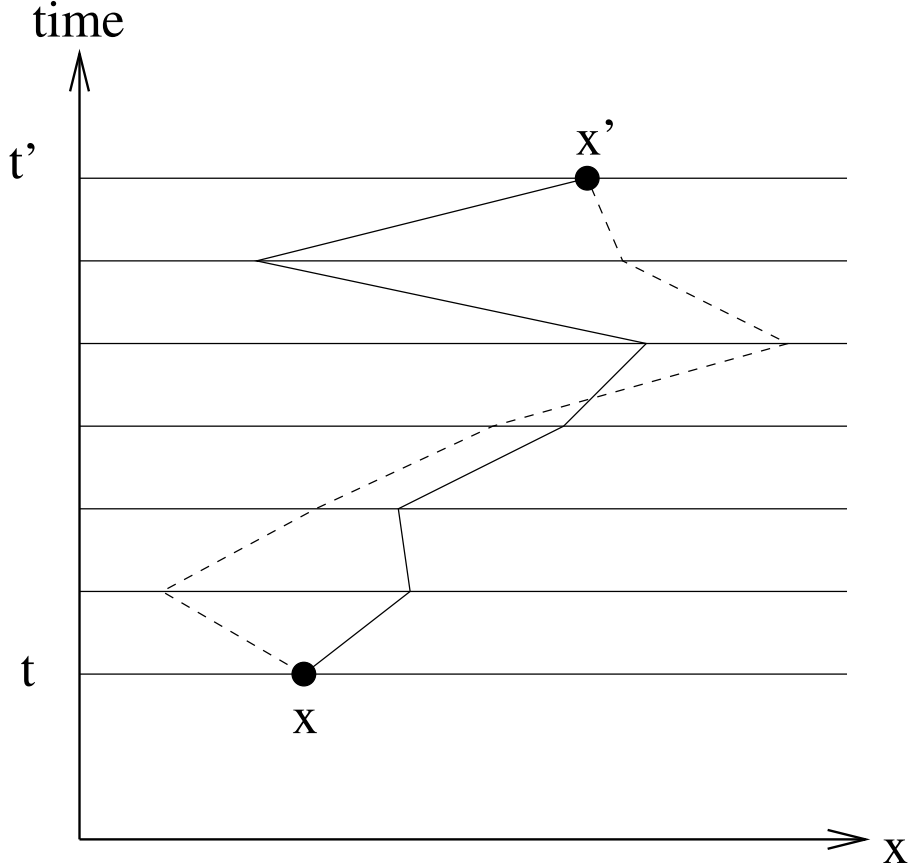


Figure 15: Two possible paths connecting fixed end points. The time scale is divided into discrete time slices. The quantum amplitude  $\langle x', t' | x, t \rangle$  is calculated by adding all possible paths with *classical* weight  $\exp\{iS[x(t)]/\hbar\}$ .

remember, however, that the imaginary time axis is now a thermal quantity and not related to the true dynamics of the particles. Coordinate space plots that cover some fixed amount of time steps are also useful. There one must remember, that the discretization to time slices is entirely artificial, and a plot obtained by simply connecting all the beads (points visited at discrete times) does not give full credit to the real situation. A more realistic picture can be obtained by taking into account, that a particle may visit all points within the thermal wavelength of any calculated bead.

## 7.4 Link action

A **link** is the pair of adjacent time slices,  $\{\mathbf{R}_{m-1}, \mathbf{R}_m\}$ , in Eq. (280). The **link action** is minus the logarithm of the *exact* density matrix:

$$S_m := -\ln [\rho(\mathbf{R}_{m-1}, \mathbf{R}_m; \tau)] . \quad (284)$$

Thus the exact density matrix reads

$$\rho(\mathbf{R}_0, \mathbf{R}_M; \beta) = \int d\mathbf{R}_1 \dots \mathbf{R}_{M-1} \exp \left[ - \sum_{m=1,M} S_m \right] . \quad (285)$$

It is customary to separate the actions coming from the kinetic and potential parts of the Hamiltonian, which are

$$K_m = \frac{3M}{2} \ln(4\pi\lambda\tau) + \frac{(\mathbf{R}_{m-1} - \mathbf{R}_m)^2}{4\lambda\tau} \quad (286)$$

and the “inter-action”  $U_m = S_m - K_m$ , which is often used in the symmetrised form. Put together, the primitive approximation for the link action is

$$S_m^{\text{prim.}} = \frac{3M}{2} \ln(4\pi\lambda\tau) + \underbrace{\frac{(\mathbf{R}_{m-1} - \mathbf{R}_m)^2}{4\lambda\tau}}_{\text{“Spring term”}} + \underbrace{\frac{\tau}{2} [V(\mathbf{R}_{m-1}) + V(\mathbf{R}_m)]}_{\text{“Potential term”}} . \quad (287)$$

In polymer analogy the spring term holds the polymer together and the potential term gives the inter-polymer interaction. For many quantities thermal averages translate to ring polymers.

## 7.5 Improving the action

The superfluid temperature is only 2.172 K for  ${}^4\text{He}$  liquid, and the number of time slices to reach the superfluid region turns out to be  $M \sim 1000$  if one uses the primitive approximation. A better action is needed, which allows to take longer time steps. The path is a **fractal**, so finding better actions is not the same thing as finding a better integrator of a differential equation (*e.g.* leap-frog in MD). The strategy is to use exact properties of the action as a guidance.

The Feynman–Kac formula gives the inter-action as the average over all free-particle paths,

$$e^{-U_m} := e^{-U(\mathbf{R}_{m-1}, \mathbf{R}_m; \tau)} = \left\langle \exp \left[ - \int_0^\tau dt V(\mathbf{R}(t)) \right] \right\rangle_{RW} , \quad (288)$$

where  $\langle \dots \rangle_{RW}$  denotes average over all random walk paths from  $\mathbf{R}_{m-1}$  to  $\mathbf{R}_m$ . Often we have (or know) only the pair potential between particles, so we have

$$e^{-U(\mathbf{R}_{m-1}, \mathbf{R}_m; \tau)} = \left\langle \prod_{i < j} \exp \left[ - \int_0^\tau dt V(r_{ij}(t)) \right] \right\rangle_{RW} , \quad (289)$$

where  $r_{ij}(t)$  is the distance between particles  $i$  and  $j$ . If one neglects three-body and higher correlations between particles, the product can be taken out of the average,

$$e^{-U(\mathbf{R}_{m-1}, \mathbf{R}_m; \tau)} \approx \prod_{i < j} \left\langle \exp \left[ - \int_0^\tau dt V(r_{ij}(t)) \right] \right\rangle_{RW}. \quad (290)$$

Now the average is the interaction of a pair of particles - a quantity that can be computed beforehand. This is the core idea of the **pair–product action**, and the improvement upon the primitive action is significant. Furthermore, it applies also to Coulomb and hard–core potentials, while many other improved action methods fail for nonintegrable potentials. A short list of possible improved actions:

- Pair–product action
- Cumulant action
- Harmonic action
- WKB action (semiclassical)

## 7.6 Bose Symmetry

In the beginning of the PIMC section I stated without hesitation that the energy eigenstates are visited according to the Maxwell–Boltzmann probability  $e^{-\beta E_N}$ . This is correct only for distinguishable particles. Bose-Einstein statistics requires that we symmetrise the density matrix (subindex  $B$  refers to bosons),

$$\rho_B(\mathbf{R}_0, \mathbf{R}_1; \beta) = \frac{1}{N!} \sum_P \rho(\mathbf{R}_0, P\mathbf{R}_1; \beta), \quad (291)$$

where the sum is over all particle–label permutations  $P$ . The permutation of coordinates can be done on either the first or the second argument of the density matrix, or to both; it makes no difference. This involves the summation of  $N!$  terms and is a computational burden. Fortunately all terms in the sum are positive and we can evaluate it by *sampling*: the bosonic simulation is a random walk through both the coordinate space *and* the permutation space. This cannot be done for fermions, because even and odd permutations have large cancellation and a MC evaluation of the sum is out of the question. I'll return to this problem later.

The partition function is a sum over all closed paths; Bose–symmetrised partition function is obtained by letting the paths close to any permutation of the starting points.

**Superfluidity** Partition function is obtained by taking all closed paths. Adding the Bose symmetrisation, this gives rise to exchange paths, where, say, particle 1 takes the place of particle 2 and vice versa. A special situation arises, when the exchange involves the periodic

image of the other particle, because then the extended plot (all periodic boxes side by side) shows that the looping path goes through the entire system. The finite size of the simulation box causes finite size effects, but the idea of **winding paths**, paths that span across the entire system, remains valid. Thus the superfluid transition can be seen visually in PIMC. The best theoretical value of the lambda transition<sup>47</sup> in <sup>4</sup>He is  $2.19 \pm 0.02$  K at SVP (saturated vapor pressure), very close to the experimental value 2.172 K. Via his path integral formulation of quantum mechanics, Feynman<sup>48</sup> has answered two important questions:

- Does the strong inter-particle potential invalidate the idea of Bose–Einstein condensation in helium? (No, it is still ok).
- Why should there be a transition at low temperature? (Feynman divides exchange paths into polygons and shows that at some low temperature large polygons that involve of the order of  $N$  particles start to contribute in the partition function).

## 7.7 Sampling paths

As Eq. (285) shows, we want to sample paths from the distribution

$$w(\mathbf{R}_0, \dots, \mathbf{R}_{M-1}) = \frac{1}{Z} \exp \left[ - \sum_{m=1,M} S_m \right], \quad (292)$$

where the normalization is again the partition function.

Consider first how to sample a single point in the path, the elementary operation in PIMC. We wish to move a bead  $\mathbf{R}$  at time  $\tau$ , which is connected to two fixed beads  $\mathbf{R}_0$  and  $\mathbf{R}_2$ , at times 0 and  $2\tau$ , respectively. The simplest choice would be the **classical sampling**, where the bead is displaced uniformly inside a cube, whose size is adjusted to get near 50 % acceptance. In the **free-particle sampling** the new position is sampled from

$$w(\mathbf{R}) = \exp \left[ - \frac{(\mathbf{R} - \mathbf{R}_{mid})^2}{2\lambda\tau} - U(\mathbf{R}, \mathbf{R}_1) - U(\mathbf{R}, \mathbf{R}_2) \right], \quad (293)$$

where  $\mathbf{R}_{mid} = \frac{1}{2}(\mathbf{R}_1 + \mathbf{R}_2)$ , so this is a Gaussian centered at  $\mathbf{R}_{mid}$  with width  $\sqrt{\lambda\tau}$ . If there is a repulsive potential between the particles, the moves suggested by the free-particle sampling will be rejected whenever the beads become too close; Further improvement would be for example a correlated Gaussian.

Unfortunately the computer time needed for a free-particle path to diffuse a fixed distance will scale as  $M^3$ . Hence large values of  $M$  will be needed and this fact combined with a non-efficient action (primitive action) can easily ruin the whole PIMC routine.

---

<sup>47</sup>E. L Pollock and K. J. Runge, Phys. **B46** (1992) 3535.

<sup>48</sup>R. P. Feynman, Phys. Rev. **90** (1953) 1116; Phys. Rev. **91** (1953) 1291; Phys. Rev. **91** (1953) 1301.

Moving the whole path at once is likely to be inefficient, as most of the attempted moves will be rejected. It is better to move path segments. One speaks of **multi-level Metropolis algorithms that uses bisection**. Their further description is beyond the scope of these lecture notes.

## 7.8 Fermion paths: The sign problem

For fermions indistinguishability is imposed by summing again over all permutations, but now terms which come from odd number of permutations have negative sign (compare with (291)):

$$\rho_F(\mathbf{R}_0, \mathbf{R}_1; \beta) = \frac{1}{N!} \sum_P (-1)^{\zeta_P} \rho(\mathbf{R}_0, P\mathbf{R}_1; \beta), \quad (294)$$

where  $\zeta_P$  is the parity of permutation  $P$ . For bosons the factor is simply  $(+1)^{\zeta_P} = 1$ .

Now we can prove for both bosons and fermions the statement made earlier, namely that the permutation of coordinates can be done on either the first or the second argument of the density matrix, or to both. (Anti)symmetrising with respect to both arguments gives

$$\rho_{B/F}(\mathbf{R}_0, \mathbf{R}_1; \beta) := \frac{1}{(N!)^2} \sum_P (\pm 1)^{\zeta_P} \sum_{P'} (\pm 1)^{\zeta_{P'}} \rho(P\mathbf{R}_0, P'\mathbf{R}_1; \beta). \quad (295)$$

Taking a particular pair of permutations  $P$  and  $P'$  we can always find a third one such that  $P'' = PP'$ , and  $\zeta_{P''} = \zeta_P + \zeta_{P'}$ . Thus we can write the above equations in the form

$$\rho_{B/F}(\mathbf{R}_0, \mathbf{R}_1; \beta) = \frac{1}{(N!)^2} \sum_P (\pm 1)^{\zeta_P} \sum_{PP''} (\pm 1)^{\zeta_P + \zeta_{P''}} \rho(P\mathbf{R}_0, PP''\mathbf{R}_1; \beta). \quad (296)$$

Sum over all permutations  $PP''$  while  $P$  is fixed is the same as summing over all permutations  $P''$ , so we get

$$\rho_{B/F}(\mathbf{R}_0, \mathbf{R}_1; \beta) = \frac{1}{(N!)^2} \sum_P \sum_{P''} (\pm 1)^{\zeta_{P''}} \rho(P\mathbf{R}_0, PP''\mathbf{R}_1; \beta). \quad (297)$$

Now  $P$  is applied to both coordinates, so it merely relabels dummy variables. Hence all  $N!$  terms give the same contribution and we can reduce this to

$$\rho_{B/F}(\mathbf{R}_0, \mathbf{R}_1; \beta) = \frac{1}{N!} \sum_{P''} (\pm 1)^{\zeta_{P''}} \rho(\mathbf{R}_0, P''\mathbf{R}_1; \beta). \quad (298)$$

This completes our proof that permuting both arguments is equivalent with permuting one argument.

The expectation value of operator  $O$  in a Fermi system is

$$\langle O \rangle = \text{Tr}[\rho_F O] = \frac{1}{N!} \sum_P (-1)^{\zeta_P} \int d\mathbf{R} d\mathbf{R}_1 \dots d\mathbf{R}_{M-1} \quad (299)$$

$$\rho(\mathbf{R}, \mathbf{R}_{M-1}, \tau) \dots \rho(\mathbf{R}_1, \mathbf{R}', \tau) O(\mathbf{R}', \mathbf{R})|_{\mathbf{R}'=\mathbf{P}\mathbf{R}}. \quad (300)$$

The Fermi antisymmetrization is a sum of alternating series of large terms of slowly decreasing magnitude. We have no precise formula available for any of the terms, and already Feynman himself found impractical any attempts to analytically rearrange the terms in such way that they are positive. In Bose case one could rather easily sample the symmetrization sum, but now one faces the problem of how to sample an alternating sum. Ceperley has given arguments, that the signal-to-noise ratio of such samplings vanishes exponentially. In particular, the efficiency of a **direct-fermion method** (straightforward sampling as in the Bose case) scales as  $e^{-N}$ , where  $N$  is the number of fermions. Clearly the method is useless for all physically interesting systems. The Restricted Path Integral Monte Carlo (RPIMC) is one of the attempts to organise the terms in the sum related to the fixed node DMC. Here one imposes an approximate nodal structure, with the aid of a trial density matrix  $\rho_T$ , to the density matrix  $\rho_F$ , and if this is correct, then the solution is exact. The theory behind RPIMC is beyond the scope of these lecture notes, I just mention that the free energy obtained using RPIMC satisfies the variational principle<sup>49</sup>

## 7.9 The excitation spectrum and the dynamic structure function

Consider liquids, which are homogeneous and isotropic (same density everywhere and no direction dependences), therefore only one wave vector  $k$  appears. Neutron scattering measures directly the dynamic structure function  $S(k, \omega)$ ,

$$S(k, w) = -\frac{1}{\pi} \Im m \mathcal{X}(k, \omega), \quad (301)$$

where  $\mathcal{X}(k, \omega)$  is the Fourier transform of the real space density-density correlation function,  $\mathcal{X}(\mathbf{r}_1, \mathbf{r}_2, t)$ . Explicitly,  $S(k, \omega)$  is given by

$$S(k, \omega) = \frac{1}{2\pi N} \int_{-\infty}^{\infty} dt e^{i\omega t} \langle \hat{\rho}_k(t) \rho_{-k}(t) \rangle \quad (302)$$

$$= \frac{1}{NZ} \sum_{m,n} \delta(\omega - E_m - E_n) e^{-\beta E_n} |\langle m | \hat{\rho}_k | n \rangle|^2, \quad (303)$$

where the density operator  $\hat{\rho}_k$ <sup>50</sup>,

$$\hat{\rho}_k = \sum_{i=1}^N e^{i\mathbf{k} \cdot \mathbf{r}_i} \quad (304)$$

---

<sup>49</sup>The RPIMC free energy is equal or larger than the exact free energy.

<sup>50</sup>Just a Fourier transform of a sum of Dirac deltas.

computed at the particle coordinates  $\mathbf{r}_i$ . The quantity that comes out of PIMC is written in imaginary time and it is the Laplace transform of the dynamic structure function,

$$F(k, t) = \int_{-\infty}^{\infty} d\omega e^{-\omega t} S(k, \omega) \quad (305)$$

$$= \frac{1}{N\bar{Z}} \text{Tr} \left\{ \hat{\rho}_{-k} e^{-Ht} \hat{\rho}_k e^{-H(\beta-t)} \right\} . \quad (306)$$

Mathematically there is no harm done, because  $F(k, t)$  and  $S(k, \omega)$  contain exactly the same information and a Laplace inversion is well defined. The problem arises because the *simulated*  $F(k, t)$  *always has some noise, which makes a perfect inversion impossible*. The time-domain structure function  $F(k, t)$  is an exponentially decaying curve plus tiny features on top. And it is these small feature that give all  $S(k, \omega)$ , so very little noise can cover the useful part of the information. Even sharp features in  $S(k, \omega)$ , such as delta-function peaks, will show only as unimpressive humps in  $F(k, t)$ .

## 7.10 Fermion PIMC methods

Fixed-node DMC can do fermions by using an antisymmetric trial wave function. Path integrals work with density matrices and do not use any trial guess at all - this makes it trickier to force antisymmetry upon a PIMC simulation. I list here a few attempts with comments.

### 1. RPIMC (Restricted Path Integral Monte Carlo)<sup>51</sup>

This could be called fixed-node PIMC. The paths are restricted so that the density matrix  $\rho(\mathbf{R}, \mathbf{R}_0; \tau)$  with a fixed  $\mathbf{R}_0$  doesn't change sign.

- Does not recover the exact ideal fermi gas limit at  $r_s \rightarrow 0$ <sup>52</sup>.<sup>53</sup>

### 2. CPIMC (Configuration Path Integral Monte Carlo)<sup>54</sup>

Instead of coordinate space, consider occupation of e.g. momentum orbitals  $|k\rangle$ , and work using second quantization. - Built to be good at  $r_s \rightarrow 0$  - Systematic deviations from RPIMC results for uniform electron gas

### 3. PB-PIMC (Permutation Blocking Path Integral Monte Carlo)

<sup>55</sup>

---

<sup>51</sup>D. Ceperley, Phys. Rev. Lett. **69** 331 (1992).

<sup>52</sup>Density is measured with  $r_s = \bar{r}/a_B$ , where  $\bar{r}$  the mean interparticle distance,  $n^{-1} = \frac{4}{3}\pi\bar{r}^3$ ,  $a_B$  is the Bohr radius.

<sup>53</sup>S. Filinov, J. Phys. A: Math. Gen. **34**, 1665-1677 (2001).

<sup>54</sup>T. Schoof, S. Groth, J. Vorberger, and M. Bonitz, Phys. Rev. Lett. **115** 130402 (2015).

<sup>55</sup>T. Dornheim, S. Groth, A. Filinov, and M. Bonitz, "Permutation blocking path integral Monte Carlo: A highly efficient approach to the simulation of strongly degenerate non-ideal fermions," New J. Phys. 17, 073017 (2015).

## 8 The fermion sign problem

Monte Carlo methods can give exact results for boltzmannons and bosons up to particle numbers  $\sim 10^3$ , sometimes  $10^4$ . Let's see what makes fermions so different.

The bosonic ground state wave function has no nodes, and the wave function is real and positive everywhere (shown by R. Penrose). With the Hamiltonian

$$\hat{\mathcal{H}} = -\frac{\hbar^2}{2m} \nabla_{\mathbf{R}}^2 + V(\mathbf{R}) , \quad (307)$$

it's a simple matter to prove that any imaginary part of the wave function increases energy, hence parting from the ground state. There are no nodes, so the wave function cannot change sign, and we may as well choose it to be positive everywhere. For bound states, such a wave function is a good probability density and we can sample it using MC methods.

The problem lies with fermions. The Hamiltonian (307) doesn't make any distinction of bosons or fermion. The lowest energy state is symmetric, so the search converges easily to the bosonic ground state, or rather the arbitrary symmetry state. Antisymmetry has to be forced upon the solution, and the lowest antisymmetric state – the ground state of the fermion system – is higher in energy than the bosonic one. The antisymmetry means that exchange of two identical fermions changes the sign of the wave function. so there must be nodes.

A function with both positive and negative values doesn't make an admissible probability density. In VMC one samples the function (Eq. (84))

$$w(\mathbf{R}) = \frac{|\varphi_T(\mathbf{R})|^2}{\int d\mathbf{R} |\varphi_T(\mathbf{R})|^2} . \quad (308)$$

This is always positive, also for fermions. For fermions, one must maintain antisymmetry in  $\varphi_T(\mathbf{R})$ , which for  $N$  identical fermions (same spin) means there must be nodes, and the dimension of the nodal surface is  $3(N - 1)$ . According to the variational principle,  $\varphi_T(\mathbf{R})$  with wrong nodal surface gives energy above the true fermion ground state value. In fixed-node DMC one keeps the nodal surface as is, and improves numerically the correlation part of the wave function. This leads to correlations with lowest energy, but the nodal surface is not improved. In short, the reason is that zero times anything is zero: DMC with importance sampling evolves the product (see Eq. (196))

$$f(\mathbf{R}; \tau) = \varphi_T(\mathbf{R}) \Psi(\mathbf{R}; \tau) , \quad (309)$$

and where  $\varphi_T(\mathbf{R})$  is zero, there also  $f(\mathbf{R}; \tau)$  is zero, no matter how far in  $\tau$  we evolve. This is again a variational problem, better nodes evolve in DMC to a lower energy fermion state, but fixed-node DMC won't evolve the nodes. The released-node DMC tries to shift the nodes a bit, but the price of the small gain is high: the computational burden is extreme and the algorithm may not even obey the variational principle.

Let's consider the general case of evaluating an average over arbitrary weights. The expectation value of some quantity  $A$  is

$$\langle A \rangle_w = \frac{\sum_i w_i A_i}{\sum w_i} , \quad (310)$$

but the weights  $w_i$  may be negative we cannot sample them using MC. Separate the sign as  $w_i = \text{sgn}(w_i)|w_i|$ ,

$$\langle A \rangle_w = \frac{\sum_i w_i A_i}{\sum w_i} = \frac{\sum_i \text{sgn}(w_i)|w_i|A_i}{\sum \text{sgn}(w_i)|w_i|} = \frac{\frac{\sum_i |w_i|\text{sgn}(w_i)A_i}{\sum_i |w_i|}}{\frac{\sum_i |w_i|\text{sgn}(w_i)}{\sum_i |w_i|}} . \quad (311)$$

This contains a good probability density

$$p_i := \frac{|w_i|}{\sum_i |w_i|} , \quad (312)$$

so can evaluate two averages,

$$\langle A \rangle_w = \frac{\sum_i p_i \text{sgn}(w_i)A_i}{\sum_i p_i \text{sgn}(w_i)} = \frac{\langle \text{sign}A \rangle_{|w|}}{\langle \text{sign} \rangle_{|w|}} . \quad (313)$$

Evaluation of this is perfectly doable in MC, but there's a catch. The denominator is related to the partition function  $Z$  of weights  $w_i$ , and another one of weights  $|w_i|$ ,

$$\langle \text{sign} \rangle_{|w|} = \sum_i p_i \text{sgn}(w_i) = \frac{\sum_i w_i}{\sum_i |w_i|} = \frac{Z_w}{Z_{|w|}} = \frac{e^{-\beta F_w}}{e^{-\beta F_{|w|}}} = e^{-\beta(F_w - F_{|w|})} , \quad (314)$$

where the free energy is  $F = -\frac{1}{\beta} \ln Z$  (from thermodynamics). As always in MC, the error of the mean diminishes as  $1/\sqrt{M}$  with  $M$  samples, but there is a factor that grows,

$$\frac{\Delta(\langle \text{sign} \rangle_{|w|})}{\langle \text{sign} \rangle_{|w|}} = \frac{1}{\sqrt{M}} \frac{\sqrt{\langle \text{sign}^2 \rangle_{|w|} - \langle \text{sign} \rangle_{|w|}^2}}{\langle \text{sign} \rangle_{|w|}} \sim \frac{e^{\beta(F_w - F_{|w|})}}{\sqrt{M}} = \frac{e^{\beta N(f_w - f_{|w|})}}{\sqrt{M}} . \quad (315)$$

The difference  $f_w - f_{|w|}$  (free energies per particle,  $F$  is extensive) is positive (because the boson energy with weights  $|w|$  is below the fermion energy with weights  $w$ ). The factor grows exponentially both with decreasing temperature, and with increasing number of fermions  $N$ . This is the **fermion sign problem**.

F. Pederiva<sup>56</sup> gives a discussion of what happens, if one has an antisymmetric trial wave function  $\varphi_T^A(\mathbf{R})$  and the exact antisymmetric ground state wave function is  $\phi_0^A(\mathbf{R})$ , and computes the energy,

$$\langle E \rangle = \frac{\langle \phi_0^A | \hat{\mathcal{H}} | \varphi_T^A \rangle}{\langle \phi_0^A | \varphi_T^A \rangle} = \frac{\int d\mathbf{R} \phi_0^A(\mathbf{R}) \varphi_T^A(\mathbf{R}) \frac{\hat{\mathcal{H}} \varphi_T^A(\mathbf{R})}{\varphi_T^A(\mathbf{R})}}{\int d\mathbf{R} \phi_0^A(\mathbf{R}) \varphi_T^A(\mathbf{R})} . \quad (316)$$

---

<sup>56</sup>In *An Advanced Course in Computational Nuclear Physics*, Ed. Hjorth-Jensen, Lombardo, and van Kolck (2017).

Assuming the nodal surfaces of  $\varphi_T^A(\mathbf{R})$  are the same as those of  $\phi_0^A(\mathbf{R})$ , one could try to invent a way to sample the integrals using MC. As such,  $\varphi_T^A(\mathbf{R})$  is not positive definite, so one cannot directly sample from it, but let's split it to positive and negative regions,

$$\phi_0^A(\mathbf{R})\varphi_T^A(\mathbf{R}) = \underbrace{f^+(\mathbf{R}^+)}_{\geq 0} - \underbrace{f^-(\mathbf{R}^-)}_{\geq 0}, \quad (317)$$

and by linearity, both positive densities,  $f^+$  and  $f^-$ , satisfy the imaginary-time Schrödinger equation with the same eigenvalue. The expectation value is now

$$\langle E \rangle = \frac{\left[ \int d\mathbf{R}^+ f^+(\mathbf{R}^+) \frac{\hat{\mathcal{H}}\varphi_T^A(\mathbf{R}^+)}{\varphi_T^A(\mathbf{R}^+)} \right] - \left[ \int d\mathbf{R}^- f^-(\mathbf{R}^-) \frac{\hat{\mathcal{H}}\varphi_T^A(\mathbf{R}^-)}{\varphi_T^A(\mathbf{R}^-)} \right]}{\left[ \int d\mathbf{R}^+ f^+(\mathbf{R}^+) \right] - \left[ \int d\mathbf{R}^- f^-(\mathbf{R}^-) \right]}, \quad (318)$$

which can be sampled using MC. However, both  $f^+$  and  $f^-$  satisfy the same imaginary-time Schrödinger equation, so as  $\tau$  increases, they converge to the same ground state probability density, and the result approaches indeterminate

$$\langle E \rangle = \frac{0}{0}. \quad (319)$$

As Pederiva points out, this shows up during a MC simulation as exponentially increasing variance of energy, so the signal-to-noise ratio gets terribly small. This is another way to express the fermion sign problem.

Troyer and Wiese<sup>57</sup> argue that the fermion sign problem is nondeterministic polynomial (NP) hard. This implies that a generic solution of the sign problem would also solve all problems in the complexity class NP in polynomial time, which hints that there maybe isn't one.

Are we out of luck? If we could solve the eigenstates and eigenvalues of  $\hat{\mathcal{H}}$ ,  $\hat{\mathcal{H}}|i\rangle = E_i|i\rangle$ , we could calculate finite temperature expectation values from the density matrix  $\hat{\rho} = \frac{1}{Z}e^{-\beta\hat{\mathcal{H}}}$ ,

$$\langle \hat{A} \rangle = \text{Tr}(\hat{\rho}\hat{A}) = \frac{\sum_i e^{-\beta E_i} \langle i|\hat{A}|i\rangle}{\sum_i e^{-\beta E_i}}. \quad (320)$$

Here the weights  $e^{-\beta E_i}$  are positive, so there *is no sign problem*. Alas, solving  $\hat{\mathcal{H}}|i\rangle = E_i|i\rangle$  is an exponentially hard problem in itself.

A question one should next ask is, just *how* accurately do we need to know the solution to  $\hat{\mathcal{H}}|i\rangle = E_i|i\rangle$  in order to avoid the sign problem? Is it enough to have the approximate solution hidden in an evolution algorithm?

Chin<sup>58</sup> argues that the sign problem is purely a consequence of a poor approximation to the exact propagator (Green's function)  $e^{-\tau\hat{\mathcal{H}}}$  and "not intrinsic to solving a fermion problem".

---

<sup>57</sup>M. Troyer and U-J Wiese, Phys. Rev. Lett. **94**, 170201 (2005)

<sup>58</sup>S. A. Chin, Phys. Rev. **E91**, 031301(R) (2015).

His opinion is based on the observation, that the culprit is the free fermion propagator  $e^{-\tau \hat{T}}$ , which appears as a factor in commonly applied approximations to the exact propagator. In coordinate representation the free fermion propagator is antisymmetrized diffusion,

$$G_T(\mathbf{R}_1, \mathbf{R}_2; \tau) = \sum_P (-1)^P \langle \mathbf{R}_1 | e^{-\tau T} | P \mathbf{R}_2 \rangle \quad (321)$$

$$= (4\pi D\tau)^{-3N/2} \sum_P (-1)^P e^{-\frac{(\mathbf{R}_1 - P\mathbf{R}_2)^2}{4D\tau}} = (4\pi D\tau)^{-3N/2} \det \mathcal{M} \quad (322)$$

$$\mathcal{M}_{ij} = e^{-\frac{(\mathbf{r}_i^{(1)} - \mathbf{r}_j^{(2)})^2}{4D\tau}} \text{ matrix elements of } \mathcal{M}, \quad (323)$$

where  $\mathbf{R}_1 = (\mathbf{r}_1^{(1)}, \mathbf{r}_2^{(1)}, \dots, \mathbf{r}_N^{(1)})$  and  $\mathbf{R}_2 = (\mathbf{r}_1^{(2)}, \mathbf{r}_2^{(2)}, \dots, \mathbf{r}_N^{(2)})$ . For two fermions this is diffusion of particles 12 to 12 minus diffusion of 12 to 21 (exchange),

$$G_T(\mathbf{R}_1, \mathbf{R}_2; \tau) = (4\pi D\tau)^{-3} \left[ e^{-\frac{(\mathbf{r}_1^{(1)} - \mathbf{r}_1^{(2)})^2}{4D\tau}} e^{-\frac{(\mathbf{r}_2^{(1)} - \mathbf{r}_2^{(2)})^2}{4D\tau}} - e^{-\frac{(\mathbf{r}_1^{(1)} - \mathbf{r}_2^{(2)})^2}{4D\tau}} e^{-\frac{(\mathbf{r}_2^{(1)} - \mathbf{r}_1^{(2)})^2}{4D\tau}} \right] \quad (324)$$

$$= (4\pi D\tau)^{-3} \begin{vmatrix} e^{-\frac{(\mathbf{r}_1^{(1)} - \mathbf{r}_1^{(2)})^2}{4D\tau}} & e^{-\frac{(\mathbf{r}_1^{(1)} - \mathbf{r}_2^{(2)})^2}{4D\tau}} \\ e^{-\frac{(\mathbf{r}_2^{(1)} - \mathbf{r}_1^{(2)})^2}{4D\tau}} & e^{-\frac{(\mathbf{r}_2^{(1)} - \mathbf{r}_2^{(2)})^2}{4D\tau}} \end{vmatrix} = (4\pi D\tau)^{-3} \det \mathcal{M}. \quad (325)$$

where  $\mathbf{r}_i^{(k)}$  is the position of particle  $i$  in  $\mathbf{R}_k$ . The antisymmetrized  $\langle \mathbf{R}_1 | e^{-\tau \hat{T}} | \mathbf{R}_2 \rangle$  is *not positive definite*, and the more frequently one applies free fermion diffusion, the more sign problem one spawns. Chin's idea is that if one can get close enough to the ground state with less than 10 free fermion propagators in the approximation of  $e^{-\tau \hat{\mathcal{H}}}$ , one obtains the solution before the

sign problem kicks in. He demonstrates the feasibility by computing the properties of up to 20 spin-polarized electrons in a two-dimensional quantum dot.

## 9 Error estimation

### 9.1 Some definitions and clarifications

Consider evaluating quantity  $A$  and a sample of size  $N$ . The mean value over the sample - or sample average - is

$$\bar{A}_N := \frac{1}{N} \sum_{i=1}^N A_i . \quad (326)$$

This is *not* the expectation value (ensemble average or the mean) of  $A$ , marked  $\langle A \rangle$ , because the sample is finite. The expectation value is the sum over every possible value of  $A_i$ ,

$$\langle A \rangle := \sum_i p_i A_i , \quad (327)$$

where  $p_i$  is the probability of  $A_i$ . For a continuous distribution this is

$$\langle A \rangle := \int dx p(x) A(x) . \quad (328)$$

The difference is that

- $\bar{A}_N$  is a random variable that depends on the chosen sample
- $\langle A \rangle$  is a fixed number

According to the law of large numbers the mean and the expectation value coincide for an infinitely large sample,

$$\lim_{N \rightarrow \infty} \bar{A}_N = \langle A \rangle . \quad (329)$$

## 9.2 Biased and unbiased estimators of variance

The variance  $\sigma^2$  is the mean square deviation from the mean value

The standard deviation  $\sigma$  is the reported error.

Monte Carlo results are given as

$$\text{result} = \underbrace{1.234}_{\text{mean value}} \pm \underbrace{0.002}_{\sigma} . \quad (330)$$

First, one must be clear about what mean value is used in evaluation of  $\sigma^2$ . If one uses the mean over  $N$  samples,  $\bar{A}_N$ , then we get the *biased estimator of the variance*,

$$\sigma_{\text{biased}}^2 := \frac{1}{N} \sum_{i=1}^N (A_i - \bar{A}_N)^2 \text{ biased estimator of the variance .} \quad (331)$$

On the other hand, the *unbiased estimator of the variance* is the mean square deviations from the *true expectation value*,

$$\sigma_{\text{unbiased}}^2 := \frac{1}{N} \sum_{i=1}^N (A_i - \langle A \rangle)^2 \text{ unbiased estimator of the variance .} \quad (332)$$

Obviously, the biased and unbiased estimators are related. Start from the definition of the biased estimator and add and subtract the constant  $\langle A \rangle$ :

$$\begin{aligned} \sigma_{\text{biased}}^2 &= \frac{1}{N} \sum_{i=1}^N (A_i - \bar{A}_N)^2 = \frac{1}{N} \sum_{i=1}^N [A_i - \langle A \rangle - (\bar{A}_N - \langle A \rangle)]^2 \\ &= \underbrace{\frac{1}{N} \sum_{i=1}^N [A_i - \langle A \rangle]^2}_{\sigma_{\text{unbiased}}^2} - 2 \frac{1}{N} \sum_{i=1}^N (A_i - \langle A \rangle) \underbrace{(\bar{A}_N - \langle A \rangle)}_{\text{no } i} + \frac{1}{N} \sum_{i=1}^N \underbrace{(\bar{A}_N - \langle A \rangle)^2}_{\text{no } i} \\ &= \sigma_{\text{unbiased}}^2 - 2(\bar{A}_N - \langle A \rangle) \underbrace{\frac{1}{N} \sum_{i=1}^N (A_i - \langle A \rangle)}_{\bar{A}_N - \langle A \rangle} + (\bar{A}_N - \langle A \rangle)^2 \\ &= \sigma_{\text{unbiased}}^2 - (\bar{A}_N - \langle A \rangle)^2 . \end{aligned} \quad (333) \quad (334)$$

Statistical error estimation is based on the central limit theorem, Eq. (47). We collect the average of data, which has unbiased variance  $\sigma_{\text{unbiased}}^2$ . In the central limit theorem the mean  $\mu$  is over all values, so it equals the expectation value

$$\mu := \langle A \rangle . \quad (335)$$

Assuming the central limit theorem is valid for our data, we know that

$$(\bar{A}_N - \langle A \rangle)^2 = (\bar{A}_N - \mu)^2 = \left[ \frac{\sigma_{unbiased}}{\sqrt{N}} \right]^2 = \frac{\sigma_{unbiased}^2}{N} . \quad (336)$$

Inserting this gives the relation

$$\sigma_{biased}^2 = \sigma_{unbiased}^2 \left[ 1 - \frac{1}{N} \right] . \quad (337)$$

This can be interpreted as a finite sample size correction to variance. To conclude, the bias-corrected Monte Carlo standard deviation, the "error", is

$$\sigma = \frac{\sigma_{unbiased}}{\sqrt{N}} = (\bar{A}_N - \langle A \rangle)^2 = \sqrt{\frac{1}{N(N-1)} \sum_{i=1}^N (A_i - \bar{A}_N)^2} . \quad (338)$$

A few notions about the result so far:

- Without bias correction finite sampling underestimates variances  
 $\Rightarrow$  Susceptibilities (response functions) are underestimated by factor  $1 - \frac{1}{N}$

Ok, so what? Just collect more data and get smaller  $1/N$ .  
True, but now comes the real bad news:

- $N$  = number of statistically independent (!) samples
- Near criticality (e.g. near  $T_c$  in Ising model) sampling may become inefficient  
 $\Leftrightarrow$  Autocorrelation times increase  
 $\Leftrightarrow$  more computational time needed to increase  $N$
- $N$  is related to the integrated autocorrelation time  $\tau_{int}$  by relation ( $\tau_{int}$  given in measurement time intervals)

$$N_{statistically\ independent\ samples} = \frac{N_{all\ samples}}{1 + 2\tau_{int}} , \quad (339)$$

so if the integrated autocorrelation time for some reason increases dramatically you need a lot more Monte Carlo steps to reach the same accuracy at the same  $N$ .

In addition to correcting the sample bias we need to discuss about correlations in samples.

### 9.3 Integrated autocorrelation time

The integrated autocorrelation time  $\tau_{int}$  jumped in the discussion without derivation. Correlations are expected die out exponentially, meaning the measured values at MC-time  $i$  and  $i + t$  satisfy

$$\langle A_i A_{i+t} \rangle - \langle A \rangle^2 \propto e^{-t/\tau_{exp}}, \quad (340)$$

where  $\tau_{exp}$  is the exponential correlation time, specific to the quantity  $A$ , is the correlation decay rate. The index  $i$  vanished by the assumption of translational invariance in simulation time, meaning that we can consider an arbitrary simulation step  $i$ ,

$$\langle A_i A_{i+t} \rangle = \langle A_0 A_{0+t} \rangle. \quad (341)$$

Naturally this is valid only in equilibrium, that is, after the thermalization steps are done. The normalized autocorrelation function of  $A$  is defined

$$\phi(t) = \frac{\langle A_i A_{i+t} \rangle - \langle A \rangle^2}{\langle A^2 \rangle - \langle A \rangle^2} \quad \forall i. \quad (342)$$

A better average is obtained by integrating - or rather summing - the autocorrelation function. One defines the integrated autocorrelation time

$$\tau_{int} := \frac{\sum_{t=1}^{\infty} (\langle A_i A_{i+t} \rangle - \langle A \rangle^2)}{\langle A^2 \rangle - \langle A \rangle^2}. \quad (343)$$

The infinite limit in the summation is not practical, and only a finite data window is available for evaluation of  $\tau_{int}$ . How is  $\tau_{int}$  related to MC error estimate?

The MC error estimate tells how far the sample mean is from the true mean. We got the formula (338)

$$\sigma^2 = \frac{\sigma_{unbiased}^2}{N} = (\bar{A}_N - \langle A \rangle)^2, \quad (344)$$

so let's see how large this is *expected* to be and evaluate

$$\langle \sigma^2 \rangle = \langle (\bar{A}_N - \langle A \rangle)^2 \rangle \quad (345)$$

There's a sum squared, so maybe it can be expressed as a convolution such as the integrated autocorrelation time in Eq. (343). Let's work out the details,<sup>59</sup>

$$\langle \sigma^2 \rangle = \langle (\bar{A}_N - \langle A \rangle)^2 \rangle = \left\langle \left( \frac{1}{N} \sum_{i=1}^N (A_i - \langle A \rangle) \right)^2 \right\rangle \quad (346)$$

$$= \left\langle \left( \frac{1}{N} \sum_{i=1}^N (A_i - \langle A \rangle) \right) \left( \frac{1}{N} \sum_{j=1}^N (A_j - \langle A \rangle) \right) \right\rangle. \quad (347)$$

---

<sup>59</sup>D. Landau and K. Binder, *A Guide to Monte Carlo Simulations in Statistical Physics*, Cambridge Univ. Press 2009, p. 91.

The idea is to assume that  $N$  is large, so that

$$\frac{1}{N} \sum_{i=1}^N A_i = \langle A \rangle + \text{small deviation} , \quad (348)$$

and see how significant the small deviation is in the square. A lonely  $A_i$  can be replaced with  $\langle A \rangle$ , but the square has terms with  $A_i A_j$ . Separate cases  $j = i$  and  $j < i$  and  $j > i$  (the latter two give the same result)

$$\langle \sigma^2 \rangle = \frac{1}{N^2} \sum_{i=1}^N \langle (A_i - \langle A \rangle)^2 \rangle + \frac{2}{N^2} \sum_{i=1}^N \sum_{j=i+1}^N \langle A_i A_j - \langle A \rangle^2 \rangle , \quad (349)$$

In the second sum  $j > i$ , so it's useful to define  $j = i + t$ ,

$$\langle \sigma^2 \rangle = \frac{1}{N^2} \sum_{i=1}^N \langle (A_i - \langle A \rangle)^2 \rangle + \frac{2}{N^2} \sum_{i=1}^N \sum_{t=1}^{N-i} (\langle A_i A_{i+t} \rangle - \langle A \rangle^2) . \quad (350)$$

Assuming the  $t$ -sum converges long before  $t = N - i$ , we may extend the sum to infinity,

$$\langle \sigma^2 \rangle \approx \frac{1}{N^2} \sum_{i=1}^N \langle (A_i - \langle A \rangle)^2 \rangle + \frac{2}{N^2} \sum_{i=1}^N \sum_{t=1}^{\infty} (\langle A_i A_{i+t} \rangle - \langle A \rangle^2) \quad (351)$$

$$= \frac{1}{N^2} \sum_{i=1}^N \langle (A_i - \langle A \rangle)^2 \rangle + \frac{2}{N} \tau_{int} (\langle A^2 \rangle - \langle A \rangle^2) \quad (352)$$

$$= \frac{\langle A^2 \rangle - \langle A \rangle^2}{N} (1 + 2\tau_{int}) . \quad (353)$$

This means that the so-called *statistical inefficiency* given by the factor  $(1 + 2\tau_{int})$  changes the number of statistically independent samples from all samples  $N$  to a smaller amount  $N/(1 + 2\tau_{int})$ .

Analysing the autocorrelations in data gives valuable information about how efficient the MC sampling algorithm is, which is a relevant question in designing Markov chain MC. However, if the algorithm is not debatable, then the discussion about autocorrelations may not be that fruitful, and there are more practical ways to estimate the error in MC results.

## 9.4 Block averaging

*The averages of sufficiently large blocks of data are statistically independent.*

How large is "sufficiently large" needs to be established. Split the collected data,  $N$  values, to blocks of size  $n$ . Say there are  $N_b$  blocks,

$$N = N_b \times n , \quad (354)$$

so we work with  $N_b$  mean values  $B_i$  computed for each block  $i$ :

$$\underbrace{A_1 A_2 \dots A_n}_{\text{mean } B_1} \quad \underbrace{A_{n+1} A_{n+2} \dots A_{2n}}_{\text{mean } B_2} \quad \underbrace{A_{2n+1} \dots}_{\text{mean } B_{N_b}} \dots \underbrace{A_N}_{\text{mean } B_{N_b}} . \quad (355)$$

If  $n$  is sufficiently large, spanning over simulation time longer than the integrated autocorrelation time  $\tau_{int}$ , then the values  $B_i$  are *stochastically independent*. If this is the case, the error is given by the unbiased standard deviation,

$$\sigma = \sqrt{\frac{1}{N_b(N_b - 1)} \sum_{i=1}^{N_b} (B_i - \bar{B}_{N_b})^2} . \quad (356)$$

If the blocks cover the whole sample of  $N$  values, then of course the average of blocks is the total average,  $\bar{B}_{N_b} = \bar{A}_N$ . An equivalent, cleaner form is obtained by evaluating the square in the previous formula,

$$\text{error} = \sqrt{\frac{1}{N_b - 1} \left( (\overline{B^2})_{N_b} - (\bar{B}_{N_b})^2 \right)} . \quad (357)$$

This method can be used to both primary variables, such as energy, that are measured directly from MC simulation, and to secondary variables, such as the specific heat, computed from energy data.

## 9.5 Resampling methods

The original set of data is collected by taking samples of a quantity during the simulation. That is sampling. In resampling one takes samples from the data that has been collected, so it's sampling from a sample.

### 9.5.1 Jackknife

Von Mises applied the jackknife resampling method in some form already in the pre-computing era (1930's), but the main work was done by Quenouille (1949) (who wanted to find a way to estimate bias) and Tukey (1958).

- Divide the data to  $N$  blocks, block size  $> \tau_{int}$   
 $\Rightarrow$  blocks are independent
- Omit the first, 2nd, 3rd, ... block from the sample of size  $N$ . The decimated set  $A_{(i)}$  has  $i^{\text{th}}$  block omitted. Case  $N = 5$ :

Full set of blocks	1	2	3	4	5	average $\bar{A}_N$
averages of blocks	$\bar{a}_1$	$\bar{a}_2$	$\bar{a}_3$	$\bar{a}_4$	$\bar{a}_5$	
$A_{(1)}$		2	3	4	5	average $\bar{A}_{(1)}$
$A_{(2)}$	1		3	4	5	average $\bar{A}_{(2)}$
$A_{(3)}$	1	2		4	5	average $\bar{A}_{(3)}$
$A_{(4)}$	1	2	3		5	average $\bar{A}_{(4)}$
$A_{(5)}$	1	2	3	4		average $\bar{A}_{(5)}$

- The standard deviation can be computed using

$$\sigma = \sqrt{\frac{N-1}{N} \sum_{i=1}^N (\bar{A}_{(i)} - \bar{A}_N)^2}. \quad (358)$$

The factor  $\frac{N-1}{N}$  can be made plausible by noticing that

$$\bar{A}_{(i)} = \frac{1}{N-1} \sum_{j(\neq i)} \bar{a}_j, \quad (359)$$

so one recovers the standard deviation of block data,

$$\sigma = \sqrt{\frac{1}{N(N-1)} \sum_{i=1}^N (\bar{a}_i - \bar{A}_N)^2}. \quad (360)$$

The resampled sets in jackknife are not really new measurements, and have less data than the original set, so their variance is smaller than the variance in the full data. The resampled sets deviate from the original set by only one data point, so in this sense jackknife is probing the near vicinity of the original set.

*Don't use jackknife to estimate the median*, it will fail miserably. Median - the middle value of the data - has what one calls "non-smooth statistics": a small change in the data set can make a big change in the median. This can be considered a sort of non-differentiability. Another quantity that is non-smooth is the maximum value of data.

### 9.5.2 Bootstrap

I'm not positive, but I suppose the name comes from baron von Münchhausen's incredible account on avoiding drowning in a swamp by pulling from his own boot straps. Our bootstrapping is a generalization of the jackknife resampling, suggested by Efron (1979).

- Resample, *with replacement*, the existing data to get a new data set. Compute the statistics from this resampled set.

•

*Original Sample* : 1 2 3 4 5  
*1st bootstrap replica* : 1 1 2 5 4  
*2nd bootstrap replica* : 5 2 2 1 3  
*3rd bootstrap replica* : 4 1 1 3 4  
*etc.*

- About  $N_{boot} = 1000$  replicas are often enough.
- Compute error using

$$\text{error} = \sqrt{\frac{1}{N-1} \left[ \overline{(A^2)}_N - (\bar{A}_N)^2 \right]}, \quad (361)$$

notice that one doesn't divide by  $(N_{boot} - 1)^{60}$

- You may block data to get independent samples but it's not necessary. Some blocking is usually done anyhow, because storing all data on disk is ineconomical.

No theoretical calculations are needed, the method works no matter how mathematically complicated the chosen estimator (such as variance) is. Just like the jackknife, the bootstrap can be used to estimate simultaneously bias, kurtosis, and other statistical properties of the data.

The bootstrap resampled sets deviate from the original one more than the jackknife resampled sets, so in this sense the bootstrap samples further away from the original set.

---

<sup>60</sup>The number of bootstrap replicas is unlimited, so having  $1/(N_{boot} - 1)$  as a factor would lead to ever diminishing error, which cannot be correct.

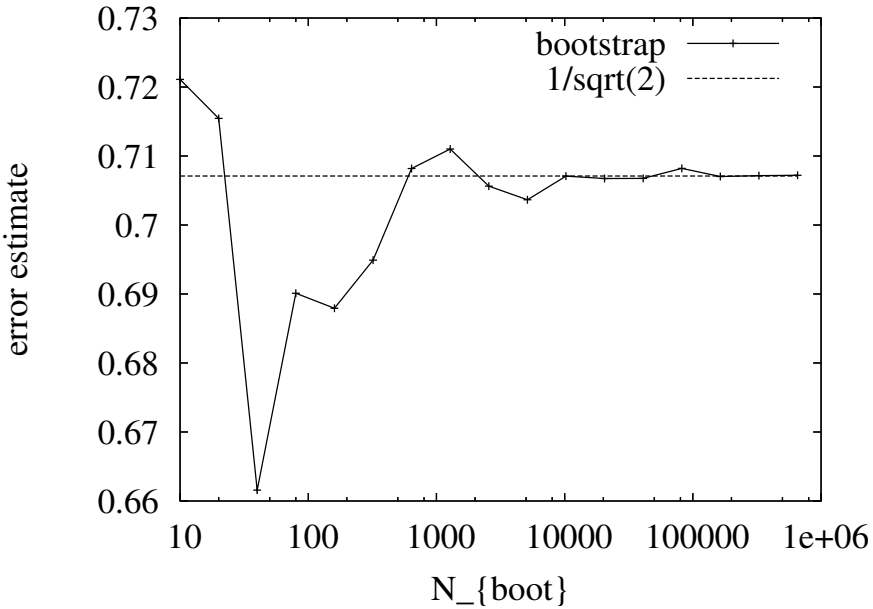


Figure 16: The convergence of the bootstrap error estimate as a function of number of bootstrap replicas. The original data set is  $\{1,2,3,4,5\}$ .

### Jackknife or bootstrap ?

- Jackknife requires as many resampled sets as there are original data points  
⇒ For over 100 data points bootstrap becomes more effective.
- But for bootstrap you need about 1000 samples to get decent estimate for variance  
⇒ **Jackknife seems to be a better up to about 1000 data points. If you have more data, use bootstrap .**
- If you don't block the data before error analysis, but choose to use statistically dependent data (=data picked more frequently than  $\tau_{int}$ ) you probably have lots of data ⇒ use bootstrap.

### How to debug error-estimation subroutines ?

- Program all three: blocking, jackknife, bootstrap
- Pick a simple set of five data points: 1,2,3,4,5
- Compare error estimates to the exact value  $\sigma = 1/\sqrt{2} = 0.70717$
- If you get “NaN” in bootstrap, your  $\bar{A}^2 - (\bar{A})^2$  is negative. Check that you divide with correct integer counts.  $\bar{A}$  should be close to 3.

- If your bootstrap error won't converge with increasing number of replicas, you haven't divided  $N_{boot}$  in computing the averages  $\bar{A}^2$  or  $\bar{A}$ .
- If your bootstrap converges to  $\sigma = \sqrt{2} = 1.414$ , you forgot to multiply with  $1/(N - 1)$  under the sqrt. In this case  $N = 5$  (but don't hardwire  $N$  to 5 ;).
- After all seems to work, generate  $N$  data points using your old reliable gaussian random number generator. Analyse the data: the average should go toward 0, and the error of average should diminish as

$$\sigma = \sigma_{input}/\sqrt{N} = 1/\sqrt{N} ,$$

because the standard normal distribution the code produces has  $\sigma_{input} = 1$ .

## 10 Large-time-step propagators

### 10.1 Propagators with fourth or higher order accuracy

Suzuki: there is no 4th order splitting

$$e^{-\tau(\hat{\mathcal{A}}+\hat{\mathcal{B}})} = \prod_{i=1}^N e^{-\tau a_i \hat{\mathcal{A}}} e^{-\tau b_i \hat{\mathcal{B}}} \quad (362)$$

without some  $a_i < 0$  and  $b_i < 0$ .<sup>61</sup>

This we cannot have in DMC, because a negative  $t_i$  means  $\langle \mathbf{R}' | e^{-\tau t_i \hat{\mathcal{T}}} | \mathbf{R} \rangle$  is inverse diffusion (backward in time), which cannot be simulated. Something has to be added, and that's some commutator(s) of  $\hat{\mathcal{T}}$  and  $\hat{\mathcal{V}}$ . A convenient one to keep is related to the classical force on particle  $i$ ,<sup>62</sup>

$$[\hat{\mathcal{V}}, [\hat{\mathcal{T}}, \hat{\mathcal{V}}]] = 2\lambda |\nabla_{\mathbf{R}} V(\mathbf{R})|^2 = 2\lambda \sum_{i=1}^N |\mathbf{f}_i(\mathbf{R})|^2, \quad \mathbf{f}_i = -\nabla_i V. \quad (363)$$

The commutator is evaluated like this,  $\hat{\mathcal{T}} = -\lambda \nabla_{\mathbf{R}}^2$ ,  $V := V(\mathbf{R})$ ,

$$\begin{aligned} [\hat{\mathcal{V}}, [\hat{\mathcal{T}}, \hat{\mathcal{V}}]]\phi(\mathbf{R}) &= [-V^2 \hat{\mathcal{T}} - \hat{\mathcal{T}} V^2 + 2V \hat{\mathcal{T}} V]\phi \\ &= \lambda [V^2 \nabla^2 \phi + \nabla^2 (V^2 \phi) - 2V \nabla^2 (V \phi)] \\ &= \lambda \left[ V^2 \nabla^2 \phi + \nabla \cdot [2V (\nabla V) \phi + V^2 \nabla \phi] \right. \\ &\quad \left. - 2V \nabla \cdot [(\nabla V) \phi + V \nabla \phi] \right] \end{aligned} \quad (364)$$

$$\begin{aligned} &= \lambda \left[ V^2 \nabla^2 \phi + \underline{2(\nabla V)^2 \phi} + \cancel{2(V \nabla^2 V) \phi} + \cancel{2V (\nabla V) \cdot \nabla \phi} \right. \\ &\quad \left. + \cancel{2V \nabla V \cdot \nabla \phi} + \cancel{V^2 \nabla^2 \phi} \right. \\ &\quad \left. - \cancel{2V \nabla^2 V \phi} - \cancel{2V \nabla V \cdot \nabla \phi} - \cancel{2V \nabla V \cdot \nabla \phi} - \cancel{2V^2 \nabla^2 \phi} \right] \end{aligned}$$

coloured terms cancel, only 2nd term survives

$$= 2\lambda (\nabla V)^2 \phi. \quad (366)$$

---

<sup>61</sup>M. Suzuki, J. Math. Phys. 32, 400 (1991).

<sup>62</sup>The operator  $[\hat{\mathcal{V}}, [\hat{\mathcal{T}}, \hat{\mathcal{V}}]]$  acts on some  $\phi(\mathbf{R})$ .

A caleidoscope of 4th order methods (incomplete list):

- **Trotter**<sup>63</sup> (divide  $\tau$  to infinitely many pieces)

$$e^{-\tau \hat{H}} = \lim_{M \rightarrow \infty} \left[ e^{-\frac{\tau}{M} \hat{T}} e^{-\frac{\tau}{M} \hat{V}} \right]^M , \quad (367)$$

- **Ruth-Forest** (Ruth (1983, private channels), Forest and Ruth (1990), re-discovered several times around 1990 by Campostrini and Rossi and by Candy and Rozmus)<sup>64</sup>
- **Takahashi-Imada** (1984)<sup>65</sup> and Li-Broughton (1987)<sup>66</sup>
- **Chin** (1997)<sup>67</sup>

### Forest-Ruth

$$\hat{G}_{\text{FR}}(\tau) = e^{-v_3 \tau \hat{V}} e^{-t_3 \hat{T}} e^{-v_2 \hat{V}} e^{-t_2 \tau \hat{T}} e^{-v_1 \tau \hat{V}} e^{-t_1 \tau \hat{T}} e^{-v_0 \tau \hat{V}} , \quad (368)$$

with  $s = 2^{1/3} = 1.25992$ ,

$$v_0 = v_3 = \frac{1}{2} \frac{1}{2-s} \quad (> 0) \quad , \quad v_1 = v_2 = -\frac{1}{2} \frac{s-1}{2-s} \quad (> 0) \quad (369)$$

$$t_1 = t_3 = \frac{1}{2-s} \quad (> 0) \quad , \quad t_2 = -\frac{s}{2-s} \quad (< 0!) . \quad (370)$$

From right to left, the potential will be evaluated at times  $0, t_1 \tau, (t_1 + t_2) \tau$  ( $< 0!$ ), and  $\tau$ . Suzuki was right, there are **negative coefficients**. These make the application quite tricky. The good thing about FR is that it only needs 6 FFT's to propagate time  $\tau$ ,

**Takahashi-Imada** "not fully fourth order"

$$\hat{G}_{\text{TI}}(\tau) = e^{-\tau \hat{T}} e^{-\tau \hat{V} - \frac{1}{24} \tau^3 [\hat{V}, [\hat{T}, \hat{V}]]} e^{-\tau \hat{T}} \quad (371)$$

---

<sup>63</sup>H. F. Trotter, Proc. Am. Math. Soc. 10, 545 (1959)

<sup>64</sup>E. Forest and R. D. Ruth, Physica D. 43, 105 (1990)

<sup>65</sup>M. Takahashi and M. Imada, J. Phys. Soc. Jpn. 53, 3765 (1984)

<sup>66</sup>X. P. Li and J. Q. Broughton, J. Chem. Phys. 86, 5094 (1987)

<sup>67</sup>S. A. Chin, Phys. Lett. A 226, 344 (1997) and S. A. Chin and C. R. Chen, J. Chem. Phys. 117, 1409 (2002)

**Chin** Several possible forms, one is

$$\hat{\mathcal{G}}_{\text{Chin}}(\tau) = e^{-v_0\tau\hat{\mathcal{V}}}e^{-t_1\tau\hat{\mathcal{T}}}e^{-v_1\tau\hat{\mathcal{W}}}e^{-t_2\tau\hat{\mathcal{T}}}e^{-v_1\tau\hat{\mathcal{W}}}e^{-t_1\tau\hat{\mathcal{T}}}e^{-v_0\tau\hat{\mathcal{V}}} \quad (372)$$

$$\hat{\mathcal{W}} := \hat{\mathcal{V}} + \frac{u_0}{v_1}\tau^2[\hat{\mathcal{V}}, [\hat{\mathcal{T}}, \hat{\mathcal{V}}]] , \quad (373)$$

$$v_0 = \frac{6t_1(t_1 - 1) + 1}{12(t_1 - 1)t_1} \quad , \quad t_2 = 1 - 2t_1 \quad (374)$$

$$v_1 = \frac{1}{2} - v_0 \quad u_0 = \frac{1}{48} \left( \frac{1}{6t_1(1 - t_1)^2} - 1 \right) , \quad (375)$$

and  $t_1$  is tunable,  $0 \leq t_1 \leq 1 - 1/\sqrt{3}$ . Even 5th order errors may cancel with  $t_1 = 0.35023$ . All coefficients are positive.

We have a good approximation for  $\hat{\mathcal{G}}(\tau) = e^{-\tau\hat{\mathcal{H}}}$ , such as

$$\hat{\mathcal{G}}_{\text{Chin}}(\tau) = \hat{\mathcal{G}}(\tau) + \mathcal{O}(\tau^5). \quad (376)$$

Nothing prevents us from overextending the validity, as long as we know that we are improving. Take a trial wave function  $\varphi_T(\mathbf{R})$  and propagate it,

$$\langle \mathbf{R} | \varphi_T(\tau_0) \rangle = \varphi_T(\mathbf{R}; \tau_0) = \int d\mathbf{R}' \langle \mathbf{R} | G_{\text{Chin}}(\tau_0) | \mathbf{R}' \rangle \varphi_T(\mathbf{R}') . \quad (377)$$

We can use VMC to see how far in  $\tau_0$  we can go until the energy begins to increase: find  $\tau_0$  were

$$E(\tau_0) = \frac{\langle \varphi_T(\tau_0) | \hat{\mathcal{H}} | \varphi_T(\tau_0) \rangle}{\langle \varphi_T(\tau_0) | \varphi_T(\tau_0) \rangle} \quad (378)$$

is at minimum (approximately).<sup>68</sup> The propagation can now be viewed as a multi-dimensional integral,

$$\begin{aligned} \varphi_T(\mathbf{R}; \tau_0) &= \int d\mathbf{R}' d\mathbf{R}_1 d\mathbf{R}_2 e^{-v_0\tau_0 V(\mathbf{R})} \langle \mathbf{R} | e^{-t_1\tau_0\hat{\mathcal{T}}} | \mathbf{R}_2 \rangle e^{-v_1\tau_0 W(\mathbf{R}_2)} \\ &\quad \langle \mathbf{R}_2 | e^{-t_2\tau_0\hat{\mathcal{T}}} | \mathbf{R}_1 \rangle e^{-v_1\tau_0 W(\mathbf{R}_1)} \langle \mathbf{R}_1 | e^{-t_1\tau_0\hat{\mathcal{T}}} | \mathbf{R}' \rangle e^{-v_0\tau_0 V(\mathbf{R}')} \varphi_T(\mathbf{R}') . \end{aligned} \quad (379)$$

Notice that this applied one  $G_{\text{Chin}}$  for a single, long time step  $\tau_0$ . The integrated coordinates can also be thought of as "shadow coordinates", as in the variational shadow wave function by L. Reatto, F. Pederiva *et al.* Large  $\tau$  means fast projection and less correlated points in DMC.  
69

---

<sup>68</sup>In VMC the normalization is irrelevant.

<sup>69</sup>H. A. Forbert and S. A. Chin, Phys. Rev. B 63, 144518 (2001).

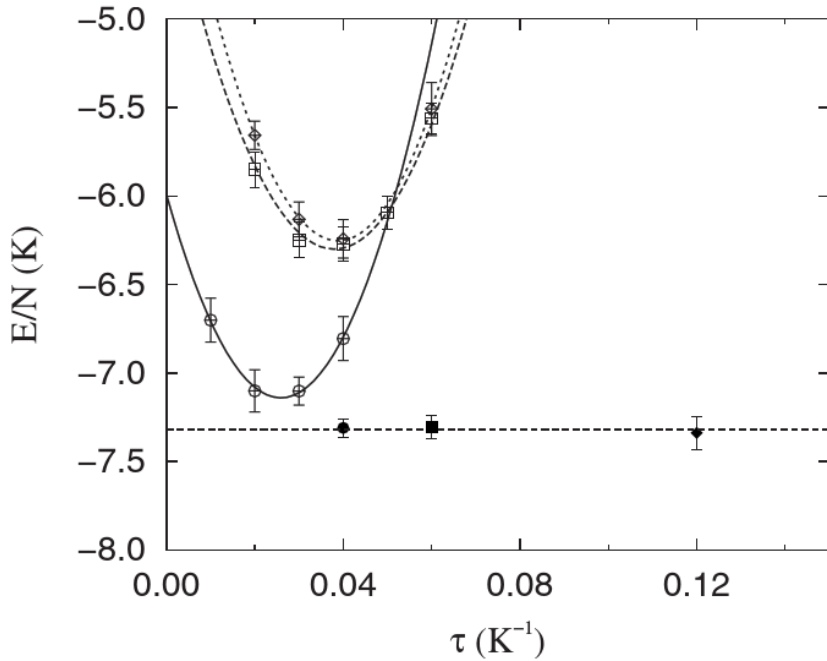


Figure 17:  $\text{He}^4$  liquid at equilibrium density, obtained by applying the single long time step propagation on various trial wave functions, from Rota *et al.*, Physical Review E 81, 016707 (2010).

Following R. E. Zillich, J. M. Mayrhofer, and S. A. Chin,<sup>70</sup> the "work horse" 2nd order propagator<sup>71</sup>

$$G_2(\tau) := e^{-\frac{\tau}{2}V} e^{-\tau T} e^{-\frac{\tau}{2}V}, \quad (380)$$

can be combined to a  $(2n)$ th order propagator,

$$G_{2n}(\tau) = \sum_{i=1}^n c_i G_2^{k_i} \left( \frac{\tau}{k_i} \right) \quad (381)$$

$$c_i = \prod_{j=1(\neq i)}^n \frac{k_i^2}{k_i^2 - k_j^2}. \quad (382)$$

For PIMC, suitable  $k_i$  sequences are  $\{12\}$  (result 4th order),  $\{124\}$  (result 6th order), and  $\{1236\}$  (result 8th order). Here "suitable" means that terms have the same amount of free

<sup>70</sup>R. E. Zillich, J. M. Mayrhofer, and S. A. Chin, J. Chem. Phys. 132, 044103 (2010).

<sup>71</sup>Other choices can be made, too.

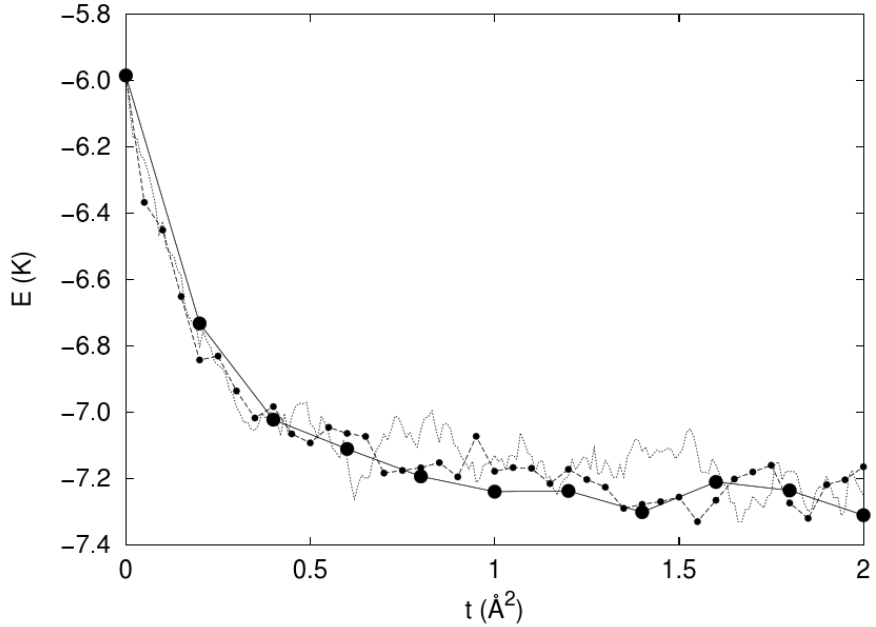


Figure 18: Liquid He<sup>4</sup> : Timesteps 0.01 (dots), 0.05 (small points) and 0.2 (large points). Getting to the ground state takes 10 times more updates with a 2nd order propagator than with a 4th order one. From H. A. Forbert and S. A. Chin, Phys. Rev. E 63, 016703 (2000).

propagators with the same timestep  $\tau$ , or those that can be *made* "commensurate" by exact splitting, e.g.  $e^{-2\tau T} = e^{-\tau T}e^{-\tau T}$ . If the sequence is commensurate, the free propagators can be neatly factored out. For example, the 6th order propagator is

$$G_6(\tau) = \frac{1}{45}G_2(\tau) - \frac{4}{9}G_2^2(\tau/2) + \frac{64}{45}G_2^4(\tau/4) . \quad (383)$$

which can be written as

$$G_6(12345; 4\tau) = G_0(12; \tau)G_0(23; \tau)G_0(34; \tau)G_0(45; \tau) \quad (384)$$

$$\left[ \frac{64}{45}e^{-\frac{\tau}{2}(V_1+2V_2+2V_3+2V_4+V_5)} - \frac{4}{9}e^{-\frac{\tau}{2}(V_1+2V_3+V_5)} + \frac{1}{45}e^{-\frac{\tau}{2}(V_1+V_5)} \right] .$$

Let's show that the last term reduces to  $\frac{1}{45}G_2(15; 4\tau)$  and un-split the free propagator,

$$\frac{1}{45}G_0(12; \tau)G_0(23; \tau)G_0(34; \tau)G_0(45; \tau)e^{-\frac{\tau}{2}(V_1+V_5)} \quad (385)$$

$$= \frac{1}{45}G_0(15; 4\tau)e^{-\frac{\tau}{2}(V_1+V_5)} = \frac{1}{45}\langle 1 | e^{-\frac{4\tau}{2}\hat{V}} e^{-4\tau\hat{T}} e^{-\frac{4\tau}{2}\hat{V}} | 5 \rangle . \quad (386)$$

Similarly, an 8th order propagator is

$$G_8(\tau) = -\frac{1}{180}G_2(\tau) + \frac{2}{15}G_2^2(\tau/2) - \frac{27}{40}G_2^3(\tau/3) + \frac{54}{35}G_2^6(\tau/6) , \quad (387)$$

so

$$\begin{aligned}
 G_8(1234567; 6\tau) &= G_0(12; \tau)G_0(23; \tau)G_0(34; \tau)G_0(45; \tau)G_0(56; \tau)G_0(67; \tau) \\
 &\quad \left[ \frac{54}{35}e^{-\frac{\tau}{2}(V_1+2V_2+2V_3+2V_4+2V_5+2V_6+V_7)} - \frac{27}{40}e^{-\frac{\tau}{2}(V_1+2V_3+2V_5+2V_7)} \right. \\
 &\quad \left. + \frac{2}{15}e^{-\frac{\tau}{2}(V_1+2V_4+V_7)} - \frac{1}{180}e^{-\frac{\tau}{2}(V_1+V_7)} \right]. \tag{388}
 \end{aligned}$$

With negative coefficients, these weights are obviously not positive definite. If used in MC, the rare negative weight moves can be systematically rejected, but the accuracy is questionable. Varying coefficients is further visualized in figure 19, where the coefficients giving a 120th order propagator are plotted. Normalizing the largest  $c$  to unity, the last one is  $c_{120} = 1.37697 \times 10^{-10}$ . A nominally larger time step is achieved in expense of intermediate time steps. Just like in

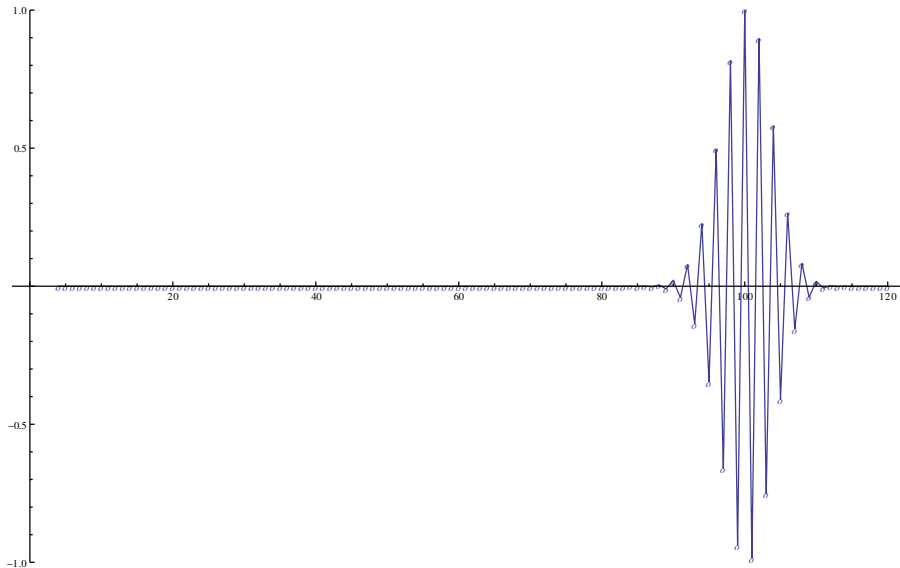


Figure 19: Taking  $k_i = i$  (not commensurate,  $i = 1, 2, 3, \dots, 120$ ), the figure shows the coefficients  $c_i$ , with the largest value normalized to 1.

solving differential equations, a larger time-to-time accuracy is achieved evaluating derivatives at intermediate times (think about, for example, the 4th order Runge-Kutta method). At about 4th order the gain and computational effort are in balance, beyond that it's a losing game.

## 10.2 Propagators with no time step error

So far the time slices have been equidistant or at least fixed. Relaxing the restriction can give "infinite order" propagators, such as the old perturbation theory expansion<sup>72</sup>,

$$e^{-\tau \hat{H}} = e^{-\tau \hat{T}} \left[ 1 - \int_0^\tau d\tau_1 \hat{\mathcal{V}}(\tau_1) + \frac{1}{2} \int_0^\tau d\tau_1 \int_0^\tau d\tau_2 \hat{\mathcal{T}}_\tau [\hat{\mathcal{V}}(\tau_1) \hat{\mathcal{V}}(\tau_2)] \dots \right],$$

often written in the time-ordered form

$$e^{-\tau \hat{H}} = e^{-\tau \hat{T}} \hat{\mathcal{T}}_\tau \left[ e^{-\int_0^\tau d\tau \hat{\mathcal{V}}(\tau)} \right], \quad \hat{\mathcal{V}}(\tau) := e^{\tau \hat{T}} \hat{\mathcal{V}} e^{-\tau \hat{T}}. \quad (389)$$

Writing the operator in coordinate space reveals a structure similar to previous combined  $G_2(\tau)$  propagators, (mark  $\mathbf{R}_k = k$  for shortness)

$$\begin{aligned} G(1, X; \tau) &= G_0(1X; \tau) - \int_0^\tau d\tau_2 \int d2 G_0(12; \tau - \tau_2) V_2 G_0(2X; \tau_2) \\ &\quad + \frac{1}{2} \int_0^\tau d\tau_2 \int_0^\tau d\tau_3 \int d2d3 \hat{\mathcal{T}}_\tau [G_0(12; \tau - \tau_2) V_2 G_0(23; \tau_2 - \tau_3) V_3 G_0(3X; \tau_3)] \dots, \end{aligned} \quad (390)$$

where 1 is on the time imaginary time  $\tau$  and  $X$  is on imaginary time 0. The expansion suffers from the common perturbation theory weakness, namely the sum doesn't converge at large  $\tau$ . The problem arises because of the so-called secular terms, which - contrary to the assumption - don't decrease term after term in the expansion. Even with known finite result, the perturbation expansion may diverge, so it's purely a technical weakness. Let's approximate this by keeping  $n$  terms and split the free propagators to a "commensurate" sequence,

$$\begin{aligned} G(1X; \tau) &\approx \tau^{-(n-1)} \int_0^\tau d\tau_2 \dots d\tau_n \int d2d3 \dots dn \hat{\mathcal{T}}_\tau [G_0(12; \tau - \tau_2) G_0(23; \tau_2 - \tau_3) \dots G_0(nX; \tau_n)] \\ &\quad \left[ 1 - \tau V_2 + \frac{\tau^2}{2!} V_2 V_3 - \dots + \frac{(-\tau)^{n-1}}{(n-1)!} V_2 V_3 \dots V_n \right]. \end{aligned} \quad (391)$$

This has the familiar structure with free propagations and a potential factor, but now the time slices move around between the limits 0 and  $\tau$ . Compared to the earlier finite order potential factors, this one is very bad: the potentials scale with particle number, and the convergence of the whole factor is poor at best. As often, perturbation expansions require heavy re-summation of terms to be of any use. Large- $V$  occurrences are perilous, they are not suppressed as in  $\exp(-\tau V)$  terms. As  $n \rightarrow \infty$  time-slices form a continuous mass with constant density, and  $G_0$ 's are almost Dirac deltas, with potential changing continuously between 0 and  $\tau$ .

<sup>72</sup>A. L. Fetter and J. D. Walecka, *Quantum Theory of Many-Particle Systems* (1971), R. P. Feynman, *Statistical Mechanics, A set of lectures* (1972-1982). The expansion can be viewed as the interaction picture representation wrt.  $\hat{\mathcal{V}}$ , and the expanded form does perturbation theory wrt.  $\hat{\mathcal{V}}$ . One way to derive is to find the integral equation for  $\hat{\mathcal{U}}(\tau)$  with  $e^{-\tau \hat{H}} = e^{-\tau \hat{T}} \hat{\mathcal{U}}(\tau) \Rightarrow \hat{\mathcal{U}}(\tau) = e^{\tau \hat{T}} e^{-\tau \hat{H}}$ , and derive this wrt.  $\tau$ .

## 11 Appendix

### 11.1 McMillan trial wave function for liquid ${}^4\text{He}$

In his 1965 PhD thesis William L. McMillan made an early application of Monte Carlo to study the ground state of liquid and solid helium<sup>73</sup>. In lack of better knowledge, back then the He-He potential was taken to be the 6-12 Lennard-Jones potential,

$$V(r) = 4\varepsilon \left[ \left( \frac{\sigma}{r} \right)^1 2 - \left( \frac{\sigma}{r} \right)^6 \right], \quad (392)$$

where  $\varepsilon = 10.22$  K and the hard core radius of He atoms is  $\sigma = 2.556$  Å, and it's customary to express distances in units  $\sigma$ . Sorry about overloading the standard deviation notation  $\sigma$ , but this length  $\sigma$  has long traditions. In order to keep the potential energy at bay and get a low energy, the trial wave function should keep atoms apart. McMillan chose the form

$$\varphi_T(\mathbf{R}) = \prod_{i < j=1}^N f(r_{ij}), \quad r_{ij} = |\mathbf{r}_i - \mathbf{r}_j|, \quad (393)$$

with two-body correlations

$$f(r) = e^{-\frac{1}{2}(\beta/r)^\mu}. \quad (394)$$

McMillan found that the best values are  $\beta \sim 2.6 - 2.7$  and  $\mu = 5$ . This wave function is computationally cheap to evaluate. The exponential form is also quite convenient, since one needs mostly the ratio

$$\frac{|\varphi_T(\mathbf{R}')|^2}{|\varphi_T(\mathbf{R})|^2} = \frac{e^{-\sum_{i < j=1}^N (\beta/r'_{ij})^\mu}}{e^{-\sum_{i < j=1}^N (\beta/r_{ij})^\mu}} = \exp \left[ -\beta^\mu \sum_{i < j=1}^N \left[ \frac{1}{(r'_{ij})^\mu} - \frac{1}{(r_{ij})^\mu} \right] \right]. \quad (395)$$

**Local energy** The Hamiltonian is

$$H = -\frac{\hbar^2}{2m} \sum_{i=1}^N \nabla_i^2 + \sum_{i < j} V(r_{ij}), \quad (396)$$

so the local energy is

$$E_L(\mathbf{R}) = -\frac{\hbar^2}{2m} \sum_{i=1}^N \frac{\nabla_i^2 \varphi_T(\mathbf{R})}{\varphi_T(\mathbf{R})} + \sum_{i < j} V(r_{ij}). \quad (397)$$

---

<sup>73</sup>W. L. McMillan, Phys. Rev. 138 (1965) A442-A451.

This form gives some hint of what is *not* meant by "local energy": The potential part of it is just the "classical" potential energy of particles located at  $\mathbf{R}$ , hence the first term should describe the kinetic energy of that system. Right? No, because thinking that way the "kinetic energy of  $i$ :th particle" can be negative! For some configurations the total kinetic part can be negative, too. This is just a warning that one shouldn't consider the terms too seriously as the kinetic and the potential energy.

Let's do the job for a slightly more general case. Use a **one-body correlation function**  $u(\mathbf{r}_i)$  for inhomogeneous cases and a **two-body correlation function** to keep particles apart:

$$\varphi_T(\mathbf{R}) = e^{\frac{1}{2}[\sum_i u(\mathbf{r}_i) + \sum_{i < j} u(\mathbf{r}_i, \mathbf{r}_j)]} . \quad (398)$$

where McMillan had  $u(\mathbf{r}_i, \mathbf{r}_j) = -(\beta/r_{ij})^\mu$ . If only the two-body correlation part is present, then this is called a Jastrow trial wave function. It is much used in any strongly interacting many-body problems, not just liquid helium. To simplify calculations we assume that  $u(\mathbf{r}_i, \mathbf{r}_j)$  depends only on the length  $r_{ij}$  and not on the spatial direction, hence  $u = u(r_{ij})$ .

The following formulas come handy; I'll write intermediate steps in 2D, final forms are valid in any dimension. First of all, we introduce the shorthand notation  $u_{ij} = u(r_{ij})$ . Let  $\nabla_k$  denote the gradient with respect to the position vector of particle  $k$ . We have

$$\begin{aligned} \nabla_k r_{ij} &= \left( \frac{\partial}{\partial x_k}, \frac{\partial}{\partial y_k} \right) \sqrt{(x_i - x_j)^2 + (y_i - y_j)^2} \\ &= r_{ij}^{-1} (x_i - x_j, y_i - y_j) (\delta_{ik} - \delta_{jk}) \\ &= \hat{\mathbf{r}}_{ij} (\delta_{ik} - \delta_{jk}) , \end{aligned} \quad (399)$$

where the hat signifies a unit vector. Similarly,

$$\begin{aligned} \nabla_k \cdot \mathbf{r}_{ij} &= \left( \frac{\partial}{\partial x_k}, \frac{\partial}{\partial y_k} \right) \cdot (x_i - x_j, y_i - y_j) \\ &= D(\delta_{ik} - \delta_{jk}) . \end{aligned} \quad (400)$$

From these we get

$$\begin{aligned} \nabla_k^2 r_{ij} &= \nabla_k \cdot \hat{\mathbf{r}}_{ij} (\delta_{ik} - \delta_{jk}) = \nabla_k \cdot [r_{ij}^{-1} \mathbf{r}_{ij}] (\delta_{ik} - \delta_{jk}) \\ &= -r_{ij}^{-2} \nabla_k r_{ij} \cdot \mathbf{r}_{ij} (\delta_{ik} - \delta_{jk}) + D r_{ij}^{-1} (\delta_{ik} - \delta_{jk})^2 \\ &= (D - 1) r_{ij}^{-1} (\delta_{ik} - \delta_{jk})^2 = (D - 1) r_{ij}^{-1} (\delta_{ik} + \delta_{jk}) . \end{aligned}$$

Then

$$\nabla_k u_i = u'_i \nabla_k r_i = u'_k \hat{\mathbf{r}}_k \quad (401)$$

$$\nabla_k u_{ij} = u'_{ij} \nabla_k r_{ij} = u'_{kj} \hat{\mathbf{r}}_{kj} - u'_{ik} \hat{\mathbf{r}}_{ik} \quad (402)$$

$$(403)$$

and

$$\nabla_k^2 u_i = u''_k \quad (404)$$

$$\begin{aligned} \nabla_k^2 u_{ij} &= u''_{ij} (\nabla_k r_{ij})^2 + u'_{ij} \nabla_k^2 r_{ij} \\ &= [u''_{ij} + u'_{ij} (D-1) r_{ij}^{-1}] (\delta_{ik} + \delta_{jk}) \\ &= u''_{ik} + u'_{ik} (D-1) r_{ik}^{-1} + (i \leftrightarrow j) . \end{aligned} \quad (405)$$

Here  $u'(r_{ij})$  stands for the derivative  $du_{ij}/dr_{ij}$ , and  $D$  is the dimension.

Back to the main task. Define

$$\varphi_T(\mathbf{R}) := e^{U(\mathbf{R})} , \quad U(\mathbf{R}) := \frac{1}{2} \left[ \sum_i u_i + \sum_{i < j} u_{ij} \right] \quad (406)$$

to get

$$\nabla_k \varphi_T = \varphi_T \nabla_k U(\mathbf{R}) , \quad (407)$$

and so

$$\begin{aligned} \varphi_T^{-1} \nabla_k^2 \varphi_T &= \varphi_T^{-1} \nabla_k \cdot [\varphi_T \nabla_k U(\mathbf{R})] \\ &= [\nabla_k U(\mathbf{R})]^2 + \nabla_k^2 U(\mathbf{R}) . \end{aligned} \quad (408)$$

The gradient is now

$$\nabla_k U(\mathbf{R}) = \frac{1}{2} \left[ u'_k \hat{\mathbf{r}}_k + \sum_{j(>k)} u'_{kj} \hat{\mathbf{r}}_{kj} - \sum_{i(<k)} u'_{ik} \hat{\mathbf{r}}_{ik} \right] \quad (409)$$

$$= \frac{1}{2} \left[ u'_k \hat{\mathbf{r}}_k + \sum_{i(\neq k)} u'_{ki} \hat{\mathbf{r}}_{ki} \right] , \quad (410)$$

and the laplacian is

$$\nabla_k^2 U(\mathbf{R}) = \frac{1}{2} \left[ u''_k + (D-1) u'_k r_k^{-1} + \sum_{i(\neq k)} u''_{ik} + (D-1) u'_{ik} r_{ik}^{-1} \right] . \quad (411)$$

From these we can collect the local energy

$$E_L(\mathbf{R}) = -\frac{\hbar^2}{2m} \sum_k \left[ [\nabla_k U(\mathbf{R})]^2 + \nabla_k^2 U(\mathbf{R}) \right] + \sum_{i < j} V(r_{ij}) , \quad (412)$$

and the drift ("quantum force") defined in Eq. (203),

$$\mathbf{F}_k(\mathbf{R}) = 2\boldsymbol{\nabla}_k U(\mathbf{R}) . \quad (413)$$

The local energy can be now computed from the drift,

$$E_L(\mathbf{R}) = -\frac{\hbar^2}{2m} \sum_k \left[ \frac{1}{4} \mathbf{F}_k^2 + \frac{1}{2} \boldsymbol{\nabla}_k \cdot \mathbf{F}_k \right] + \sum_{i < j} V(r_{ij}) , \quad (414)$$

If the trial wave function is the exact eigenstate, then this simplifies to

$$E_L(\mathbf{R})_{exact} = \frac{\hbar^2}{8m} \sum_k \mathbf{F}_k^2 + \sum_{i < j} V(r_{ij}) \quad \text{for an exact eigenstate ,} \quad (415)$$

because you can partially integrate the  $\boldsymbol{\nabla}_k \cdot \mathbf{F}_k$  away. An unchecked idea: evaluate both local energies and get a measure for how far the trial wave function is from an eigenstate? For a good trial wave function the local energy should be as close to a constant as possible; that's variance optimization.

Let's see what comes out with a two-body correlation function  $u_{ij}$ . The local energy is

$$\begin{aligned} E_L &= -\frac{\hbar^2}{2m} \sum_k \left[ \frac{1}{4} \left( \sum_{i \neq k} u'_{ki} \hat{\mathbf{r}}_{ki} \right)^2 + \frac{1}{2} \sum_{i \neq k} u''_{ik} + (D-1) u'_{ik} r_{ik}^{-1} \right] + \sum_{i \neq j} \frac{1}{2} V(r_{ij}) \\ &= -\frac{\hbar^2}{2m} \frac{1}{4} \sum_k \left( \sum_{i \neq k} u'_{ki} \hat{\mathbf{r}}_{ki} \right)^2 + \sum_{i \neq j} \left[ -\frac{\hbar^2}{2m} \left( \frac{1}{2} u''_{ij} + \frac{1}{2} (D-1) u'_{ij} r_{ij}^{-1} \right) + \frac{1}{2} V(r_{ij}) \right] . \end{aligned} \quad (416)$$

The first term is a square of a sum,

$$\begin{aligned} \sum_k \left( \sum_{i \neq k} u'_{ki} \hat{\mathbf{r}}_{ki} \right)^2 &= \sum_k \left( \sum_{i \neq k} u'_{ki} \hat{\mathbf{r}}_{ki} \right) \left( \sum_{j \neq k} u'_{kj} \hat{\mathbf{r}}_{kj} \right) = \sum_{k \neq i} (u'_{ki})^2 + \sum_{i \neq j \neq k} u'_{ki} u'_{kj} \hat{\mathbf{r}}_{ki} \cdot \hat{\mathbf{r}}_{kj} \\ &= \sum_{i \neq j} \left[ (u'_{ij})^2 + \sum_{k \neq i, j} u'_{ki} u'_{kj} \hat{\mathbf{r}}_{ki} \cdot \hat{\mathbf{r}}_{kj} \right] = \sum_{i \neq j} \left[ (u'_{ij})^2 + \sum_{k \neq i, j} \boldsymbol{\nabla}_k u_{ki} \cdot \boldsymbol{\nabla}_k u_{kj} \right] . \end{aligned} \quad (417)$$

Putting all together,

$$E_L = \sum_{i \neq j} \left[ -\frac{\hbar^2}{2m} \sum_{k(\neq i,j)} \nabla_k u_{ki} \cdot \nabla_k u_{kj} - \frac{\hbar^2}{2m} \left( (u'_{ij})^2 + \frac{1}{2} u''_{ij} + \frac{1}{2} (D-1) u'_{ij} r_{ij}^{-1} \right) + \frac{1}{2} V(r_{ij}) \right].$$

The  $\nabla_k u_{ki} \cdot \nabla_k u_{kj}$  is actually a three-body function, which gain importance at high density when three particles are probable to get close. Some density dependence is present already in the two-body correlation part, in coordinates  $i$  and  $j$ . For a repulsive potential  $u'(r)$  is large at small distances, so the three-body term gets largest contributions from nearest neighbours, which are arranged to a suitable stacking structures at elevated densities.

The question what correlation function really belongs to  $n$ -body correlations is answered by the *cluster condition*:

*If one pulls far any number of particles from 1 to  $n-1$ , then the  $n$ -body correlation function  $u_n$  goes to zero.*

This tries to say the function goes to zero unless the  $n$  particles form a tight cluster in space. For example,

$$u_2(r_{ij}) := u_{ij} = - \left( \frac{\beta}{|\mathbf{r}_i - \mathbf{r}_j|} \right)^{\mu} \quad (418)$$

is a two-body correlation function as indicated, because pulling  $i$  far from  $j$  reduces this to zero. Similarly, using this  $u_2$  as a "seed",

$$\nabla_k u_{ki} \cdot \nabla_k u_{kj} + \text{cyclic permutations of } (i, j, k) \quad (419)$$

is a three-body correlation function. Why do we need a three-body correlation function? Looking back at the  $E_L$  resulting from  $u_2$  only, there's no way to get

$$\sum_{i \neq j \neq k} \nabla_k u_{ki} \cdot \nabla_k u_{kj} \neq \text{constant} \quad \forall \mathbf{R} \quad (420)$$

The only way to get  $E_L$  more constant is to add a  $u_3$  that cancels this culprit term. So let's assume you do exactly that, and write an improved trial wave function,

$$\varphi(\mathbf{R}) = \exp \left[ -\frac{1}{2} \sum_{i < j} u_{ij} + \frac{1}{3!} \sum_{i < j < k} u_{ijk} \right] := e^{U_2(\mathbf{R}) + U_3(\mathbf{R})} \quad (421)$$

$$u_{ijk} = \nabla_k u_{ki} \cdot \nabla_k u_{kj} + \text{cyclic permutations of } (i, j, k). \quad (422)$$

and re-compute the local energy. But computing gradients you add more to  $E_L$  than you bargained for,

$$\sum_k \nabla_k^2 U = \sum_k \nabla_k^2 U_2 + \sum_k \nabla_k^2 U_3 \quad \text{2- and 3-body corr. functions} \quad (423)$$

$$\begin{aligned} \sum_k (\nabla_k U)^2 &= \sum_k (\nabla_k U_2 + \nabla_k U_3)^2 \\ &= \underbrace{\sum_k (\nabla_k U_2)^2}_{\text{part of this is the original culprit}} + 2 \underbrace{\sum_k \nabla_k U_2 \cdot \nabla_k U_3}_{\text{up to 4-body}} + \underbrace{\sum_k (\nabla_k U_3)^2}_{\text{up to 5-body}}, \end{aligned} \quad (424)$$

so cancelling the original culprit, we got new non-constant culprits, up to a five-body correlation term. This goes out of hand.



Figure 20: The three-body term generated by two-body correlations in the  $[\nabla_k U(\mathbf{R})]^2$  local energy term.

Forgetting this term one would get

$$E_L(\mathbf{R}) \approx \sum_{i \neq j} \left[ -\frac{\hbar^2}{2m} \left( \frac{1}{4}(u'_{ij})^2 + \frac{1}{2}u''_{ij} + \frac{1}{2}(D-1)u'_{ij}r_{ij}^{-1} \right) + \frac{1}{2}V(r_{ij}) \right], \quad (425)$$

so obviously choosing  $u(r)$  that solves the equation

$$-\frac{\hbar^2}{2m} \left( \frac{1}{4}(u'(r))^2 + \frac{1}{2}u''(r) + \frac{1}{2}(D-1)u'(r)r^{-1} \right) + \frac{1}{2}V(r) = C \quad (426)$$

one gets *nearly* a constant local energy for every  $\mathbf{R}$ ,

$$E_L(\mathbf{R}) \approx \sum_{i \neq j} C = N(N-1)C = N(E_0/N) . \quad (427)$$

where the last equality target the assumed ground state energy per particle  $E_0/N$ . Practise shows that this two-body correlation keeps atoms too far apart, and the three-body term that gains importance at increasing density. This determines an approximate  $u(r)$  up to a constant, which doesn't matter since it will be absorbed to the wave function normalization.

Specifically, the local energy of the McMillan trial wave function is

$$\begin{aligned} u'_{ij} &= \frac{\partial}{\partial r_{ij}} \left[ - \left( \frac{\beta}{r_{ij}} \right)^\mu \right] = \mu \beta^\mu r_{ij}^{-\mu-1} \\ u''_{ij} &= -\mu(\mu+1) \beta^\mu r_{ij}^{-\mu-2} , \end{aligned} \quad (428)$$

so

$$\begin{aligned} E_L^{\text{McMillan}}(\mathbf{R}) &= 2 \underbrace{\frac{\hbar^2}{8m} \left[ \mu(\mu+2-d) \beta^\mu \sum_{i \neq j} r_{ij}^{-\mu-2} \right]}_{T_1} \\ &\quad - \underbrace{\frac{\hbar^2}{8m} (\mu \beta^\mu)^2 \sum_i \left[ \sum_{j(\neq i)} r_{ij}^{-\mu-2} \mathbf{r}_{ij} \right]^2}_{T_2} + \sum_{i < j} V(r_{ij}) \\ &= 2T_1(\mathbf{R}) - T_2(\mathbf{R}) + \sum_{i < j} V(r_{ij}) . \end{aligned} \quad (429)$$

The kinetic part of the local energy has two terms, which correspond to evaluating the expectation values  $\langle \varphi_T | \nabla_{\mathbf{R}}^2 | \varphi_T \rangle$  and  $\langle \nabla_{\mathbf{R}} \varphi_T | \nabla_{\mathbf{R}} \varphi_T \rangle$ . Although mathematically equivalent, these two forms give different variance in Monte Carlo. Sometimes mathematical manipulations *may* lead to increase of variance. A rule of thumb says, that one should evaluate expressions in their most basic form. The mathematical equivalence of the two forms of the kinetic energy ensures that their *mean* values should be the same. This is a very useful test: Evaluate expectation values of both forms and see if they approach the same value. If not, then either expression has programming error or the derivatives are not correct.

For completeness we spell out also the drift force corresponding to the McMillan trial wave function :

$$[\mathbf{F}(\mathbf{R})]_i = \mu \beta^\mu \sum_{j(\neq i)} r_{ij}^{-\mu-2} \mathbf{r}_{ij} . \quad (430)$$

For a repulsive potential the quantity in the exponent has to be negative to keep walkers apart. The choice  $\mu = 5$  pulls them strongly apart: the He-He potential is very repulsive in short range.

Figs. 21 and 22 show some selected results for the McMillan correlation factor. For comparison we show the fully optimised  $u_{ij}$ , as given by the HyperNetted Chain (HNC) theory. Clearly the McMillan two-body correlation function is able to keep atoms apart, but it doesn't describe the structure near 5 Å, and hence the radial distribution oscillates with smaller amplitude than the experimental one. The DMC radial distribution by Boronat and Casulleras<sup>74</sup> is practically identical to the experimental one.

The local energy of the Slater-Jastrow trial wave function (225) is also fairly simple to evaluate, if we define

$$L(\mathbf{R}) = \ln [\det(A_\uparrow) \det(A_\downarrow)] U(\mathbf{R}), \quad (431)$$

so that again

$$\nabla_{\mathbf{R}}^2 \varphi_T(\mathbf{R}) = [\nabla_{\mathbf{R}}^2 L(\mathbf{R}) + (\nabla_{\mathbf{R}} L(\mathbf{R}))^2] \varphi_T(\mathbf{R}). \quad (432)$$

The gradient of the Slater determinant is obtained using the identity

$$\frac{\partial}{\partial x_k} \ln \det(A) = \text{Tr} \left[ A^{-1} \frac{\partial}{\partial x_k} A \right]. \quad (433)$$

## 11.2 Cusp conditions in Coulomb systems

We must make sure that the trial wave function satisfies the so-called **cusp condition**, so that the infinities of the potential energy are cancelled by those of the kinetic energy<sup>77</sup>. Here we deal with the conditions for an  $N$ -electron system<sup>78</sup>

The Hamiltonian of  $N$  electrons is

$$H = -\frac{1}{2} \sum_{i=1}^N \nabla_i^2 + V(\mathbf{R}). \quad (434)$$

Move electrons 1 and 2 so that other electrons and the total center of mass  $\mathbf{R}_{CM}$  are fixed. The  $N$ -electron wave function is

$$\Psi(\mathbf{R}) := \Psi(\mathbf{r}_1, \dots, \mathbf{r}_N) = \Psi'(\mathbf{r}, \mathbf{R}_{CM}, \mathbf{r}_3, \dots, \mathbf{r}_N), \quad (435)$$

where  $\mathbf{r} := \mathbf{r}_1 - \mathbf{r}_2$ . Assume next that the trial wave function is of the Jastrow form,

$$\Psi'(\mathbf{r}, \mathbf{R}_{CM}, \mathbf{r}_3, \dots, \mathbf{r}_N) \propto e^{-u(\mathbf{r})} f(\mathbf{r}), \quad (436)$$

where  $f$  obeys the following rules:

---

<sup>74</sup>J. Boronat and J. Casulleras, Phys. Rev. **B49** (1994) 8920.

<sup>77</sup>T. Kato, Comm. Pure Appl. Math. 10, 151 (1957).

<sup>78</sup>This appendix follows closely the one given by M. L. Stedman in his PhD thesis.

1.  $f(0) \neq 0$ , if the spins at  $\mathbf{r}_1$  and at  $\mathbf{r}_2$  are anti-parallel
2.  $f(0) = 0$ , if the spins at  $\mathbf{r}_1$  and at  $\mathbf{r}_2$  are parallel
3.  $f(-\mathbf{r}) = -f(\mathbf{r})$ , if the spins at  $\mathbf{r}_1$  and at  $\mathbf{r}_2$  are parallel.

First we need to rewrite the Hamiltonian using  $\mathbf{r}$  and  $\mathbf{R}_{CM}$ . One has

$$\nabla_1^2 + \nabla_2^2 = 2\nabla_{\mathbf{r}}^2 + \frac{1}{2}\nabla_{\mathbf{R}_{cm}}^2 , \quad (437)$$

where  $\nabla_i$  on the left hand side operates on  $i$ th particle.

*Proof:*

We have

$$\begin{aligned} \mathbf{X} &= \frac{\mathbf{r}_1 + \mathbf{r}_2}{2} \\ \mathbf{x} &= \mathbf{r}_1 - \mathbf{r}_2 , \end{aligned} \quad (438)$$

so

$$\begin{aligned} \frac{\partial}{\partial(\mathbf{r}_1)_k} &= \frac{\partial\mathbf{X}_k}{\partial(\mathbf{r}_1)_k} \frac{\partial}{\partial\mathbf{X}_k} + \frac{\partial\mathbf{x}_k}{\partial(\mathbf{r}_1)_k} \frac{\partial}{\partial\mathbf{x}_k} \\ &= \frac{1}{2} \frac{\partial}{\partial\mathbf{X}_k} + \frac{\partial}{\partial\mathbf{x}_k} \\ \frac{\partial}{\partial(\mathbf{r}_2)_k} &= \frac{1}{2} \frac{\partial}{\partial\mathbf{X}_k} - \frac{\partial}{\partial\mathbf{x}_k} , \end{aligned} \quad (439)$$

and further

$$\nabla_1^2 = \sum_{k=1}^3 \frac{\partial^2}{\partial(x_1)_k^2} \quad (440)$$

$$= \sum_{k=1}^3 \left( \frac{1}{2} \frac{\partial}{\partial\mathbf{X}_k} + \frac{\partial}{\partial\mathbf{x}_k} \right)^2 \quad (441)$$

$$= \sum_{k=1}^3 \frac{1}{4} \frac{\partial^2}{\partial\mathbf{X}_k^2} + \frac{\partial^2}{\partial\mathbf{X}_k\partial\mathbf{x}_k} + \frac{\partial^2}{\partial\mathbf{x}_k^2} .$$

Similarly we get

$$\nabla_2^2 = \sum_{k=1}^3 \frac{1}{4} \frac{\partial^2}{\partial\mathbf{X}_k^2} - \frac{\partial^2}{\partial\mathbf{X}_k\partial\mathbf{x}_k} + \frac{\partial^2}{\partial\mathbf{x}_k^2} , \quad (442)$$

hence

$$\nabla_1^2 + \nabla_2^2 = \sum_k \frac{1}{2} \frac{\partial^2}{\partial \mathbf{x}_k^2} + 2 \frac{\partial^2}{\partial \mathbf{x}_k^2} = \frac{1}{2} \nabla_{\mathbf{R}_{CM}}^2 + 2 \nabla_{\mathbf{r}}^2 , \quad (443)$$

what we set out to prove.

The Hamiltonian reads now

$$H = - \left( \frac{1}{4} \nabla_{\mathbf{R}_{CM}}^2 + \nabla_{\mathbf{r}}^2 \right) - \frac{1}{2} \sum_{i=3}^N \nabla_i^2 + V(\mathbf{r}, \mathbf{R}_{CM}, \mathbf{r}_3, \dots, \mathbf{r}_N) . \quad (444)$$

Our goal is to keep the local energy  $E_L = \varphi_T^{-1} H \varphi_T$  finite as  $\mathbf{r} \rightarrow 0$ . The potential part diverges as  $1/r$ .

$$\lim_{\mathbf{r} \rightarrow 0} \frac{1}{e^{-u(\mathbf{r})} f(\mathbf{r})} \left( -\nabla_{\mathbf{r}}^2 + \frac{1}{r} \right) e^{-u(\mathbf{r})} f(\mathbf{r}) < \infty , \quad (445)$$

and expanding the operator gives

$$\begin{aligned} \left( -\nabla_{\mathbf{r}}^2 + \frac{1}{r} \right) e^{-u(\mathbf{r})} f(\mathbf{r}) &= \left( \frac{2u'}{r} + u'' - u'^2 \right) e^{-u(\mathbf{r})} f(\mathbf{r}) + \frac{e^{-u(\mathbf{r})}}{r} f(\mathbf{r}) \\ &\quad + 2u' e^{-u(\mathbf{r})} \hat{\mathbf{r}} \cdot \nabla_{\mathbf{r}} f(\mathbf{r}) - e^{-u(\mathbf{r})} \nabla_{\mathbf{r}}^2 f(\mathbf{r}) , \end{aligned} \quad (446)$$

where  $u' := du/dr$ .

**Electrons with anti-parallel spins** Since now  $f(0) \neq 0$  there is only one singular terms in (447) and the cusp condition reduces to

$$\lim_{r \rightarrow 0} \frac{2u' + 1}{r} < \infty , \quad (447)$$

so we must have

$$\boxed{\left. \frac{du}{dr} \right|_{r=0} = -\frac{1}{2}} . \quad (448)$$

**Electrons with parallel spins** Taking into account the antisymmetry of  $f(\mathbf{r})$ , the Taylor expansion of  $f(\mathbf{r})$  around zero is

$$f(\mathbf{r}) = \mathbf{a} \cdot \mathbf{r} + \mathcal{O}(r^3) , \quad (449)$$

so the derivatives are

$$\begin{aligned}\nabla_{\mathbf{r}} f(\mathbf{r}) \Big|_{r=0} &= \mathbf{a} \\ \nabla_{\mathbf{r}}^2 f(\mathbf{r}) \Big|_{r=0} &= 0 .\end{aligned}\tag{450}$$

The operator in the local energy (445) is

$$\left( -\nabla_{\mathbf{r}}^2 + \frac{1}{r} \right) e^{-u(\mathbf{r})} f(\mathbf{r}) = \left( \frac{4u'}{r} + u'' - u'^2 + \frac{1}{r} \right) e^{-u(\mathbf{r})} f(\mathbf{r}) ,\tag{451}$$

so the only singular terms in the cusp condition give

$$\lim_{r \rightarrow 0} \left( \frac{4u'}{r} + \frac{1}{r} \right) < \infty ,\tag{452}$$

which gives the cusp condition for two electrons with parallel spins:

$$\boxed{\frac{du}{dr} \Big|_{r=0} = -\frac{1}{4}} .\tag{453}$$

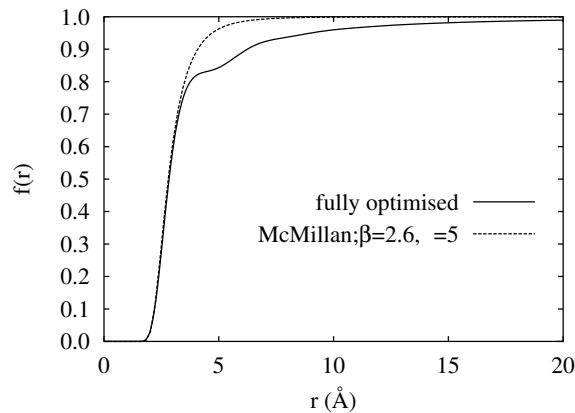


Figure 21: The McMillan correlation factor for few parameters, compared with the two-body correlations optimised fully using the HNC theory and the Aziz (1979) He-He potential at saturation density  $\rho = 0.02185\text{\AA}^{-3}$ .

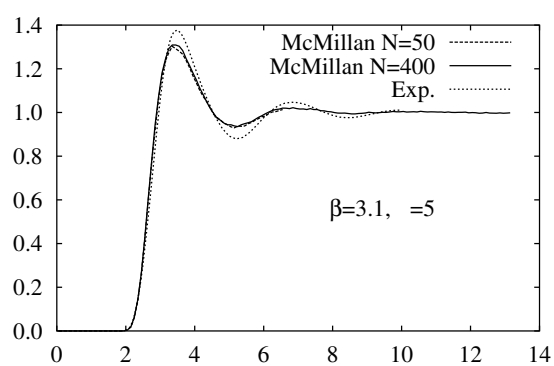


Figure 22: The radial distribution function corresponding to the McMillan wave function using  $N$  walkers with periodic boundary conditions of 3D liquid helium at saturation density. For comparison we show the experimental results by Svensson *et al.*<sup>76</sup>